

## Use Authorization

In presenting this thesis in partial fulfillment of the requirements for an advanced degree at Idaho State University, I agree that the Library shall make it freely available for inspection. I further state that permission to download and/or print my thesis for scholarly purposes may be granted by the Dean of the Graduate School, Dean of my academic division, or by the University Librarian. It is understood that any copying or publication of this thesis for financial gain shall not be allowed without my written permission.

Signature \_\_\_\_\_

Nawamee Shrestha

Date \_\_\_\_\_

**IMPROVED MODELING AND SENSITIVITY ANALYSIS OF  
SEISMIC BEHAVIOR OF WASHINGTON STREET OVERPASS IN  
MONTPELIER, IDAHO**

by

Nawamee Shrestha

A thesis

submitted in partial fulfillment

of the requirements for the degree of

**MASTER OF SCIENCE**

**IN**

**CIVIL ENGINEERING**

**DEPARTMENT OF CIVIL AND ENVIRONMENTAL ENGINEERING**

**IDAHO STATE UNIVERSITY**

May 2014

## Committee Approval

To the Graduate Faculty:

The members of the committee appointed to examine the thesis of  
Nawamee Shrestha find it satisfactory and recommend that it be accepted.

---

Major Advisor:

**Dr. Arya Ebrahimpour**

---

Committee Member:

**Dr. Bruce Savage**

---

Graduate Faculty Representative:

**Dr. Marco P. Schoen**

## **Acknowledgements**

I would like to express my sincere gratitude to my advisor Dr. Arya Ebrahimpour, who offered the continuous support, advice and encouragement throughout my education at Idaho State University. His systematic guidance and great effort into my thesis is more than that I can express in words.

I would also like to thank Idaho Transportation Department (ITD) for providing funding and project to work on without which I could not have completed my master's degree. I am grateful to Dr. Bruce Savage, committee member and Dr. Marco Schoen, Graduate Faculty Representative, help on correcting and revising my thesis and providing their great knowledge.

I would also like to thank help from Andrea Miller, former graduate student of Civil Engineering in ISU, for providing the important information required for this thesis.

Finally I would thank to my family and especially to my husband, Niroj K. Shrestha for providing me support and encouragement for my education.

This work is dedicated to my family

# Table of Contents

List of Figures .....	viii
List of Tables .....	x
ABSTRACT.....	xi
1.0 INTRODUCTION .....	1
1.1 Project Background.....	1
1.2 Literature Review.....	4
1.3 Objectives and Scopes .....	5
1.4 Outline of the Thesis.....	6
2.0 METHODS .....	8
2.1 Washington Street Overpass Description .....	9
2.2 AASHTO Guide Specifications for LRFD Seismic Bridge Design .....	12
2.2.1 Background.....	12
2.2.2 Seismic Risk Assessment.....	13
2.2.3 Selection of Analysis Procedures.....	18
2.3 Modeling in OpenSees.....	25
2.3.1 Pier Modeling.....	26
2.3.1.1 Reinforced Concrete Pier Elements .....	28
2.3.2 Neoprene Bearings.....	36
2.3.3 Guide Angles and Key Plates .....	37
2.3.4 Superstructure .....	38
2.3.5 Mass Distribution.....	40
2.3.6 Foundation .....	40
2.3.7 Abutments and Expansion Joints .....	41
2.4 Sensitivity Analysis .....	49
3.0 RESULT .....	51
3.1 Seismic Analysis.....	51
3.1.1 Pushover Analysis.....	51
3.1.2 Nonlinear Time History Analysis .....	54
3.2 Sensitivity Analysis .....	72
4.0 DISCUSSION.....	79
5.0 CONCLUSION.....	83
5.1 Conclusions of the Research.....	83
5.1.1 Seismic Analysis.....	83

5.1.2 Response of the Model With Contact Elements Versus the Bridge Model Without Contact Elements .....	84
5.1.3 Sensitivity Analysis .....	84
5.2 Future Research Recommendations .....	84
REFERENCES .....	86
APPENDIX.....	90
Appendix A: Confined Concrete Properties Calculations .....	91
Appendix B: OpenSees Commands.....	96
Appendix C: Verification.....	99

## List of Figures

Figure 1.1: Earthquake in State of Idaho as of 2007.....	3
Figure 2.1: Washington Street Overpass Showing Substructure Components [18] .....	9
Figure 2.2: Washington Street Overpass Showing Superstructure Components [18] .....	10
Figure 2.3: Plan and Elevation View of the Washington Street Overpass [11, 19].....	11
Figure 2.4: Design Response Spectrum Curve (AASHTO Figure 3.4.1-1 [1]).....	17
Figure 2.5: Seismic Design Category Core Flowchart [1].....	19
Figure 2.6: Force-Displacement Relationship [21].....	20
Figure 2.7: Modification of Seed Response Spectrum to Design Response Spectrum [18, 23] .....	23
Figure 2.8: Landers Station Horizontal (Longitudinal) Displacement Time History .....	24
Figure 2.9: Landers Station Horizontal (Transverse) Displacement Time History .....	24
Figure 2.10: Typical Pier Showing OpenSees Pier Element Numbers [11, 19] .....	27
Figure 2.11: General Pier Model [13].....	28
Figure 2.12: Concrete Stress Strain Relationship [25].....	29
Figure 2.13: Concrete Stress-Strain Model [17] .....	30
Figure 2.14: Typical Section of Pier Element [11, 19] .....	32
Figure 2.15: Steel Stress-Strain Relationship [25].....	34
Figure 2.16: Coffin-Manson Hysteric Model with Fatigue and Degradation Parameter Values [25].....	35
Figure 2.17: Guide Angle [11, 19].....	37
Figure 2.18: Key Plate [11, 19].....	38
Figure 2.19: Typical Section of Overpass Superstructure [11, 19] .....	39
Figure 2.20: A Schematic Pier 2 OpenSees Model With Nodes and Elements Numbers	41
Figure 2.21: Expansion Joint at Abutment 1 and Pier 4[11].....	43
Figure 2.22: Expansion Joint at Abutment 2[11].....	43
Figure 2.23: Abutment 1 Model.....	44
Figure 2.24: Schematic of Piers 4, 2 and 6 OpenSees Model.....	45
Figure 2.25: Landers Station Longitudinal Displacement Time History Applied to the Bottom of Piers 2, 3, 5 and 6 .....	46
Figure 2.26: Landers Station Longitudinal Displacement Time History Applied at the Abutments .....	47
Figure 2.27: Schematic of the OpenSees Washington Street Overpass Model .....	48
Figure 3.1: General Pier Model in OpenSees .....	52
Figure 3.2: Bending moment Vs. Deflection of Element 3 of Pier 2 .....	53
Figure 3.3: Bending moment Vs. Deflection of Element 3 of Pier 4 .....	53
Figure 3.4: Relative Displacement of Abutment1 and Bridge Deck .....	56
Figure 3.5: Bending Moment in Element 3, Pier 2.....	57
Figure 3.6: Shear in Element 3, Pier 2.....	57
Figure 3.7: Bending Moment in Element 3, Pier 4.....	58
Figure 3.8: Shear in Element 3, Pier 4.....	58
Figure 3.9: Bending Moment in Element 3, Pier 6.....	59
Figure 3.10: Shear in Element 3, Pier 6.....	59
Figure 3.11: Relative Displacement of Top and Bottom of Element 3, Pier 2 .....	61

Figure 3.12: Relative Displacement of Top and Bottom of Element 3, Pier 4 .....	61
Figure 3.13: Relative Displacement of Top and Bottom of Element 3, Pier 6 .....	62
Figure 3.14: Shear Force in Guide Angles, Pier 2 .....	65
Figure 3.15: Shear Force in Key Plates, Pier 3 .....	65
Figure 3.16: Shear Force in Guide Angles, Pier 4 .....	66
Figure 3.17: Shear Force in Key Plates, Pier 5 .....	66
Figure 3.18: Shear Force in Guide Angles, Pier 6 .....	67
Figure 3.19: Relative Displacement of Abutment 1 and Bridge Deck, Z-direction .....	68
Figure 3.20: Total Displacement of the Deck and the Relative Displacement of Deck and Top of the Pier 2, Z-Direction.....	68
Figure 3.21: Total Displacement of the Deck and the Relative Displacement of Deck and Top of the Pier 4, Z-Direction.....	69
Figure 3.22: Total Displacement of the Deck and the Relative Displacement of Deck and Top of the Pier 6, Z-Direction.....	69
Figure 3.23: Relative Displacement of Abutment 1 and Bridge Deck, X-Direction .....	70
Figure 3.24: Relative Displacement of the Deck to the Top of Pier 4, X-Direction .....	71
Figure 3.25: Relative Displacement at Abutment 1, Z-direction, for a Total of 80 Seconds .....	72
Figure 3.26: Sensitivity of Bending Moment to Compressive Strength of Concrete .....	74
Figure 3.27: Sensitivity of Shear Force to Compressive Strength of Concrete .....	74
Figure 3.28: Sensitivity of Displacement to Compressive Strength of Concrete .....	75
Figure 3.29: Sensitivity of Bending Moment to Coefficient of Friction of Contact Element .....	75
Figure 3.30: Sensitivity of Shear Force to Coefficient of Friction of Contact Elements..	76
Figure 3.31: Sensitivity of Displacement to Coefficient of Friction of Contact Elements	76
Figure 3.32: Sensitivity of Bending Moment to Damping Constant .....	77
Figure 3.33: Sensitivity of Shear Force to Damping Constant .....	77
Figure 3.34: Sensitivity of Displacement to Damping Constant .....	78

## List of Tables

Table 2.1: Partitions for Seismic Design Categories (AASHTO Table 3.5-1[1]) .....	14
Table 2.2: Site Class Definitions [1, 19].....	15
Table 2.3 : Regular Bridge Requirements [1].....	19
Table 2.4: Element Concrete Properties for 3000 psi 28- day Compressive Strength [19] .....	33
Table 2.5: Input Parameters for Reinforcing Steel [19].....	35
Table 2.6: PlanView of Neoprene Bearings on Pier 3 [11] .....	36
Table 2.7: Weight of Piers [19].....	40
Table 2.8: Input Parameters Values Used for the Sensitivity Analysis .....	49
Table 3.1: Bending Moment and Yield Displacement, Using Pushover Analysis .....	54
Table 3.2: Demand to Capacity Ratio of Bending Moment, Shear Force and Displacement of Element 3 of Piers.....	62
Table 3.3: Comparison of Bending Moment Demand (Kip-in.) to Capacity Ratio of Elements 2 and 3 of Piers 2, 4 and 6 of Bridge Model With and Without Contact Element (CE) .....	63
Table 3.4: Comparison of Shear Force (Kip) Demand to Capacity Ratio of Elements 2 and 3 of Piers 2, 4 and 6 of Bridge Model With and Without Contact Element (CE).....	64
Table 3.5: Comparison of Displacement Ductility of element 2 and 3 of Piers 2, 4, and 6 of Bridge Model With and Without Contact Element .....	64

# Improved Modeling and Sensitivity Analysis of Seismic Behavior of Washington Street Overpass in Montpelier, Idaho

Thesis Abstract - Idaho State University - 2014

The Washington Street Overpass in Montpelier, Idaho, was built in 1971 prior to the major changes in seismic design code. The bridge is located in a seismically active region of the state of Idaho. A project entitled “Seismic Analysis of US-89 Overpass at Union Pacific Railroad in Montpelier, Idaho” was conducted by Andrea Miller. In that project, OpenSees software was used for developing an analytical three-dimensional finite element bridge model and the procedure specified in the AASHTO *Guide Specifications for LRFD Seismic Bridge Design* (2009) was used to analyze the response of the bridge. It was concluded that the bridge may not collapse due to a 1033-year mean recurrence interval event, but horizontal restrainer guide angles and key plates are likely to fail.

In the present study, the bridge expansion joints were modeled with contact elements. Gaps were created in the joints to allow for pounding effects. Seismic analysis of the bridge model was performed using the improved bridge model. It was concluded that the bridge may not collapse from the forces induced due to an earthquake event of 1,033 years return period (7% probability of exceedence in 75 years). However guide angles may fail leaving key plates and neoprene bearings as only the lateral movement restrainers. To evaluate the extent of the earthquake damage, all the guide angles and key plates were removed and another analysis was performed. Removal of the restrainers allowed the superstructure to move freely on the substructure, but failed to unseat the superstructure. The response of the improved bridge model was compared to the first

phase of the project. It was observed that the contact elements and gaps did not have significant influence on the bridge seismic response.

Sensitivity analysis of the bridge response to compressive strength of concrete, coefficient of friction of contact element and damping constant were performed using the improved OpenSees bridge model. From the analysis it is concluded that the damping constant affects the bridge response the most.

# CHAPTER 1

## INTRODUCTION

### 1.1 Project Background

The *American Association of State Highway Officials (AASHO) 1958 Standard Specifications for Highway bridges* specified the requirements of considering seismic loading in the design of highway bridges in the United States which remained unchanged for more than 15 years [5]. Extensive damages of a significant number of bridges in San Fernando (California) earthquake of 1971 revealed existence of deficiencies in the bridge seismic design code of that time. The bridge design code prior to 1974 did not account for fault proximity, site conditions, dynamic structural response and ductile details for reinforced concrete construction [26].

Following the 1994 Northridge earthquake, various research studies have been conducted to improve the design code and significant changes were made. However the bridges built in and prior to 1971 are still serving as important structure to the transportation system today. Washington Street Overpass in Montpelier, Idaho is one of those highway bridges constructed in 1971 and is located in a seismically active region. Geological studies show active faults are located near the bridge and movement on the faults can cause earthquakes of magnitude 6.5 to 7.5. Disruption of this bridge can result in a large economic loss to the state of Idaho, since the bridge serves as one of the two routes to access Montpelier and it crosses Union Pacific Railroad (UPRR). The railroad is one of the vital ways of transporting goods for the area. It also serves as a primary route for emergency vehicles, so the bridge should be usable soon after a major earthquake

event. Figure 1.1 shows the location of bridges, faults, and earthquakes in Idaho as of 2007.

A project “Seismic Analysis of US-89 Overpass at Union Pacific Railroad in Montpelier, Idaho” was conducted by Andrea Miller in which she developed a three-dimensional finite element model of the bridge in the Pacific Earthquake Engineering Research (PEER) Center Open System for Earthquake Engineering Simulation (OpenSees) software. Information from the Idaho Transportation Department (ITD) and OpenSees manual were used for modeling the bridge. AASHTO *Guide Specifications for LRFD Seismic Bridge Design* (2009) was used to analyze the bridge which included pushover and nonlinear time history analyses. The project concluded that restrainers such as guide angles and key plates will fail under a 1,033-year seismic event (7% probability of exceedence in 75 years), but the forces and moment induced during the earthquakes are not enough to fail the substructure. In addition, the displacements resulted from the earthquakes did not unseat the bridge superstructure from the piers. However, Miller did not have enough time to properly model the expansion joints. Therefore, the project herein presents an improved OpenSees bridge model using contact elements for expansion joints. In addition, a sensitivity analysis is performed to evaluate the bridge response to changes in selected material properties.

# Earthquake in State of Idaho, USA

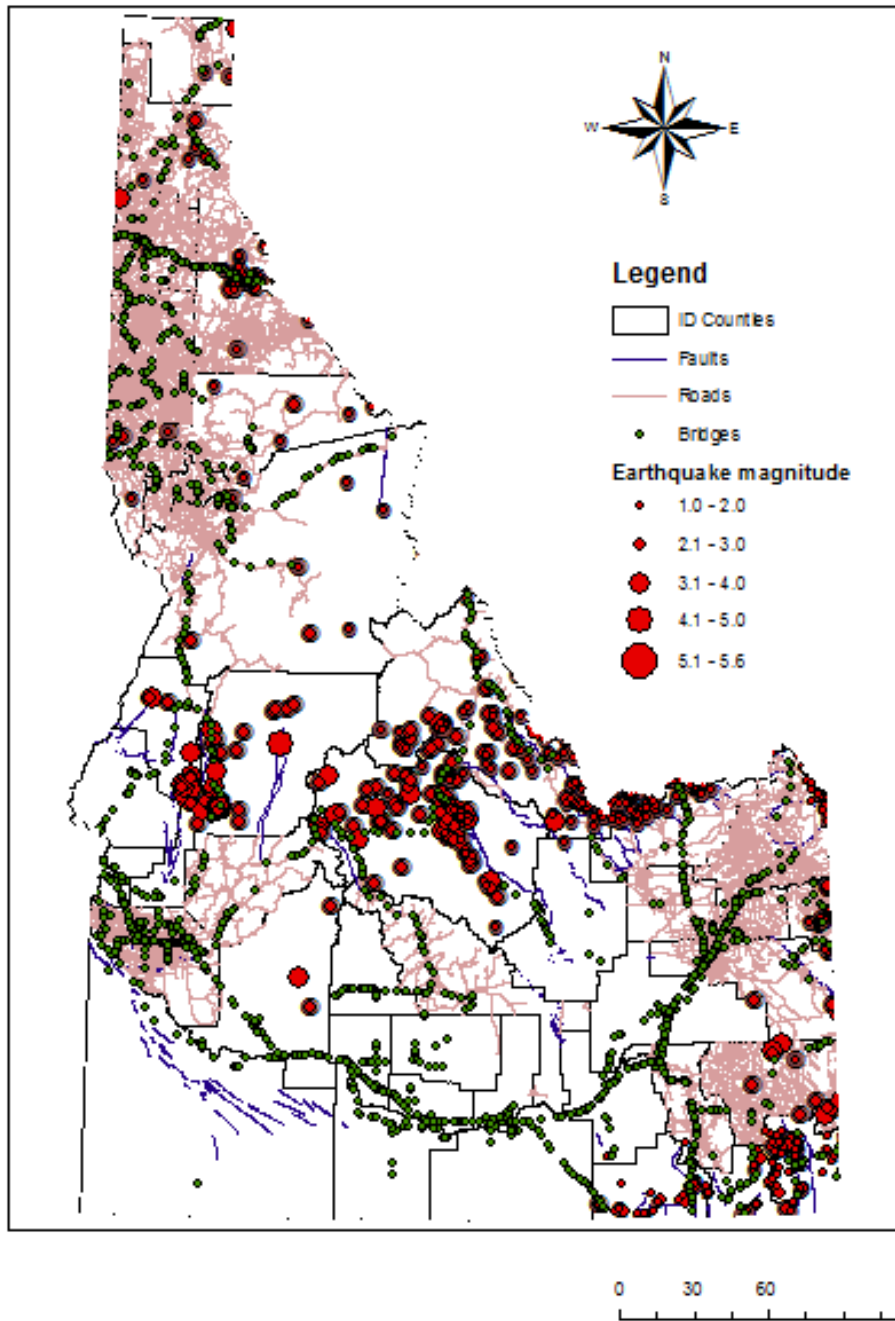


Figure 1.1: Earthquake in State of Idaho as of 2007

## 1.2 Literature Review

Past earthquakes, particularly the 1989 Loma Prieta and 1994 Northridge caused severe damages to a considerable number of major bridges that were designed with consideration of seismic forces. This remarkably increased the discussion about the seismic design of new bridges and retrofit of existing bridges that was initiated following the 1971 San Fernando earthquake [20]. Lessons learned from the damage experienced were seriously taken into consideration for further research work on seismic analysis of bridges.

Various methods have been developed and used by researchers to determine the seismic demand of highway bridges. Seismic demand of bridges can be determined by linear and nonlinear methods. Some of the procedures to determine the seismic demand of structure include linear static, linear dynamic, nonlinear static, and nonlinear dynamic [24]. Nonlinear analysis is sophisticated and produces much more realistic results than linear analysis under strong seismic ground motions [15]. A bridge-foundation-soil system may include material, geometrical and boundary nonlinearities. Consideration of these nonlinear behaviors for bridge seismic analysis gives realistic response.

Experimental and analytical approaches have been used worldwide for seismic analysis of bridges. However due to the challenge of creating a prototype bridge model and with the advent of high speed computers, analytical approach has been popular for the last few decades. Several computer software packages are available to determine the seismic demand of a structure. SEISBA, SAP 2000, WFRAME, ADINA, STRUDL, SC-Push3D, ABAQUS, LS-DYNA, ANSR-I, SEISAB, and OpenSees are some of the most reliable computer software used for analytical study [24, 28].

With the use of advanced computer software, it is found that the abutment response considerably influences the overall response of short to medium length bridges. An OpenSees bridge model was developed to conduct sensitivity analysis on how bridge abutment model affects the overall seismic demand of bridge with varying abutment characteristics [16]. ABAQUS software was used to model and study the nonlinear soil-pile interaction [24]. A 3D nonlinear finite element model of the girder-abutment connection was developed using the computer program ADINA (2008) [24]. The OpenSees software has been widely used because of its easy accessibility and capability of modeling and analyzing the nonlinear response of structural and geotechnical systems. Availability of a wide range of material models, variety of elements, and solution algorithms allows the OpenSees users to develop models with higher accuracy [25].

### **1.3 Objectives and Scopes**

The 40 years old highway bridge was constructed according to the 1969 AASHTO specifications which does not meet the current seismic bridge design. Hence the major objectives of the project are to perform the seismic analysis and study the behavior of the nonlinear response of the bridge following guidelines provided in the AASHTO *Guide Specifications for LRFD Seismic Bridge Design* (2009). The major objectives can be achieved by performing the following:

- Improve the OpenSees bridge model developed for the first phase of the project by simulating the abutment-deck interaction and the interaction between the adjacent deck segments using contact elements.
- Provide the boundary nonlinearity to the bridge model by creating gaps between the deck segments and between the deck and the abutment.

- Compare the nonlinear response from the improved bridge model and the bridge model developed in the first phase of the project when subjected to a probable earthquake event.
- Perform sensitivity analysis of the bridge response due to changes in selected parameters. The selected parameters for the study are compressive strength of the concrete, coefficient of friction of contact element and the bridge damping constant.
- Determine the parameter that influences the seismic response of the bridge the most.

#### **1.4 Outline of the Thesis**

This thesis is composed of five chapters. The first chapter describes the project statement, literature review, objectives and scopes. Chapter 2 covers the methodologies used for performing seismic analysis of the bridge and parametric sensitivity analysis of the bridge response to the considered earthquake loading. This includes the procedure for bridge seismic analysis using the guidelines provided in *AASHTO Guide specifications for LRFD Seismic Bridge Design (2009)*, modeling a three-dimensional finite element bridge model using OpenSees software and procedure for sensitivity analysis. Chapter 3 presents the result. This includes the results for evaluation of the bridge seismic performance and the study of the behavior of the nonlinear response of the bridge using the improved bridge model. The results obtained are then compared to the response of the previous bridge model when subjected to the same earthquake loading. Chapter 3 also includes the results from a sensitivity analysis. Chapter 4 contains the discussion of the results obtained for seismic analysis of the bridge and

sensitivity analysis. Chapter 5 contains the conclusions and recommendations for future work.

## CHAPTER 2

### METHODS

This chapter describes the methods used for seismic analysis of the Washington Street Overpass and the determination of the selected input parameters that influence the bridge nonlinear response to a probable earthquake. The methods include the use of *AASHTO Guide specifications for LRFD Seismic Bridge Design*, procedure for seismic analysis of the bridge, modeling of the bridge using OpenSees software and the procedure for the sensitivity analysis of the bridge response to an earthquake event. Following are the methodology overview.

- Visit the site and study the structural plans of the bridge
- Perform seismic risk assessment according to the information obtained
- Select the seismic analysis procedure
- Develop an analytical bridge model using an appropriate structural software as required by the seismic analysis procedure
- Generate the ground motion inputs as required by the procedure and software used for developing an analytical bridge model
- Analyze the bridge response following the procedure selected
- Perform sensitivity analysis of the bridge response by varying the values of the selected input parameters

The methods mentioned above are described in detail in the succeeding sections.

## 2.1 Washington Street Overpass Description

The steel and concrete Washington Street Overpass built in 1971 is located over Union Pacific Railroad (UPRR) and 12<sup>th</sup> street in Montpelier, Idaho. Figure 2.1 and 2.2 shows the elevation view of the bridge and its components. Figure 2.3 shows the plan and elevation view of the bridge. The bridge was constructed with the structural design in accordance with 1969 AASHO specifications. The 720 feet long bridge is composed of five reinforced concrete piers, deep pile foundations, reinforced concrete superstructure with two steel box girders, steel key plates, steel guide angles, neoprene bearings, two abutments and three expansion joints. Two of the expansion joints are located at the abutments and one at the middle pier.

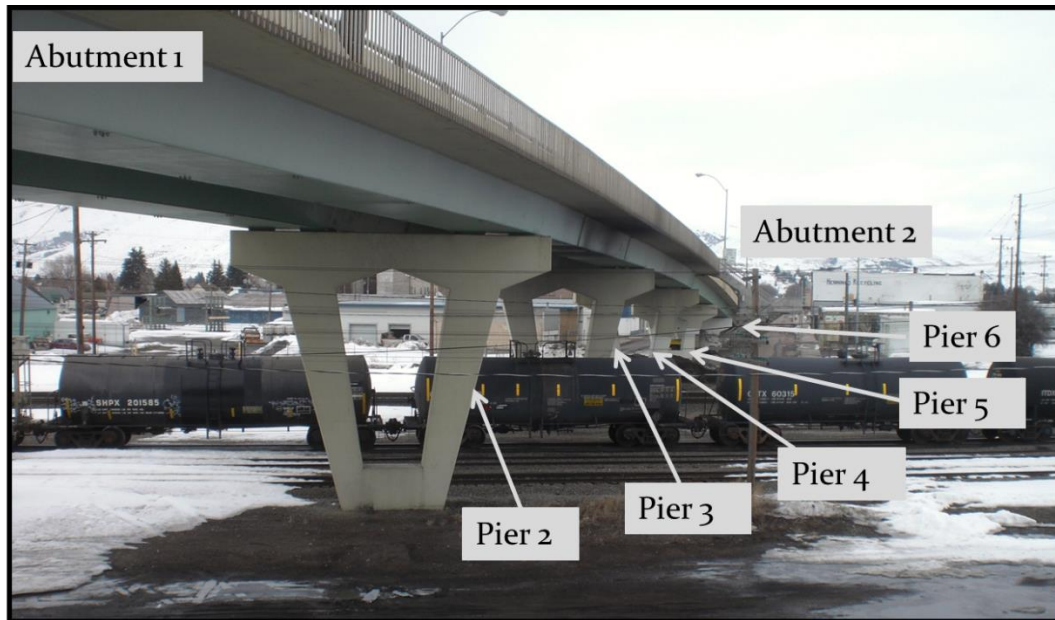


**Figure 2.1: Washington Street Overpass Showing Substructure Components [18]**

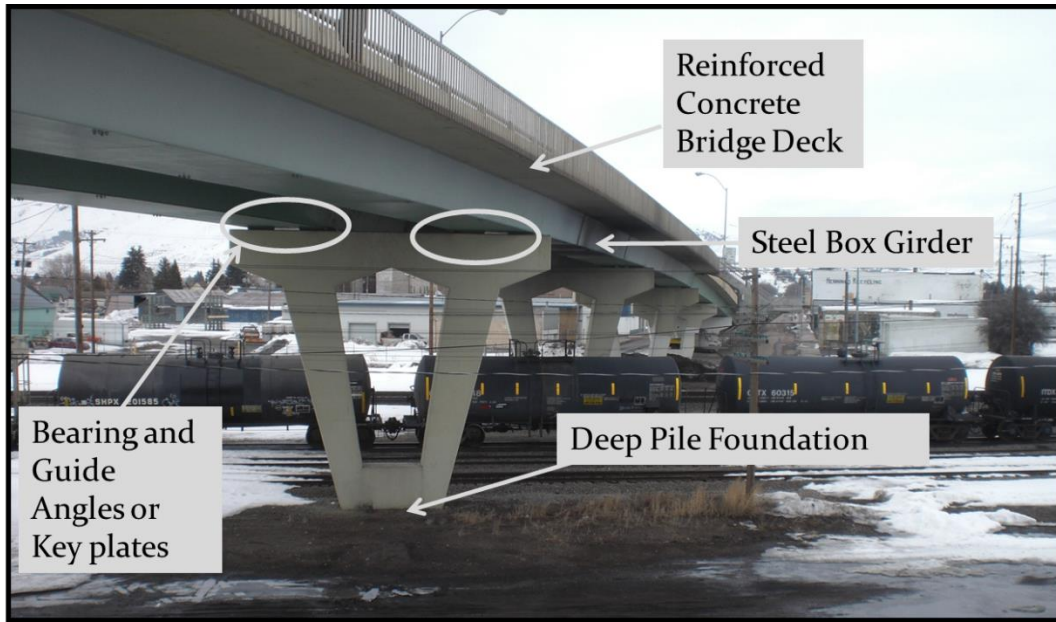


**Figure 2.2: Washington Street Overpass Showing Superstructure Components [18]**

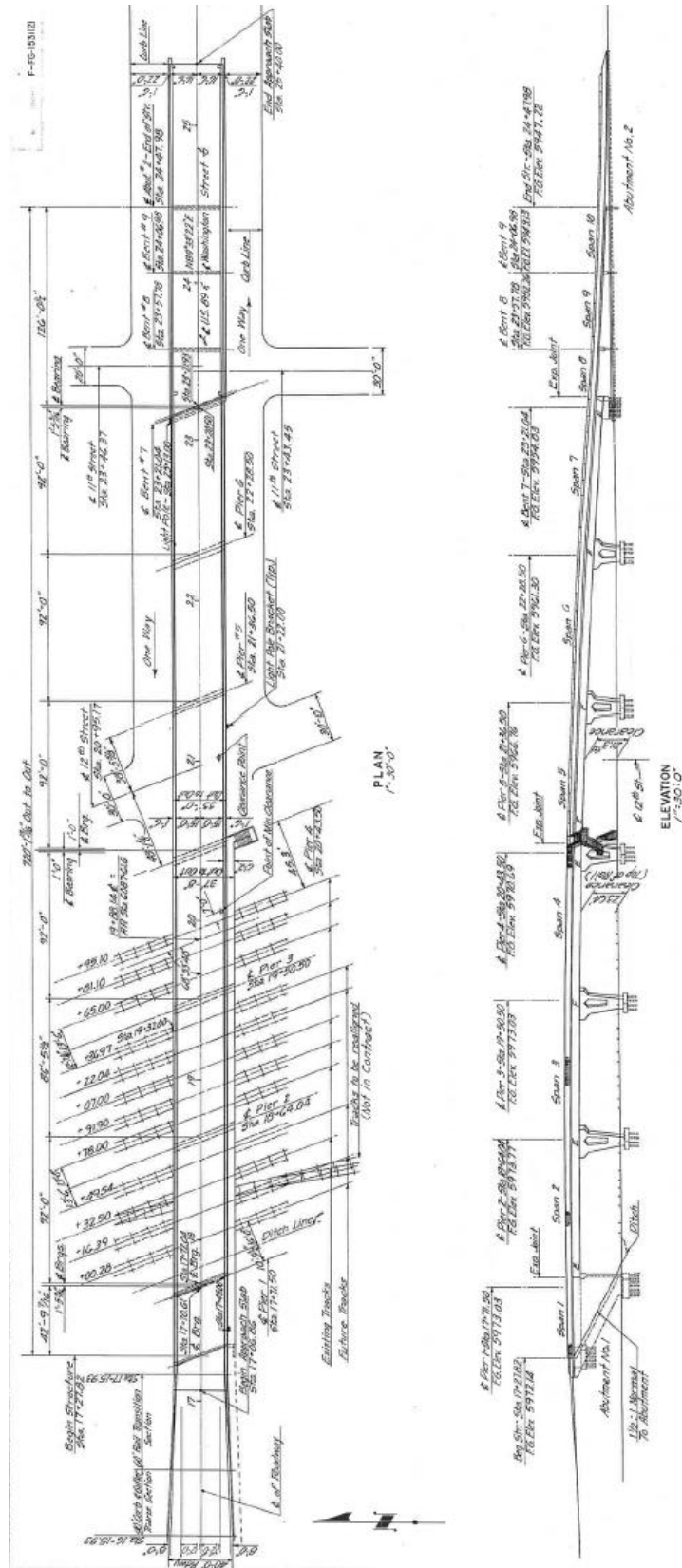


Figure 2.3: Plan and Elevation View of the Washington Street Overpass [11, 19]

## **2.2 AASHTO Guide Specifications for LRFD Seismic Bridge Design**

The AASHTO *Guide Specifications for LRFD Seismic Bridge Design* (2009) covers seismic analysis and design for typical bridge types [1]. It incorporates recent best practices and research results providing significantly improved seismic design approach. It provides detailed guidelines for selecting the appropriate procedure for seismic analysis of a bridge based on Seismic Design Category (SDC) and the required analysis procedures. It also provides guidance on developing an appropriate analytical bridge model.

### **2.2.1 Background**

As a consequence of severe damages of significant number of bridges in 1971 San Fernando earthquake, efforts were made to improve the seismic design of bridges. These efforts resulted in developing the ATC-6, *Seismic Design Guidelines for Highway Bridges* which was published in 1981. The ATC-6 was adopted by AASHTO as a Guide Specifications in 1983 [1]. Later in 1991 the guidelines were adopted into the *Standard Specifications for Highway Bridges* which was revised and reformatted to develop Division I-A. AASHTO LRFD *Bridge Design Specifications* included Division I-A as the basis for the seismic provisions.

Extensive research was conducted to improve the bridge seismic design further after damaging earthquakes in 1980s and 1990s. The efforts resulted in (a) publication of ATC-32, *Improved Seismic Design Criteria for California Bridges: Provisional Recommendations* in 1996; (b) the development of Caltrans' *Seismic Design Criteria*; (c) publication of MCEER/ATC-49 (NCHRP 12-49), *Recommended LRFD Guidelines for the Seismic Design of Highway Bridges* in 2003; and (d) the development of the South

Carolina *Seismic Design Specifications* in 2001. From the four publications the best practices were combined to form a single new seismic design specification for AASHTO. The new guide specifications contained the displacement based principles which were modified in 2008.

The new approach is divided into a simplified displacement check procedure and a pushover assessment of displacement capacity. These specifications provide the selection of procedure to use according to the seismic design categories and it could be used on a national level. Key features of the guide specifications are seven percent in 75 year design event for development of a design spectrum, use of NEHRP Site Classification, sufficient conservatism (1.5 safety factors) for minimum support length requirement and establish four Seismic Design Categories (SDCs) [1].

The requirement of 1.5 safety factor for minimum support length is necessary to provide a high level of safety against the superstructure being unseated at the abutments or expansion joints during the maximum considered earthquake. The use of 1.5 safety factor for minimum support length maximizes the chances of forming inelastic deformation in columns which can be readily inspected and repaired after an earthquake event. A shake table test was performed at the university of Nevada, Reno to evaluate the performance of a bridge model which was constructed using the *AASHTO Guide Specifications for LRFD Seismic Bridge Design* (2009) [27]. The project concluded that the overall objective of the seismic design of the bridge model was obtained.

### **2.2.2 Seismic Risk Assessment**

According to the *AASHTO Guide Specifications for LRFD Seismic Bridge Design*, selection of procedure to analyze seismic behavior of a bridge is based on

Seismic Design Categories (SDC's). The design categories are divided into four SDC ranging from A to D based on the 1-sec period design spectral acceleration for the design earthquake. Table 2.1 was used to determine the SDC of the bridge site. This requires the Site Class for the local soil conditions. Table 2.2 is used to define the site class. This method divides the site class on the basis of average shear wave velocity, average standard penetration test blow count, average undrained shear strength, plasticity index, and moisture content for the upper 100 feet of the soil profile. However for the Washington Street Overpass, limited soils investigation was performed. The soils investigation consisted of 12 test holes ranging from 30 feet to 55 feet deep with an average standard penetration test blow count ( $\bar{N}$ ) of 8.6 blows/foot (19). Using the average blow count value and Table 2.2, this site falls under site class E.

**Table 2.1: Partitions for Seismic Design Categories (AASHTO Table 3.5-1[1])**

<b>Value of <math>S_{DI} = F_v S_I</math></b>	<b>SDC</b>
$S_{DI} < 0.15$	<b>A</b>
$0.15 \leq S_{DI} < 0.30$	<b>B</b>
$0.30 \leq S_{DI} < 0.50$	<b>C</b>
$0.50 \leq S_{DI}$	<b>D</b>

To determine the SDC, the next step is to find the design response spectrum coefficients. The acceleration coefficients are determined using the United States Geologic Survey (USGS) Seismic Design Parameter software. The latitude and longitude of the site is used to obtain the accurate values of the required coefficients for Site Class B.

**Table 2.2: Site Class Definitions [1, 19]**

Site Class	Soil Type and Profile
A	Hard rock with measured shear wave velocity, $\bar{v}_s > 5000$ ft/sec
B	Rock with $2500$ ft/sec $< \bar{v}_s < 5000$ ft/sec
C	Very dense soil and soil rock with $1200$ ft/sec $< \bar{v}_s < 2500$ ft/sec, or with either $\bar{N} > 50$ blows/ft or $\bar{s}_y > 2.0$ ksf
D	Stiff soil with $600$ ft/sec $< \bar{v}_s < 1200$ ft/sec, or with either $15$ blows/ft $< \bar{N} < 50$ blows/ft or $1.0$ ksf $< \bar{s}_y < 2.0$ ksf
E	Soil profile with $\bar{v}_s < 600$ ft/sec, or with either $\bar{N} < 15$ blows/ft or $\bar{s}_y < 1.0$ ksf, or any profile with more than $10$ ft of soft clay defined as soil with $PI > 20$ , $w > 40\%$ , and $\bar{s}_y < 0.5$ ksf
F	Soils requiring site-specific ground motion response evaluations, such as: <ul style="list-style-type: none"> <li>• Peats or highly organic clays (<math>H &gt; 10</math> ft of peat or highly organic clay, where <math>H</math> = thickness of soil)</li> <li>• Very high plasticity clays (<math>H &gt; 25</math> ft with <math>PI &gt; 75</math>)</li> <li>• Very thick soft/medium stiff clays (<math>H &gt; 120</math> ft)</li> </ul>
<p>Exceptions:</p> <p>Where the soil properties are not known in sufficient detail to determine the site class, a site investigation shall be undertaken sufficient to determine the site class. Site Class E or F should not be assumed unless the authority having jurisdiction determines that Site Class E or F could be present at the site or in the event that Site Class E or F is established by geotechnical data.</p> <p>where:</p> <p><math>\bar{v}_s</math> = average shear wave velocity for the upper 100 ft of the soil profile as defined in <a href="#">Article 3.4.2.2</a></p> <p><math>\bar{N}</math> = average standard penetration test (SPT) blow count (blows/ft) (ASTM D 1586) for the upper 100 ft of the soil profile as defined in <a href="#">Article 3.4.2.2</a></p> <p><math>\bar{s}_y</math> = average undrained shear strength in ksf (ASTM D 2166 or D 2850) for the upper 100 ft of the soil profile as defined in <a href="#">Article 3.4.2.2</a></p> <p><math>PI</math> = plasticity index (ASTM D 4318)</p> <p><math>w</math> = moisture content (ASTM D 2216)</p>	

The following are the acceleration coefficients for Site Class B:

$$PGA = 0.321$$

$$S_s = 0.755$$

$$S_1 = 0.256$$

Where,

PGA = Peak Ground Acceleration Coefficient on Class B Rock

$S_s$  = 0.2-sec Period Spectral Acceleration Coefficient on Class B Rock

$S_1$  = 1.0-sec Period Spectral Acceleration Coefficient on Class B Rock

The acceleration coefficients for the Site Class B rock have to be scaled to the Site Class E. Hence the following site amplification coefficients are found from the USGS.

$$F_{pga} = 1.14$$

$$F_a = 1.19$$

$$F_v = 2.98$$

Where,

$F_{pga}$  = Site Coefficient for the Peak Ground Acceleration Coefficient

$F_a$  = Site Coefficient for 0.2-sec Period Spectral Acceleration

$F_v$  = Site Coefficient for 1.0-sec Period Spectral Acceleration

The response spectrum acceleration coefficients are determined using Equations 2.1, 2.2 and 2.3 which are specified in AASTHO *Guide Specifications for LRFD Seismic Bridge Design*. The values of the acceleration coefficients  $A_s$ ,  $S_{DS}$  and  $S_{D1}$  are found to be 0.366, 0.898 and 0.763 respectively.

$$A_s = F_{pga} * PGA \tag{2.1}$$

$$S_{DS} = F_a * S_s \tag{2.2}$$

$$S_{D1} = F_v * S_1 \tag{2.3}$$

Where,

$A_s$  = Effective Peak Ground Acceleration Coefficient

$S_{DS}$  = Design Earthquake Response Spectral Acceleration Coefficient at 0.2-sec Period

$S_{D1}$  = Design Earthquake Response Spectral Acceleration Coefficient at 1.0-sec Period

The design response spectrum curve is developed using the acceleration coefficients determined for the site and following Figure 2.4.

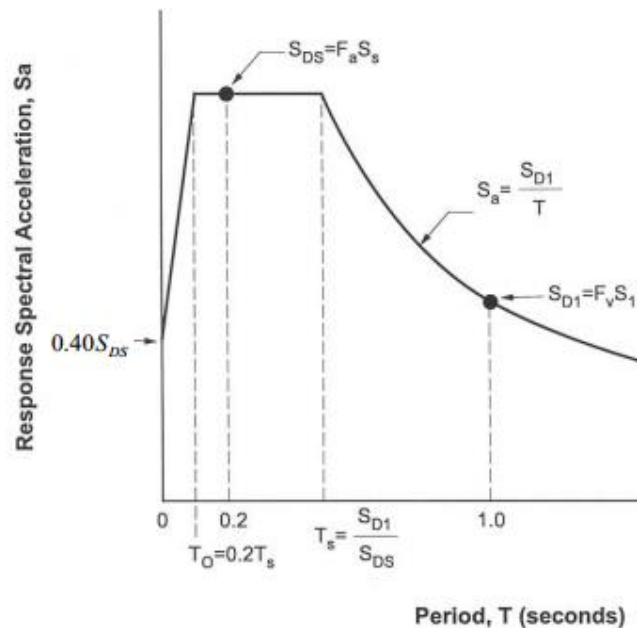


**Figure 2.4: Design Response Spectrum Curve (AASHTO Figure 3.4.1-1 [1])**

Finally, using the calculated value of  $S_{D1} = 0.763$  and Table 2.1, the Washington Street Overpass is assigned to Seismic Design Category (SDC) D. Based on the SDC assigned to the bridge and following the guidelines in the AASHTO *Guide Specifications*

for *LRFD Seismic Bridge Design*, seismic analysis procedures are selected for the bridge. The analysis procedures are described in detail in the following section.

### **2.2.3 Selection of Analysis Procedures**

The required analysis procedure for bridges assigned to each of the SDCs is described in Article 3.5 of *AASHTO Guide Specifications for LRFD Seismic Bridge Design* [1]. Figure 2.5 also outlines the procedure required for a bridge analysis based on SDC. The procedure for analyzing bridges in SDC D requires determination of displacement capacity which is then compared to the seismic displacement demand. Shear capacity of columns should also be checked. To determine the displacement capacity, an inelastic static analysis also commonly known as pushover analysis is required. However the demand analysis for a bridge depends on other factors besides SDC.

Selection of analysis procedure to determine seismic demand of a bridge is outlined in Article 4.2 of *AASHTO Guide Specifications for LRFD Seismic Bridge Design*. The recommended procedure for normal bridges in SDC D is Equivalent Static Analysis (ESA) or Elastic Dynamic Analysis (EDA) depending on the bridge's regularity. Regular bridges are defined as the bridges having fewer than seven spans, no abrupt or unusual changes in weight, stiffness, or geometry and that satisfy the requirements in Table 2.3 [1] However for essential or critical bridges within 6 miles of active faults, nonlinear time history analysis is recommended. This method is more comprehensive because it takes in account of the effect of inelastic behavior on the demand analysis.

**Table 2.3 : Regular Bridge Requirements [1]**

Parameter	Value				
	2	3	4	5	6
Maximum subtended angle (curved bridge)	90°	90°	90°	90°	90°
Maximum span length ratio from span-to-span	3	2	2	1.5	1.5
Maximum bent/pier stiffness ratio from span-to-span (excluding abutments)	-	4	4	3	2

Note: All ratios expressed in terms of the smaller value.

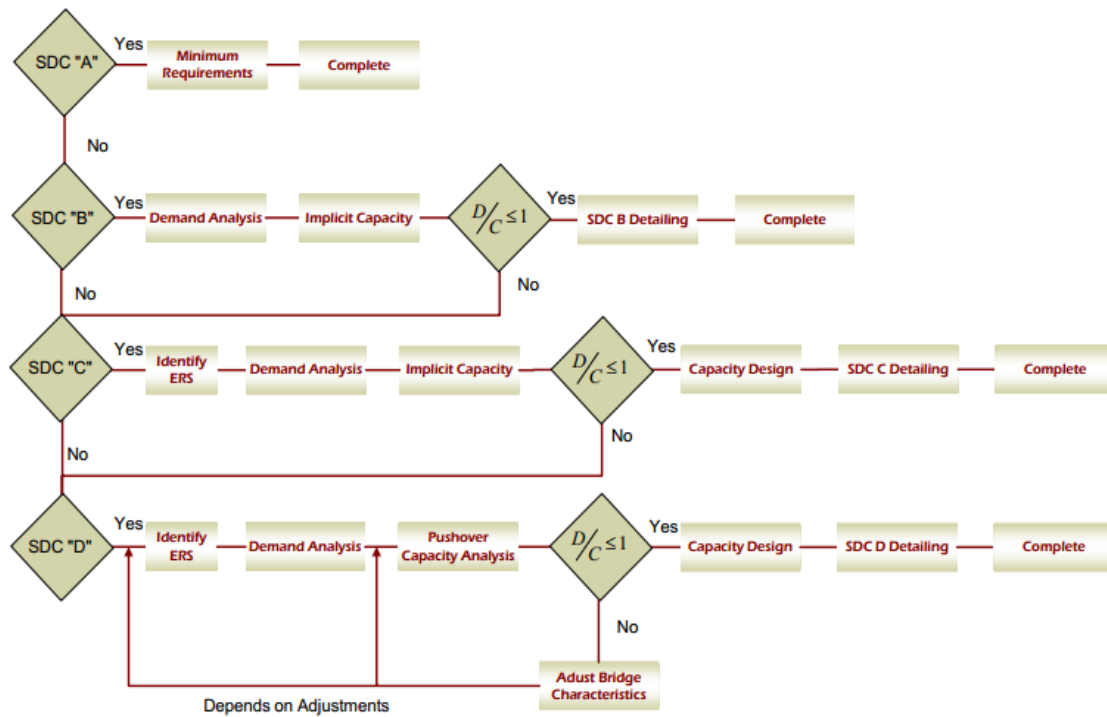


**Figure 2.5: Seismic Design Category Core Flowchart [1]**

### 2.2.3.1 Pushover Analysis

The objective of the pushover analysis is to determine the displacement capacity of an individual pier. The displacement capacity determines the displacement of a component of a pier when it reaches the inelastic deformation. The displacement capacity obtained from the analysis should be greater than displacement demand.

To perform pushover analysis of a pier, a pier is developed in OpenSees software. Detail descriptions on modeling the bridge and its components in OpenSees are provided in the later sections. An incremental lateral force is applied to the top of the pier until a target displacement is reached. The displacement at which the structure exceeds the elastic limit is defined as the displacement capacity of the pier. The elastic limit is the threshold value at which a structure cannot retain its original shape, size and position. When the elastic limit is exceeded a small increment in force forms extensive deformations. Figure 2.6 shows an example of force-displacement relationship of structure where  $d_y^*$  is the displacement capacity of a structure.

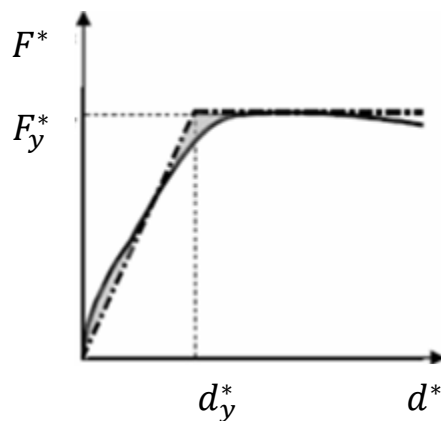


**Figure 2.6: Force-Displacement Relationship [21]**

### 2.2.3.2 Nonlinear Time History Analysis

Nonlinear time history analysis is more realistic and sophisticated procedure to analyze the seismic response of bridges. For the procedure, a set of displacement time histories is required to be applied at the base of each pier and abutments of the bridge. According to the requirements mentioned in the AASHTO *Guide Specifications for LRFD Seismic Bridge Design*, the analysis should be performed with two horizontal components and one vertical component of ground motion time histories. However, only two horizontal components of the time histories are used in this project because of the complexity in analyzing the bridge response. Difficulty in running the bridge model when subjected to all three components of an earthquake event was also one of the reasons in not using the vertical component. The model could not converge with “*NonlinearBeamColumn*” element and the OpenSees crashed. This element is used to model the reinforced concrete piers of the bridge.

As mentioned earlier, Miller performed the seismic analysis of the overpass by applying four different sets of displacement time histories which were scaled to the bridge site response spectrum. They were Landers, Borah, Lamont and Duzce displacement time histories. Out of the four displacement time histories, Landers earthquake loading had the largest values for displacement, internal shear force and bending moment. According to Dr. Robert Spears, professional from Idaho National Laboratory, the landers earthquake also matched better with the site response spectrum [19]. Considering the two reasons mentioned, displacement time histories for Landers station are used for this project.

Idaho National Laboratory (INL) assisted in obtaining the displacement time histories. The first step in obtaining the time histories was to define a design response spectrum for the site of the overpass. As shown in Figure 2.4, the input required to generate the design response spectrum were the design spectral acceleration coefficients at 1.0 second period ( $S_{D1}$ ), design spectral acceleration coefficients at 0.2 second period ( $S_{DS}$ ) and the long-period transition period ( $T_L$ ). The calculations and procedure required to obtain the design spectral acceleration coefficients are provided in Section 2.2.2 and maps in ASCE 7-05 [2] is used to find the long-period transition period.

The second step was to find the “seed” time histories with the similar site effects, attenuation and source of the location of the overpass. The Pacific Earthquake Engineering Research (PEER) Center database was used to find the seed time histories [20]. The time histories for Landers station (Landers, Lucern 1992 earthquake) was one of the selected seed time histories. The selected seed response spectrum was then modified by Dr. Spears of INL to match the overpass site response spectrum [23]. Figure 2.7 shows the modified design response spectrum from the seed response spectrum. The figure also shows the values of  $S_{D1}$ ,  $S_{DS}$  and the fundamental natural frequency of the bridge,  $f_n$ .

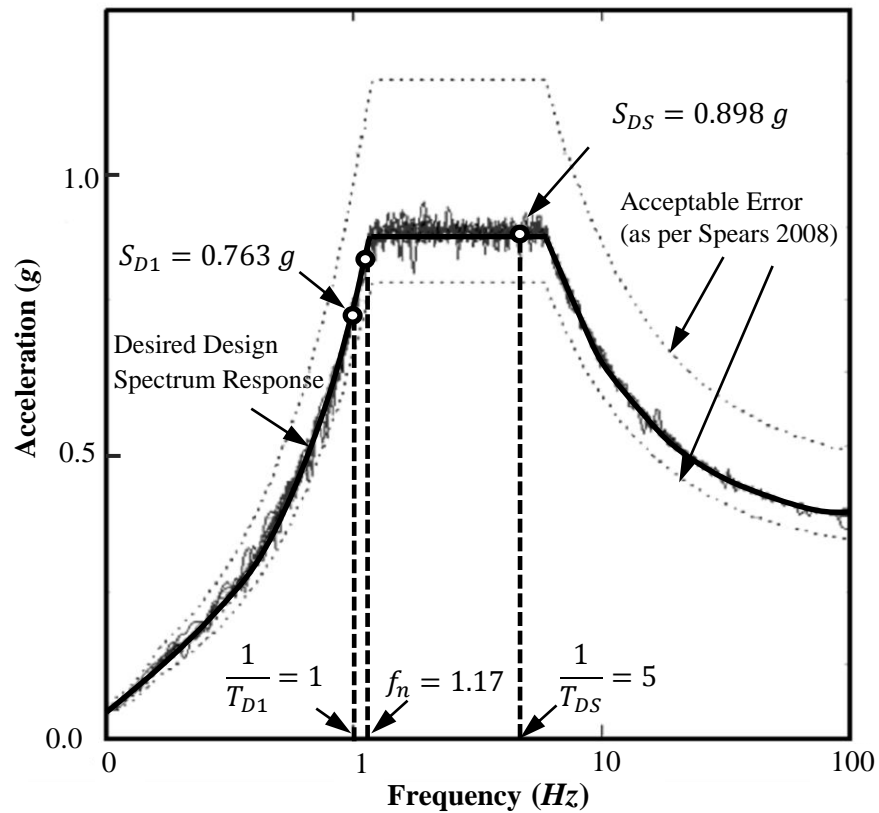


**Figure 2.7: Modification of Seed Response Spectrum to Design Response Spectrum [ 18, 23]**

OpenSees requires the ground excitation inputs as displacement time histories. Therefore, the acceleration time histories scaled to the overpass site response spectrum were integrated to obtain the displacement time histories by using the Trapezoidal Rule. Figures 2.8 and 2.9 show the longitudinal and transverse displacement time histories for Landers station, respectively.

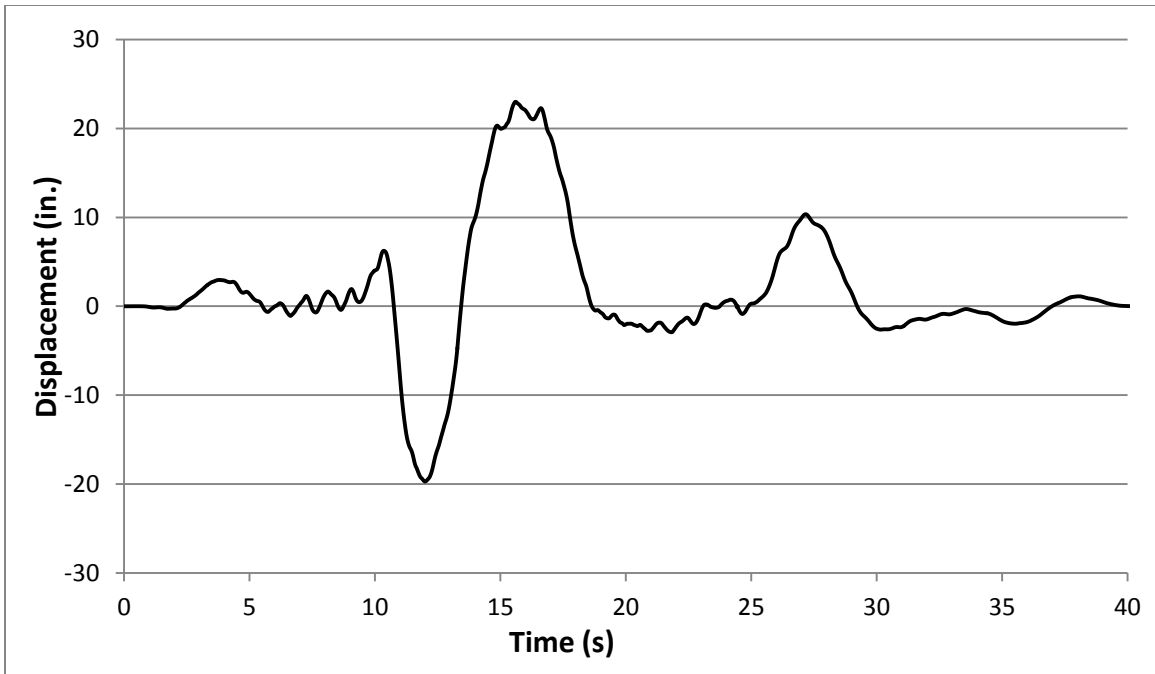


**Figure 2.8: Landers Station Horizontal (Longitudinal) Displacement Time History**

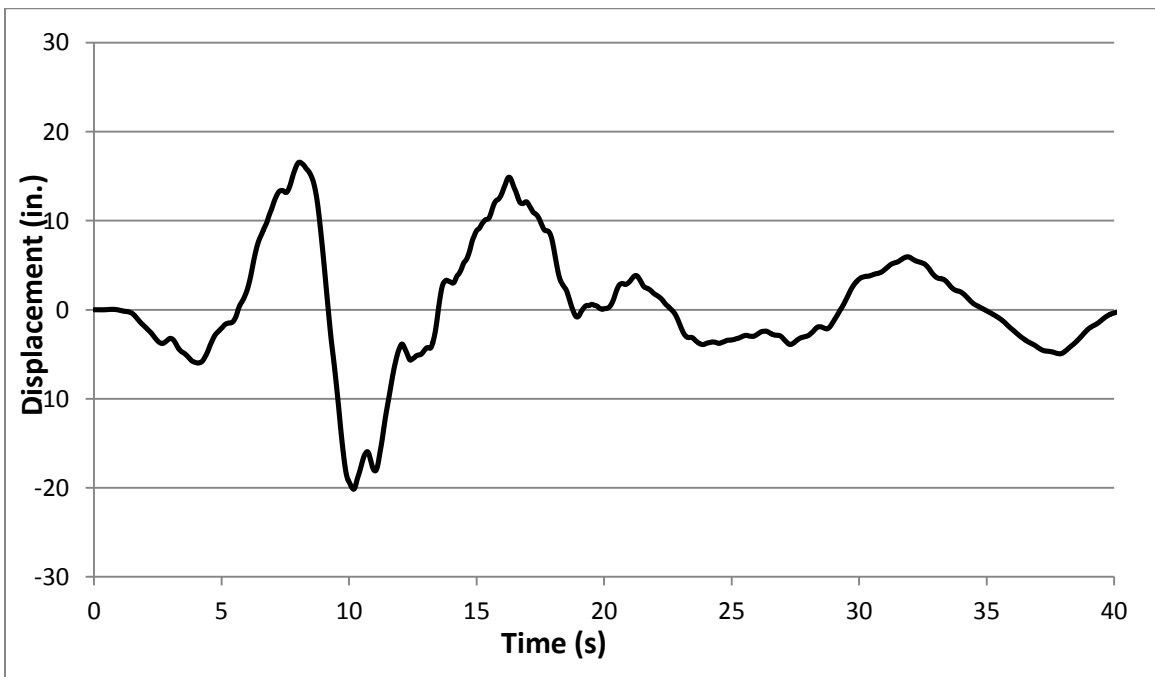


**Figure 2.9: Landers Station Horizontal (Transverse) Displacement Time History**

### **2.3 Modeling in OpenSees**

The OpenSees object-oriented finite element software is used for modeling the overpass. This finite element based software has been widely used in earthquake engineering. The open source software was developed at University of California, Berkeley at the Pacific Earthquake Engineering Research (PEER) Center for performance-based earthquake engineering analysis. The advanced software is capable of simulating the nonlinear behavior of structural and geotechnical systems. OpenSees uses Tcl programming language which enables users to program models without learning the complex computer language. It is a community-based software which allows the users and researchers to include their efforts in improving the software.

Modeling in OpenSees requires codes defining each element of the structure and their respective materials. The OpenSees library has a wide range of material models and elements. This enables users to obtain a realistic and more accurate structural response.

The following sections provide detailed descriptions of modeling of the bridge elements in OpenSees. The bridge model consists of reinforced concrete decks with two box girders, five reinforced concrete piers, abutments, deep pile foundations, steel guide angles, steel key plates, neoprene bearings and expansion joints. The interaction of each of the components with its adjacent components affects the global response of the bridge. To obtain more accuracy in the bridge seismic response, appropriate OpenSees elements have been selected.

To develop a bridge model in OpenSees, it is necessary to set up global and local coordinate systems. The Global coordinate system is used for creating nodes of each elements of the bridge and each element has its own local coordinate system. Global X-

axis is set along the length of the bridge and right hand rule is used to fix the other two axes. The global Y-axis is along the height of the bridge and Z-axis is the remaining axis. Origin of the axis is set towards the Abutment 1 and bottom of the Pier 2. Local X-axis is along the length of the element or the line connecting the two nodes of the element. Geometric-transformation command was used to construct geometric transformation object [25]. Dimension of each elements were used to create the nodes.

Actual geometry or smaller dimension of each component has been taken in consideration while preserving the shape of overall bridge. Verifications have been performed to ensure the proper usage of OpenSees elements used. Detail methods, calculations and verifications performed for modeling the bridge in OpenSees has been provided in Miller's thesis [19].

### **2.3.1 Pier Modeling**

The bridge superstructure is supported by two abutments and five reinforced concrete piers. A typical pier is divided into four elements as shown in Figure 2.10. Figure 2.2 and 2.3 also show the bridge piers. The pile cap acts as a foundation, so the element is excluded from pier. To be conservative smallest cross section dimension of each element is selected to represent the element model except Element 4. For Element 4, the average value of the smallest and largest dimensions was considered.

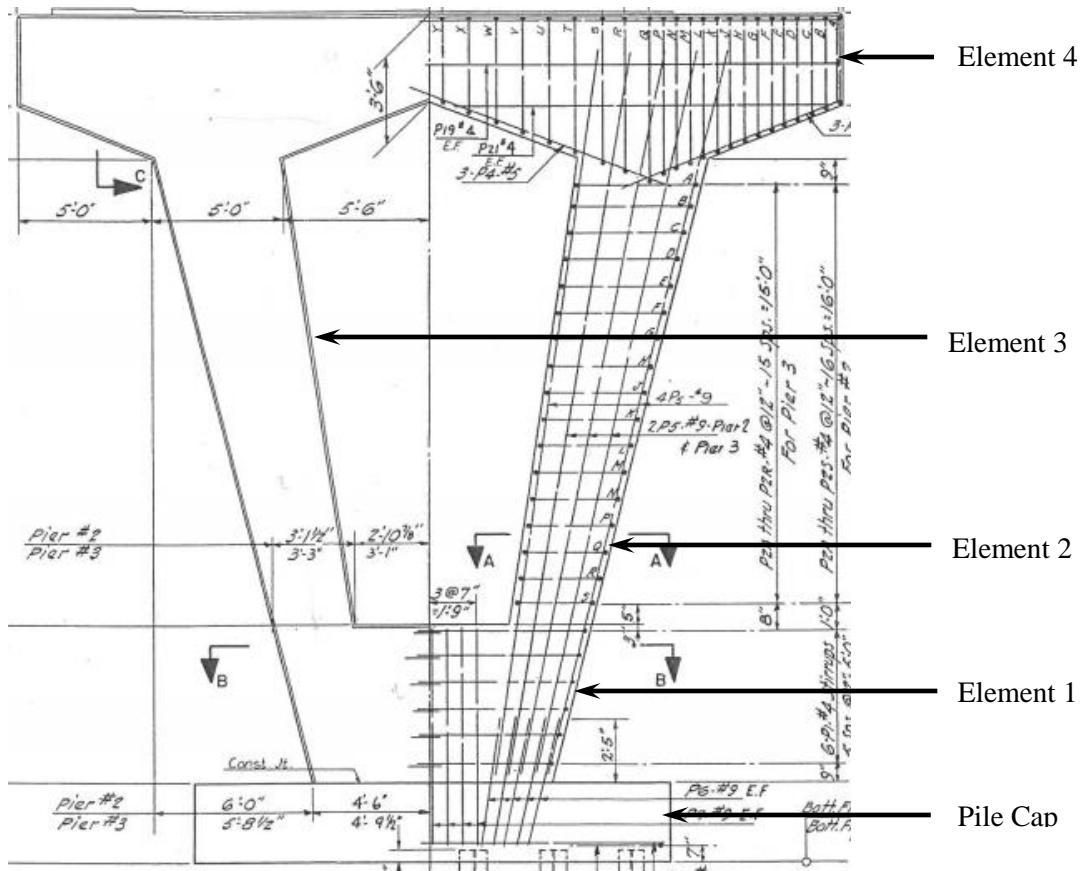


**Figure 2.10: Typical Pier Showing OpenSees Pier Element Numbers [11, 19]**

Figure 2.11 is the general OpenSees pier model which shows node and element numbers. The nodes were created such that each element could connect the adjacent elements and form the pier shape. For this reason Element 4 of each pier is divided into five pieces.

Nodes 411 and 422 are created to be able to model the guide angles, key plates and neoprene bearings. The nodes are the locations of neoprene bearings on which the bridge deck sits with lateral movement restrainers like guide angles or key plates. Modeling of these components is described in Sections 2.3.2 and 2.3.3 of this thesis.

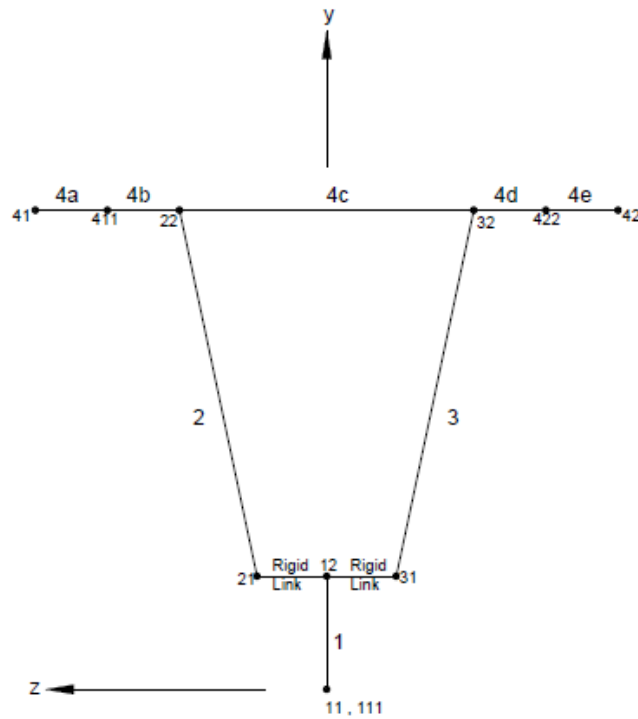


**Figure 2.11: General Pier Model [13]**

### 2.3.1.1 Reinforced Concrete Pier Elements

Each pier (Piers 2, 3, 4, 5 and 6) were discretized as shown in Figure 2.11 and the pier elements were defined by the line element “*NonlinearBeamColumn*” with fiber section. The fiber sections allow the user to define the reinforcements providing dimension to the one directional element. The two rigid link elements are used to connect the Elements 2 and 3 to Element 1 which help in forming the shape of the actual piers.

To represent the nonlinear response of the bridge system under earthquake loading, modeling the cyclic response of the materials in the structure is very important [7]. The following section describes the material models used in the bridge model.

## Concrete01 Material

According to the structural plans provided by Idaho Transportation Department the 28- day compressive strength of the concrete for the pier is found to be 3000 psi. Concrete considered for modeling the piers is a “Concrete01” uniaxial material available in OpenSees library. The “Concrete01” material model assumes no tensile strength for concrete as shown in Figure 2.12. The maximum compressive strength ( $f_{pc}$ ), strain at maximum strength ( $\epsilon_{psc0}$ ), crushing strength ( $f_{pcu}$ ) and strain at crushing strength ( $\epsilon_{psu}$ ) are the required input for this concrete model [25].

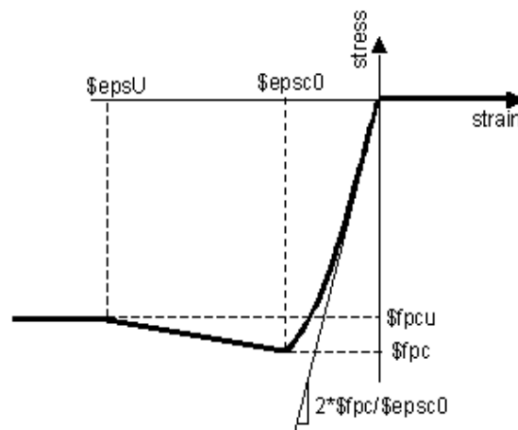


**Figure 2.12: Concrete Stress Strain Relationship [25]**

Mander’s model for concrete has been widely used and referred by AASHTO *guide specifications for LRFD Seismic Bridge Design*. Therefore Mander’s stress-strain model for confined concrete was used [17]. Figure 2.13 shows the concrete stress-strain model.

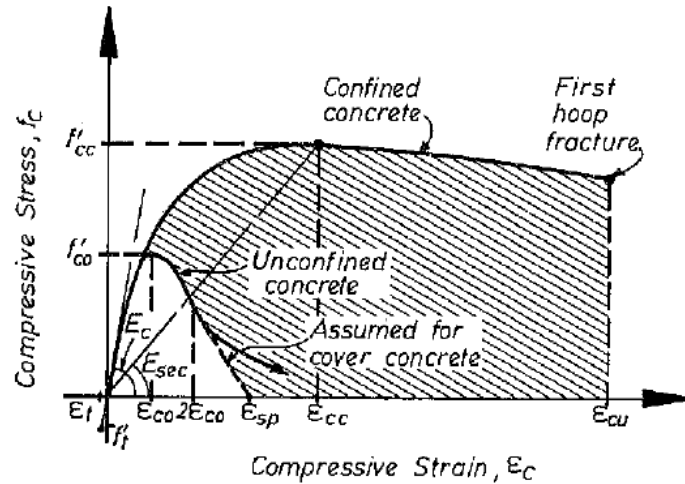


**Figure 2.13: Concrete Stress-Strain Model [17]**

Where,

$f'_{co}$  = Maximum strength of cover concrete

$\epsilon_{co}$  = Strain at maximum strength of cover concrete

$\epsilon_{sp}$  = Strain at ultimate compressive strength of cover concrete

$f'_{cc}$  = Maximum compressive strength of confined concrete

$\epsilon_{cc}$  = Strain at maximum compressive strength of confined concrete

$\epsilon_{cu}$  = Strain at ultimate compressive strength of confined concrete

To determine the concrete properties for confined concrete, unconfined concrete properties are required. The following concrete properties are recommended in Article 8.4.4 of the AASHTO *guide specifications for LRFD Seismic Bridge Design*.

$$f'_{co} = 1.3 * f'_c \quad (2.4)$$

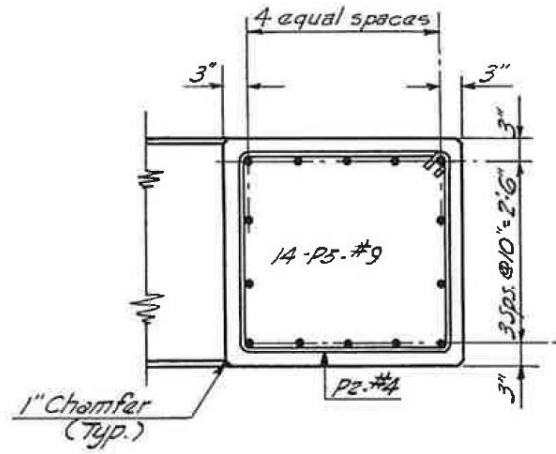
$$\epsilon_{co} = 0.002$$

$$\varepsilon_{sp} = 0.005$$

Where,

$f'_c$  = compressive strength of concrete

The unconfined concrete properties are then used to determine the confined concrete properties. The confined concrete maximum strength and the corresponding strain are the values given for the unconfined concrete multiplied by the factors  $k_1$  and  $k_2$  respectively [19, 17]. These factors are the function of dimension and the amount of transverse confinement reinforcement. Appendix A shows the procedure used to determine the appropriate confined concrete properties according to the Mander's model in the *AASHTO Guide Specifications for LRFD Bridge Design*. Figure 2.14 represents the typical concrete cross section of the pier element. Table 2.4 shows the confined concrete properties of each element of all piers.



SECTION A-A  
 3/4" = 1'-0"

Figure 2.14: Typical Section of Pier Element [11, 19]

**Table 2.4: Element Concrete Properties for 3000 psi 28- day Compressive Strength [19]**

<b>Pier</b>	<b>Element</b>	<b>Max. compressive Strength, fpc (psi)</b>	<b>Strain at Max. Strength, epsc0</b>
2	1	4035	0.002347
	2,3	4168	0.002687
	4a,b,d,e	4411	0.00331
	4c	4117	0.002557
3	1	4030	0.002332
	2,3	4164	0.002677
	4a,b,d,e	4411	0.00331
	4c	4117	0.002557
4	1	4017	0.0023
	2,3	4141	0.002618
	4a,b,d,e	4383	0.00324
	4c	4110	0.002539
5	1	4024	0.002318
	2,3	4141	0.002619
	4a,b,d,e	4411	0.00331
	4c	4117	0.002557
6	2,3	4141	0.002619
	4a,b,d,e	4411	0.00331
	4c	4117	0.002557
<b>Crushing Strength, fpcu</b>		0.7*fpc	
<b>Strain at Crushing Strength, epsu</b>		0.01	

## Steel

“*ReinforcingSteel*” in OpenSees library is selected for the longitudinal reinforcement in the reinforced concrete elements. To define the materials referred to as “*uniaxialMaterial*” in OpenSees, the following input are required as shown in Figure 2.15.

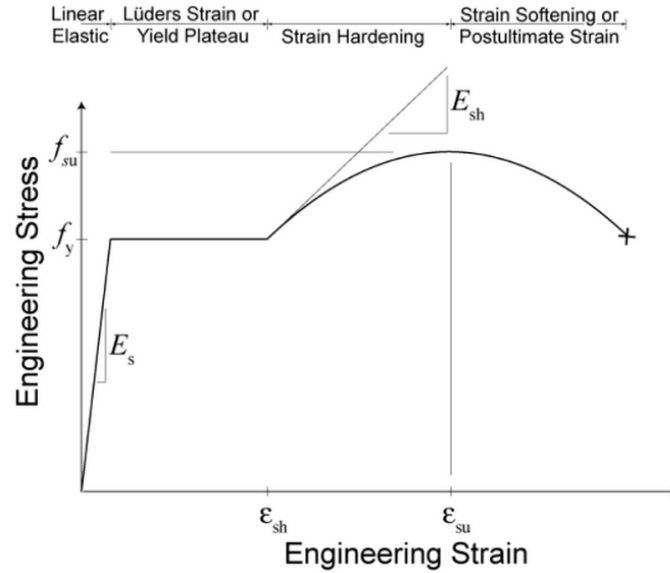


**Figure 2.15: Steel Stress-Strain Relationship [25]**

Where,

$f_y$  = Yield Stress in Tension

$f_{su}$  = Ultimate Stress in Tension

$E_s$  = Initial Elastic Tangent

$E_{sh}$  = Tangent at Initial Strain Hardening

$\epsilon_{sh}$  = Strain at Initial Strain Hardening

$\epsilon_{su}$  = Strain at Peak Stress

A realistic material model for reinforcing steel must be capable of predicting both bar rupture and strength degradation [14]. The Coffin-Manson model in OpenSees library for the reinforcing steel is used for modeling the cyclic degrading behavior of reinforced concrete structures [25]. The parameters required for the model are;  $\alpha$  that relates damage from one strain range to an equivalent damage to another strain range, “ $C_f$ ” is the

ductility constant and “ $C_d$ ” is the strength constant. Figure 2.16 shows the values of parameters required which is given in OpenSees.

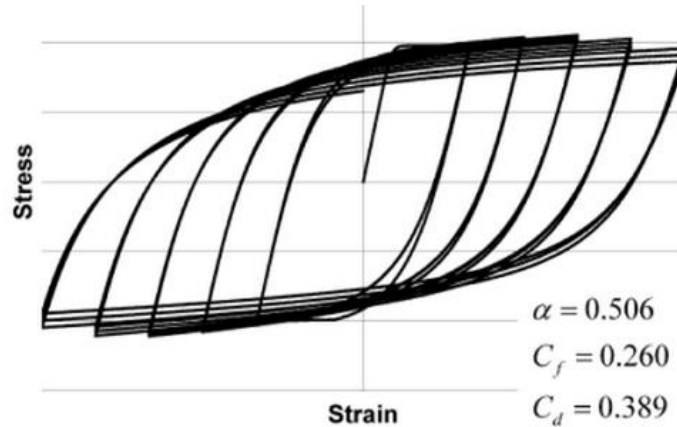


**Figure 2.16: Coffin-Manson Hysteric Model with Fatigue and Degradation Parameter Values [25]**

According to the overpass plans, Number 9 longitudinal bars are used as the reinforcing steel. Table 2.5 provides the values of input parameters required to define the reinforcing steel in OpenSees.

**Table 2.5: Input Parameters for Reinforcing Steel [19]**

Parameters	Values
$f_y$	$68 \times 10^3$ psi
$f_{su}$	$95 \times 10^3$ psi
$E_s$	$29 \times 10^6$ psi
$E_{sh}$	$3.5 \times 10^5$ psi
$\epsilon_{sh}$	0.0125
$\epsilon_{su}$	0.090

To develop the reinforced concrete element “*fiber section*” command is used. This command combines the concrete and reinforcing steel model. Detail description on the fiber section command is given in Miller’s thesis.

### 2.3.2 Neoprene Bearings

The box girders rest on two bearings on each pier of the bridge. Figure 2.6 shows the bearings on Pier 3. Bearings are shown by the black circles. A *zeroLength*” element is used to represent the bearing with the stiffness calculated in accordance with the information obtained from Idaho Transportation Department. Horizontal stiffness is applied to the element representing bearings. Stiffness of the bearings on each piers and abutments are provided in Appendix D of Miller’s thesis [19].

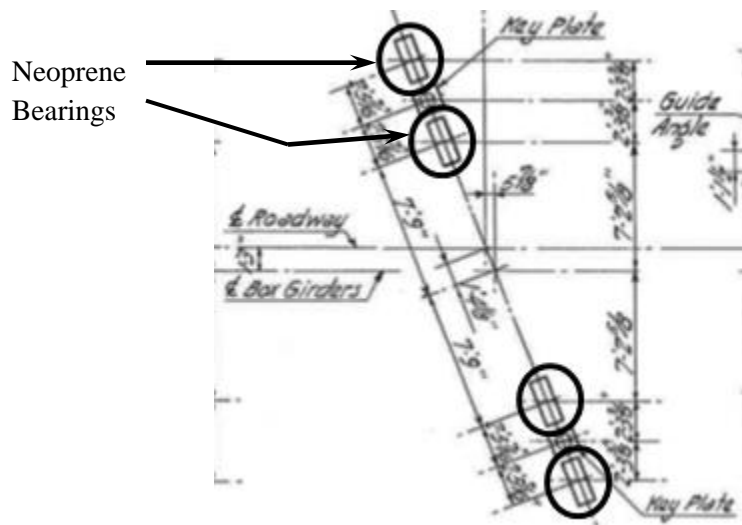


**Table 2.6: PlanView of Neoprene Bearings on Pier 3 [11]**



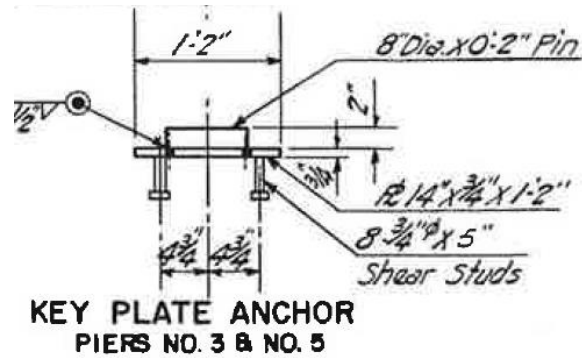


Figure 2.18: Key Plate [11, 19]

### 2.3.4 Superstructure

The superstructure of the highway bridge consists of a reinforced concrete deck and steel box girders. Figure 2.19 shows the typical section of the bridge superstructure. The superstructure behaves elastically under seismic loading [22]. Hence the line element “*elasticBeamColumn*” is used to represent the superstructure elements. Cross-sectional area, Young’s modulus, shear modulus, torsional moment of inertia and second moment of area about both axes are the required input parameters for the “*elasticBeamColumn*” element. The concrete bridge deck was transformed into an equivalent steel area to determine the input parameters for the “*elasticBeamColumn*” element. Calculation and the values obtained for the parameters are provided in Appendix F of Miller’s thesis [19]. Twenty elements are used to model each span of the bridge. An example of OpenSees command for the element is provided in Appendix J of Miller’s thesis.



### 2.3.5 Mass Distribution

Table 2.7 shows the total weight of the bridge piers. For gravity load, the weight of Element 4 and half of the Elements 2 and 3 of each pier (see Figures 2.10 and 2.11) are applied to the top of the Elements 2 and 3 (Nodes 22 and 32). The total weight of the superstructure is calculated to be 309 pounds per inch in which the corresponding mass is applied as lumped masses on each node of the elements representing the superstructure.

**Table 2.7: Weight of Piers [19]**

Pier	Weight (kips)
2	90
3	90
4	102
5	78
6	78

### 2.3.6 Foundation

The foundation of each of the piers consists of an array of 12BP53 H-piles. Six degrees of freedom is provided to the spring representing the foundation. The springs are modeled using a “*zeroLength*” element at the bottom of the piers. The stiffnesses provided to the element are given in Table 2-6 in Miller’s thesis [19]. Figure 2.20 shows a schematic of Pier 2 which shows the elements representing foundation. It also shows the nodes and elements numbers used for the pier.

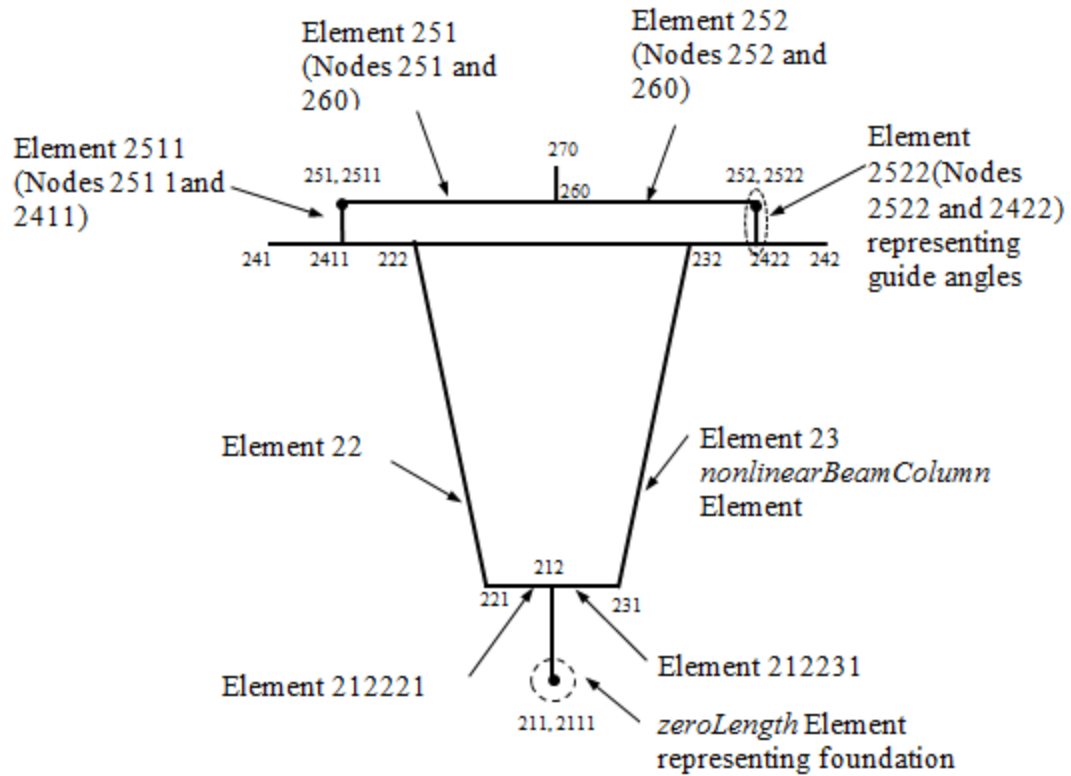


**Figure 2.20: A Schematic Pier 2 OpenSees Model With Nodes and Elements Numbers**

### 2.3.7 Abutments and Expansion Joints

The bridge superstructure is supported by two abutments at the end of the bridge deck and five piers. The bridge deck sits on bearings at the abutments and separated by expansion joints. Modeling abutments are essential when assessing the seismic behavior of a bridge as they limit the displacements and transfer the forces from the bridge deck to the embankment [7]. The bridge abutment damages experienced in 1971 San Fernando earthquake show that abutments carry a large portion of the seismic forces specially in longitudinal direction [13]. The California Department of Transportation (Caltrans) has a simplified method for modeling bridge abutments for seismic applications which is presented in the Caltrans' *Bridge Design Practice*, Section 8, Seismic Analysis of Bridge

Structures [4]. The stiffness determined by using Equation (2.5) for Abutment 1 and Abutment 2 are 4,813 kips/in and 3,300 kips/in respectively.

$$k = 25 * W * h \quad (2.5)$$

Where,

$k$  = stiffness of the abutment

$W$  = width of the abutment

$h$  = height of the abutment

A “*zeroLength*” element is used at the each end of the bridge deck. The element was given stiffness of the abutment in longitudinal direction, stiffness of guide angles in transverse direction and large stiffnesses in vertical and all rotational directions [19]. The OpenSees commands for the elements are provided in Appendix J of Miller’s thesis [19].

For more realistic nonlinear response of the bridge, elements representing expansion joints should be used in the bridge model. These elements simulate the bridge deck-abutment interaction and interaction of adjacent decks. The OpenSees “*zeroLengthContact3D*” element is used for this purpose. Figures 2.21 and 2.22 show the expansion joints at Abutment 1, Pier 4, and Abutment 2, respectively.



coefficient of friction and cohesion respectively. Commands for the contact element are provided in Appendix B of this thesis.

Each abutment is modeled with four long rigid links, four short rigid links and two contact elements. The long rigid links represent the width of the bridge deck and abutment while the short rigid links are used to fit the contact elements. Figures 2.23 and 20.24 show the Abutment 1 and expansion joint model on Pier 4 with contact elements respectively.

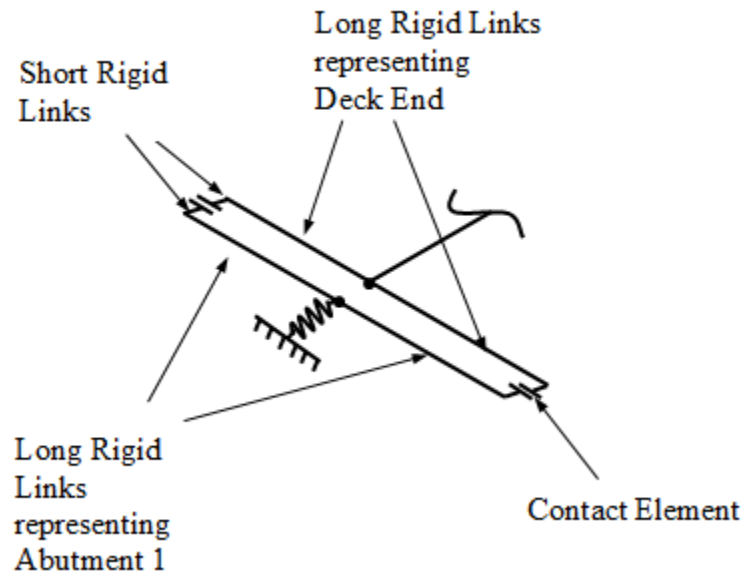


**Figure 2.23: Abutment 1 Model**

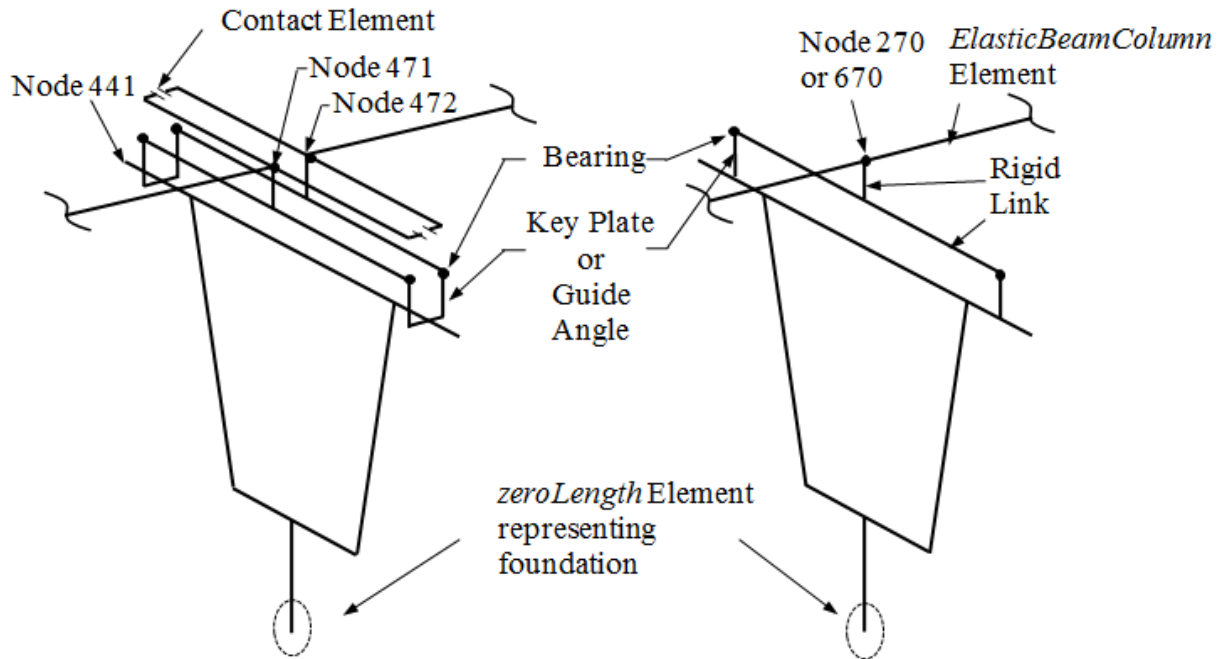


**Figure 2.24: Schematic of Piers 4, 2 and 6 OpenSees Model**

The bridge gap plays an important role in adding to the pounding effect at the abutments and expansion joint at Pier 4. The seismic pounding can amplify the global response of the participating structural systems [6]. Hence, the gaps are created by adjusting the longitudinal loading applied at the abutments and Piers 2, 3, 5 and 6.

The gap in the expansion joint on Pier 4 is 1.75 in. To create the gap the longitudinal displacement time histories that are supposed to be applied to the bottom of Piers 2 and 3 are subtracted by half of 1.75 in. (0.875 in.). Similarly, 0.875 in. displacement is added to the longitudinal displacement time histories applied to the bottom of Piers 5 and 6. Figure 2.25 shows the longitudinal displacement time histories applied to the bottom of Piers 2, 3, 5 and 6.

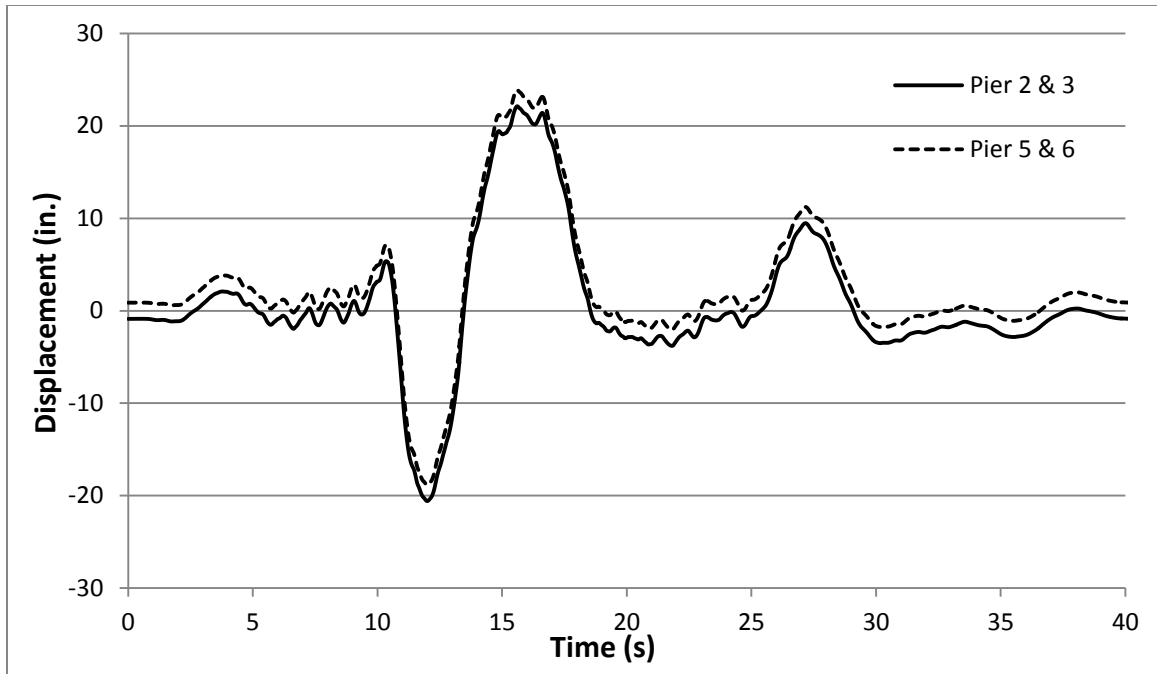


**Figure 2.25: Landers Station Longitudinal Displacement Time History Applied to the Bottom of Piers 2, 3, 5 and 6**

Now the gap in the expansion joint on Pier 4 is created, but the half of the gap size (0.875 in.) should be added to the gap size of the expansion joint at the abutments. The gap sizes of expansion joints at Abutments 1 and 2 are 1.75 in. and 2 in. respectively. Hence, half of the gap size of expansion joint on Pier 4 (0.875 in.) and gap size of expansion joint at Abutment 1 (1.75 in.) or a total of 2.625 in. is subtracted from the longitudinal displacement time history of Abutment 1. Similarly, half of the gap size of expansion joint on Pier 4 (0.875 in.) and gap size of the expansion joint at Abutment 2 (2 in.) or a total of 2.875 in. is added to the longitudinal displacement time history of Abutment 2. Figure 2.26 shows the displacement time histories that are applied to the bottom of the abutments.

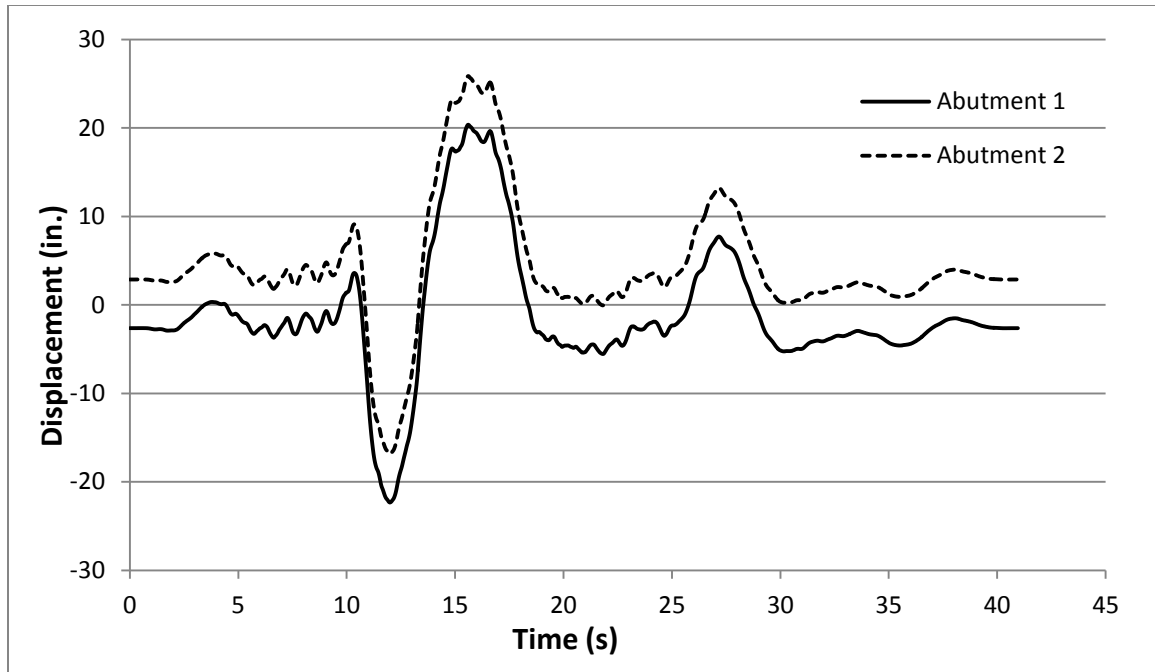


**Figure 2.26: Landers Station Longitudinal Displacement Time History Applied at the Abutments**

Figure 2.27 shows the overall schematic of the OpenSees Washington Street Overpass model. The model contains all the components of the bridge. They are five concrete reinforced piers with deep pile foundations, bridge superstructure with steel box girders and reinforced concrete deck, abutments and expansion joints with contact elements, steel guide angles, steel key plates, and neoprene bearings. More details on bridge OpenSees modeling is provided in Miller’s thesis [19]. Validation of the bridge model has been performed using the basic concept of force. This validation is explained in Appendix C of this thesis.

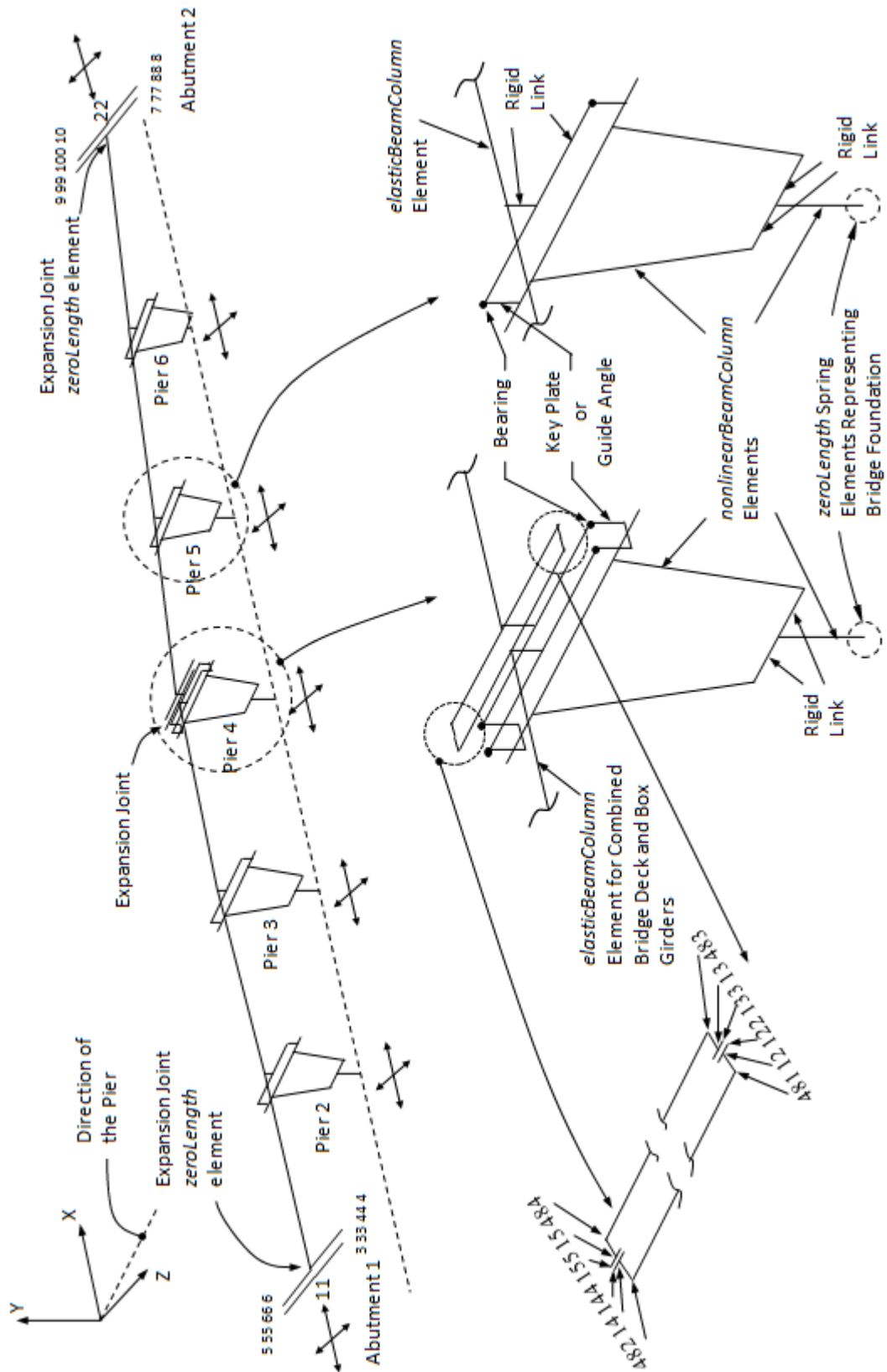


Figure 2.27: Schematic of the OpenSees Washington Street Overpass Model

## 2.4 Sensitivity Analysis

The input parameters that influence the bridge model the most may be determined by a sensitivity analysis. There are many methods of conducting sensitivity analysis. However the simplest approach is used for the study. The simplest method of sensitivity analysis is to repeatedly vary the value of one parameter at a time, while keeping the others constant [9]. This method helps to understand the sensitivity of the seismic response of the bridge to each of the parameters. Herein parameters considered for the study are the compressive strength of the concrete, coefficient of friction of contact element and damping constant of the bridge. Comparing or quantifying the model output changes can determine the parameter with the most influence on the bridge response. The various values of the parameters mentioned above for sensitivity analysis are shown in the Table 2.8.

**Table 2.8: Input Parameters Values Used for the Sensitivity Analysis**

Parameters	Values			
	1	2	3	4
Coefficient of Friction	0.1	0.3	<b>0.5</b>	0.7
Damping Constant	0.01	0.03	<b>0.05</b>	0.07
Compressive Strength of Concrete (psi)	3000	<b>3500</b>	4000	4500

The references values chosen for coefficient of friction of contact element, damping constant of the bridge and 28-day compressive strength of concrete are 0.5, 0.05 and 3500 psi, respectively; these values are shown with bold text in Table 2.8. Sensitivity

of the bridge seismic response to coefficient of friction of contact element can be determined by varying the values 0.1 through 0.7 and keeping damping constant at 0.05 and the compressive strength at 3500 psi. Similarly, sensitivity of the bridge response to the other two parameters can be determined. Parameter with the maximum changes in output is the most influencing input parameter. Sensitivity of aforementioned parameters to bending moment, shear force and displacement ductility of elements of Piers 2, 4 and 6 under earthquake loading will be analyzed. The concrete properties used for the elements of piers with 3500, 4000, and 4500 psi 28-day compressive strength are presented in Table A.1, A.2 and A.3 respectively in Appendix A.

## **CHAPTER 3**

### **RESULT**

This chapter provides the detail results obtained for the seismic analysis of the Washington Street Overpass and the parametric sensitivity analysis of the bridge response using the improved OpenSees bridge model. The improved bridge model contains all the bridge components and the contact elements in expansion joints. Gaps in all the expansion joints are also created.

#### **3.1 Seismic Analysis**

As described in Chapter 2 seismic analysis of a bridge under SDC D requires pushover and nonlinear time history analyses. The pushover analysis was performed to estimate the displacement capacity of the elements of the Piers 2, 4 and 6. For the demand analysis, a nonlinear time history analysis was performed under the bi-directional Landers earthquake loading. The nonlinear response obtained from the improved bridge model was compared to that of the bridge model without contact elements and gaps in expansion joints. Followings are the results of the analyses performed for the bridge.

##### **3.1.1 Pushover Analysis**

The pushover analyses were performed on Piers 2, 4 and 6. To perform the analysis individual reinforced concrete piers were modeled as described in Chapter 2. Weight of the Element 4 and half of the weight of Elements 2 and 3 of the corresponding pier and tributary weight of the superstructure of the bridge ( $W$ ) to individual piers was applied on top of the pier (Nodes 22 and 32). Incremental linear loads were applied to the

top of the piers (Nodes 22 and 32) in global Z-direction. Figure 3.1 shows the general OpenSees pier model with the location of the tributary load applied. The bases of the piers were fixed. The incremental horizontal load was applied to the pier until the collapse mechanism is reached. The point where the structure behaves nonlinearly is the displacement capacity of the structure. For this case, the deflection of the Node 32 which is the top node of the Element 3 of the piers and maximum bending moment of the Element 3 are taken into account for the capacity curve plotted. Figures 3.2 and 3.3 show the pushover curves for the Piers 2 and 4 obtained from the pushover analyses.

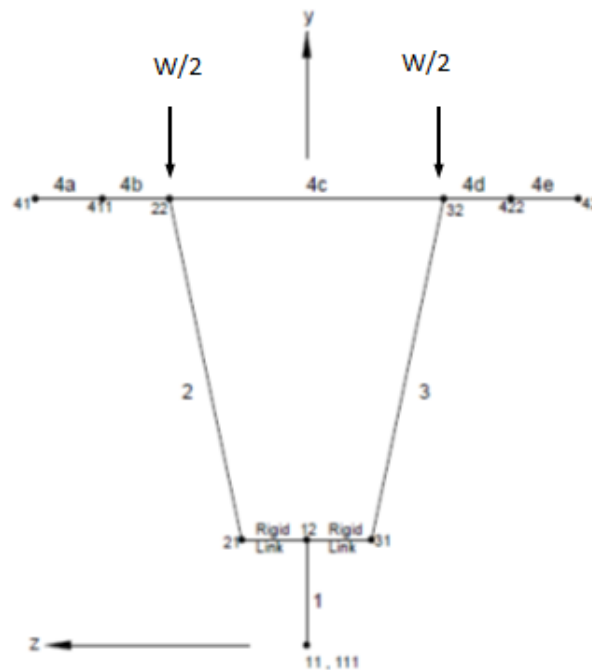


**Figure 3.1: General Pier Model in OpenSees**

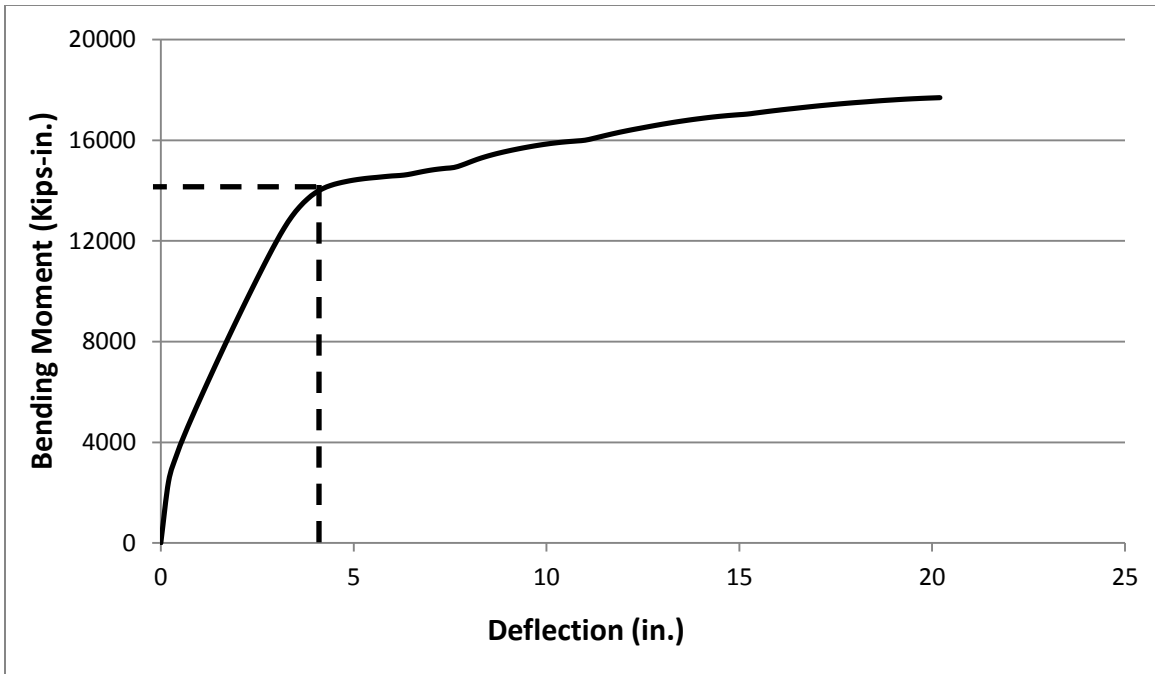


**Figure 3.2: Bending moment Vs. Deflection of Element 3 of Pier 2**

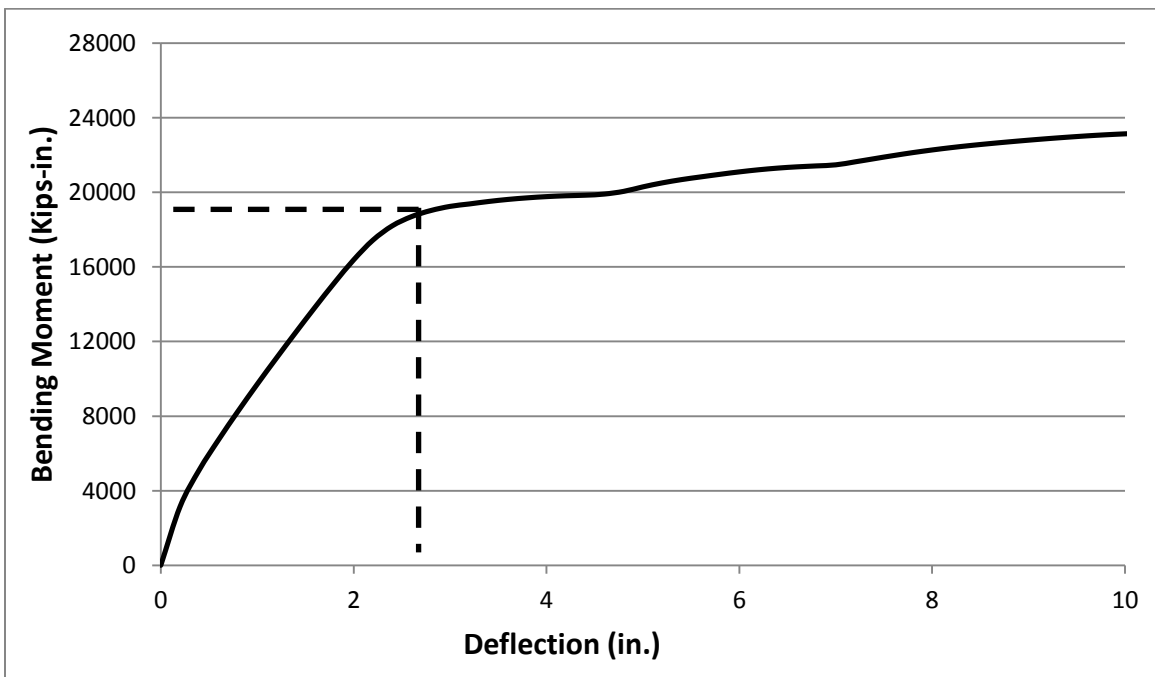


**Figure 3.3: Bending moment Vs. Deflection of Element 3 of Pier 4**

Table 3.1 shows the resulting bending moment and displacement capacities obtained from the analyses using OpenSees. It also shows the bending moment capacities by hand calculations which are approximately same as the capacities obtained from the pushover analysis. This also proves that the piers are modeled appropriately. The values given in the table are for Elements 3, but they are considered to be same as Elements 2. The elements are symmetric to each other.

**Table 3.1: Bending Moment and Yield Displacement, Using Pushover Analysis**

Piers	Estimated by Hand calculation, Bending Moment (Kips-in.)	Estimated by Pushover (OpenSees)	
		Bending Moment (Kips-in.)	Yield Displacement (in.)
2	15,500	14,200	3.9
4	18,200	18,600	2.6
6	20,300	20,400	2.0

### 3.1.2 Nonlinear Time History Analysis

The Nonlinear Time History Analysis is selected for the Washington Street Overpass demand analysis. To achieve more realistic nonlinear response of the bridge to a probable earthquake event, contact elements and gaps are implemented in all the expansion joints of the bridge model developed for the first phase of the project. The contact elements and gaps simulate the decks-abutments interaction and the interaction of the adjacent decks of the bridge which are highly nonlinear behavior. The bridge model with 3000 psi of 28 day- compressive strength of concrete, damping constant of 5 % and

coefficient of friction of contact elements of 0.1 is used for the analysis. Figure 2.24 shows the complete bridge model developed in OpenSees.

A set of transverse and longitudinal displacement time histories for Landers station which are scaled to the bridge site acceleration spectrum was applied to the base of each piers and abutments. The capacities of individual piers obtained using pushover analysis are compared with the demand displacement obtained from the entire bridge system (global model). Bending moment and shear demand of the bridge system are also checked against the bending moment and shear capacities respectively. Bending moment and shear capacities of the individual piers are obtained by hand calculation. The hand calculations are provided in Miller's thesis [19].

The results obtained from the improved bridge model with contact elements and gaps are compared to that of the bridge model without contact elements. Following are the results obtained from the nonlinear time history analysis performed for the bridge.

The relative displacement of the abutments and bridge decks in the longitudinal direction were observed. Figure 3.4 shows the relative displacement of the Abutment 1 and bridge deck.

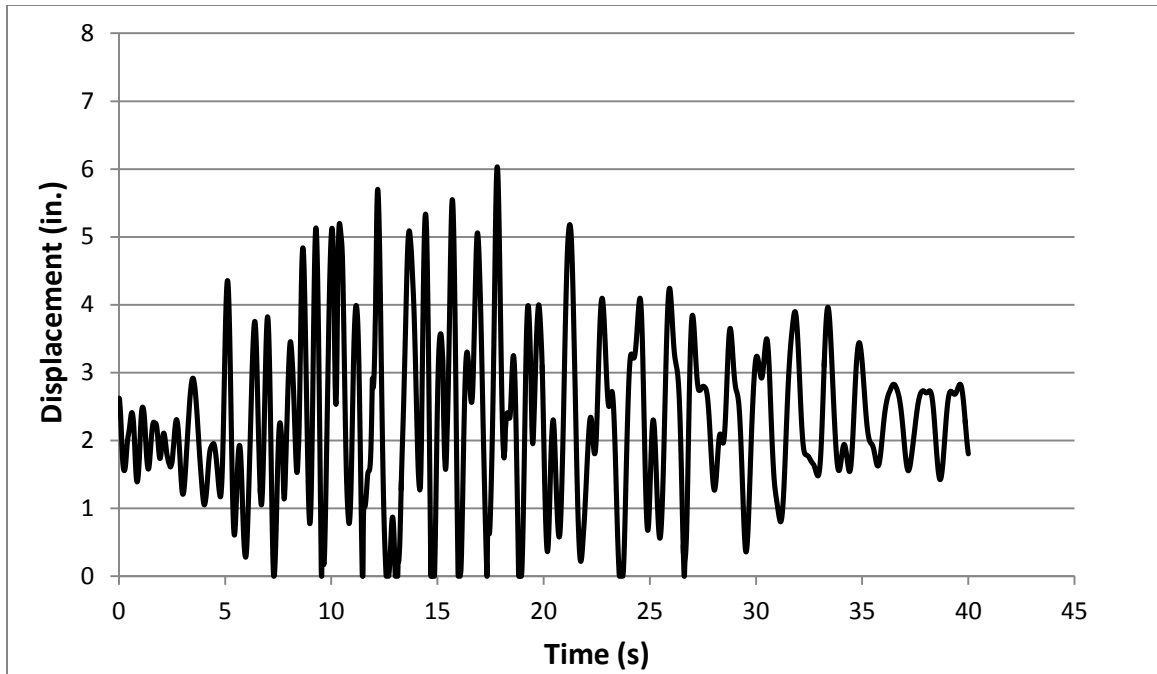


**Figure 3.4: Relative Displacement of Abutment1 and Bridge Deck**

From the figure, it can be found that the contact element is performing as desired. The relative displacements of the adjacent structures in all the location of expansion joints are found to be entirely positive or negative in all the locations. Hence it can be said that the adjacent structures are not penetrating to each other. The relative displacement is zero few times, which shows that the abutment and bridge deck come in contact closing the gap in between them. Similar observation was made for other two locations of the expansion joints.

Bending moment and shear force in Element 3 of Piers 2, 4 and 6 were observed. Figure 3.5 through 3.10 show the resulting bending moment and shear force.

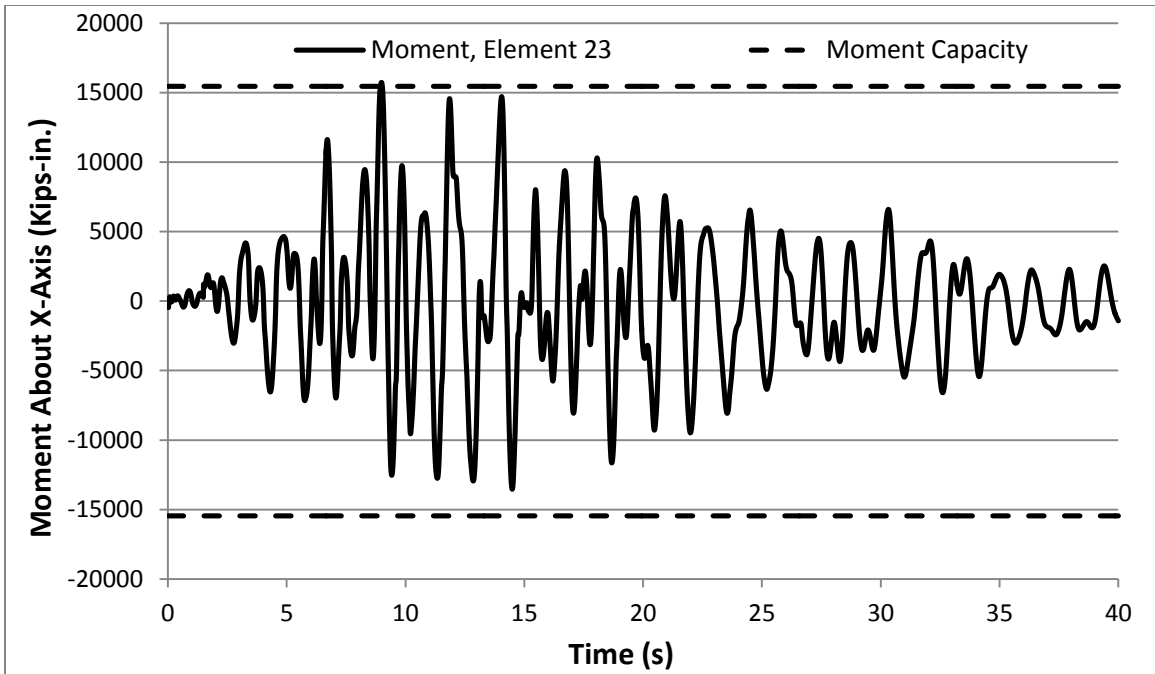


**Figure 3.5: Bending Moment in Element 3, Pier 2**

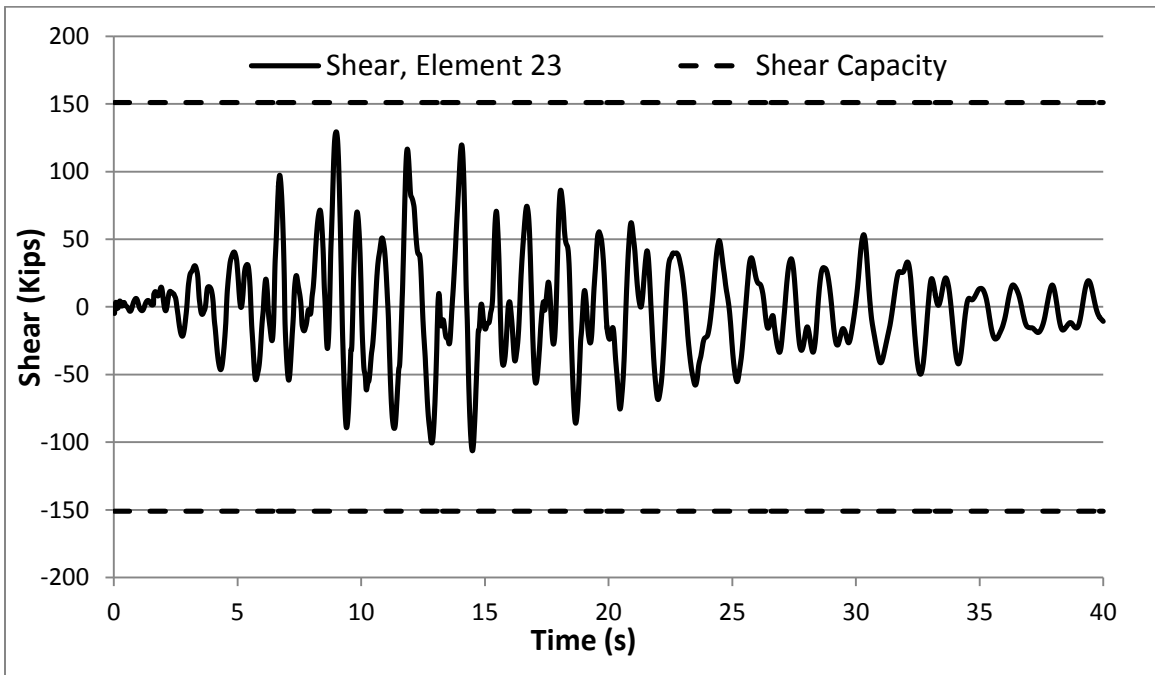


**Figure 3.6: Shear in Element 3, Pier 2**

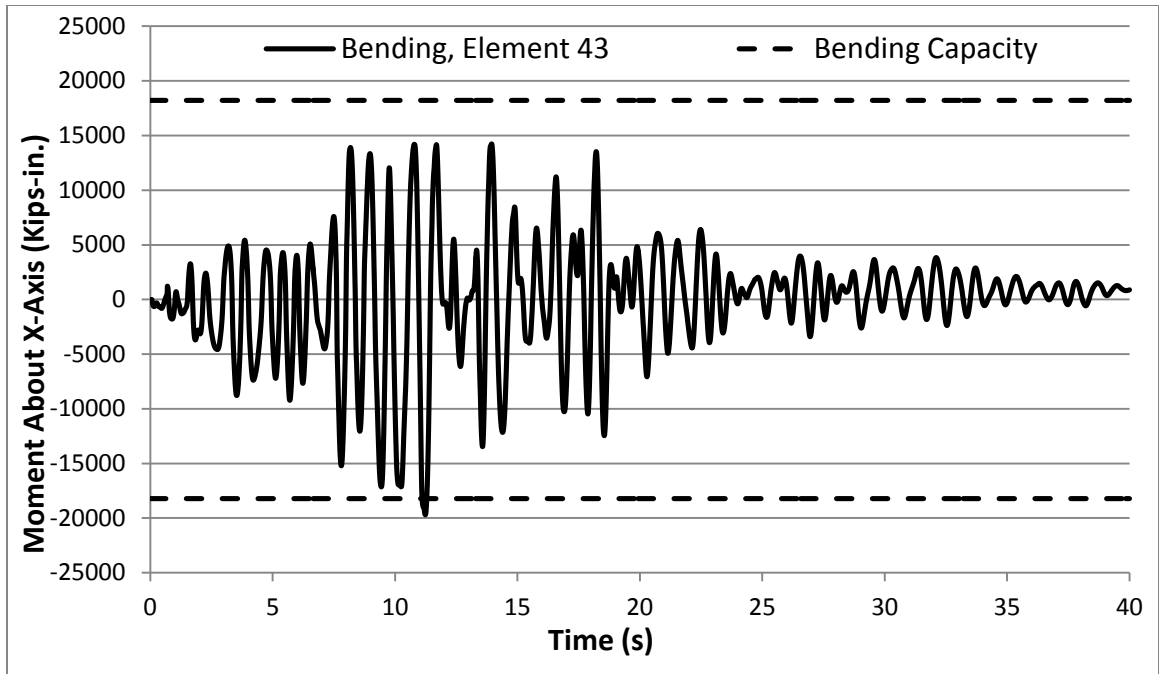


**Figure 3.7: Bending Moment in Element 3, Pier 4**

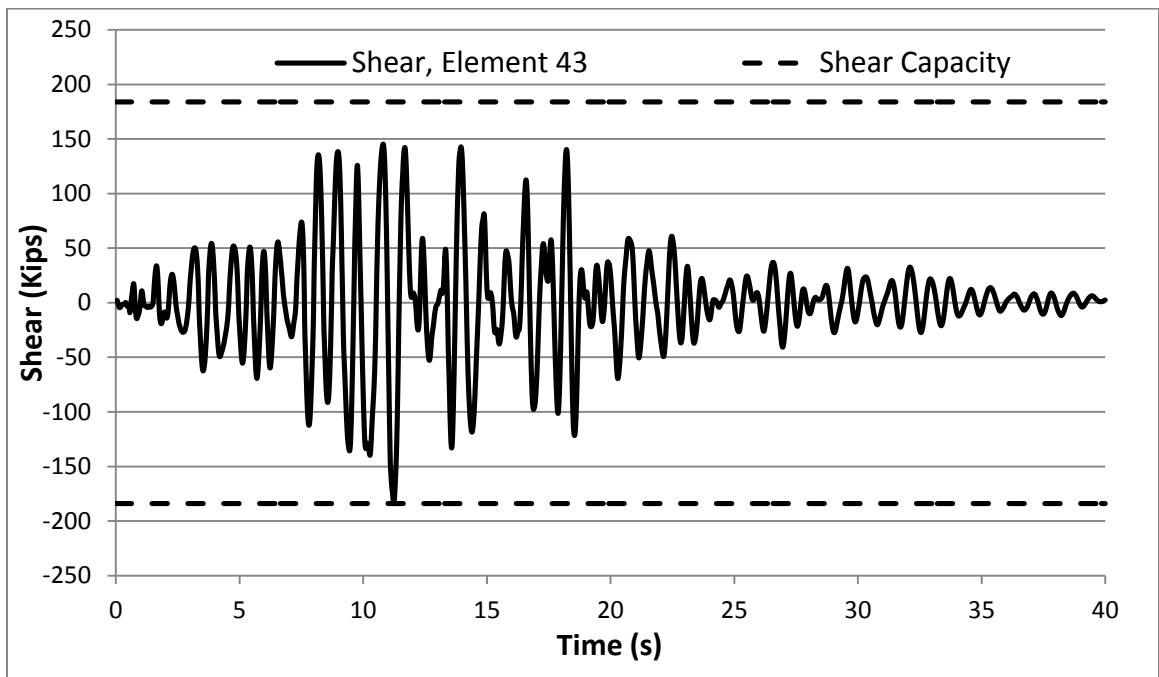


**Figure 3.8: Shear in Element 3, Pier 4**

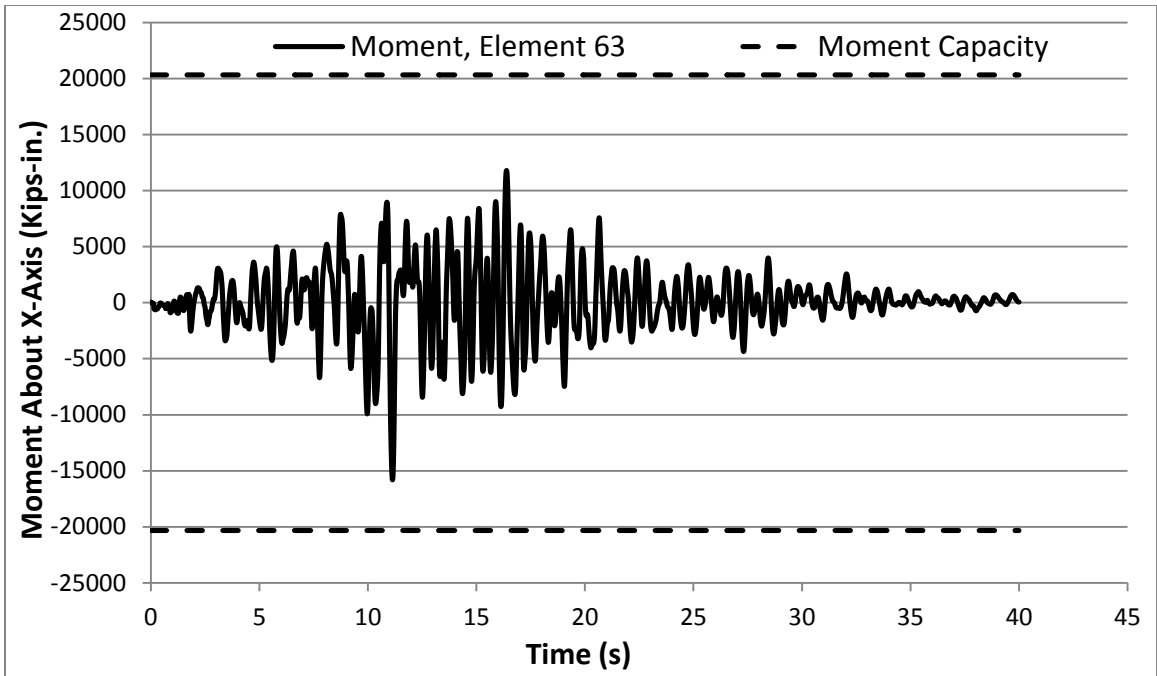


**Figure 3.9: Bending Moment in Element 3, Pier 6**

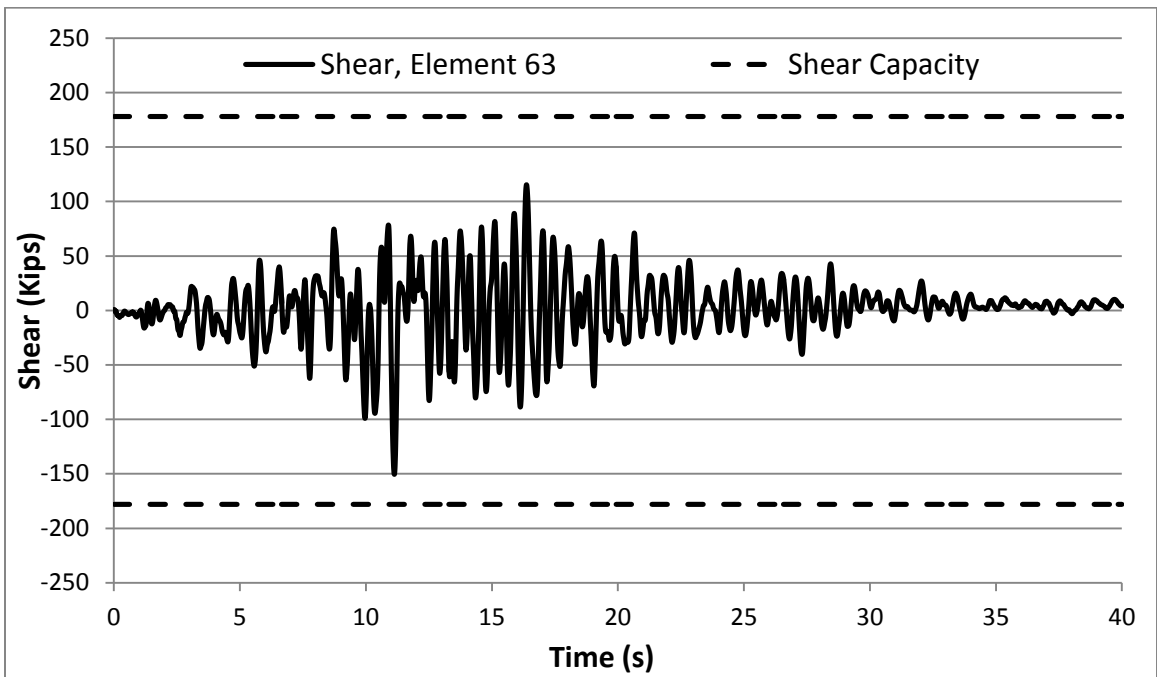


**Figure 3.10: Shear in Element 3, Pier 6**

From the figures it can be seen that the bending moment and shear force induced in Element 3 of Pier 4 are the largest. However, the bending moment in Elements 3 of Piers 2 and 4 exceed the capacity by a small amount whereas the bending moment induced in Element 3 of Pier 6 does not reach the capacity. Shear force in Elements 3 of Piers 2 and 6 does not reach their capacities. Shear force demand in Element 3 of Pier 4 reaches but do not exceed the capacity. Hence, it can be said that the piers do not fail by shearing off or creating failure mechanism.

Displacement ductility of the Elements 3 of Piers 2, 4 and 6 were also observed. Displacement ductility is the ratio of displacement demand to capacity. As noted in Section 3.1.1, the displacement capacity of the elements was obtained by performing pushover analysis on Element 3 of the piers. For comparison, the displacement demands are the transverse relative displacement of the top and bottom of the Elements 3 of the piers when the bridge was subjected to the earthquake loading. Figures 3.11, 3.12 and 3.13 show the relative displacement of top and bottom of Elements 3 of Piers 2, 4, and 6.

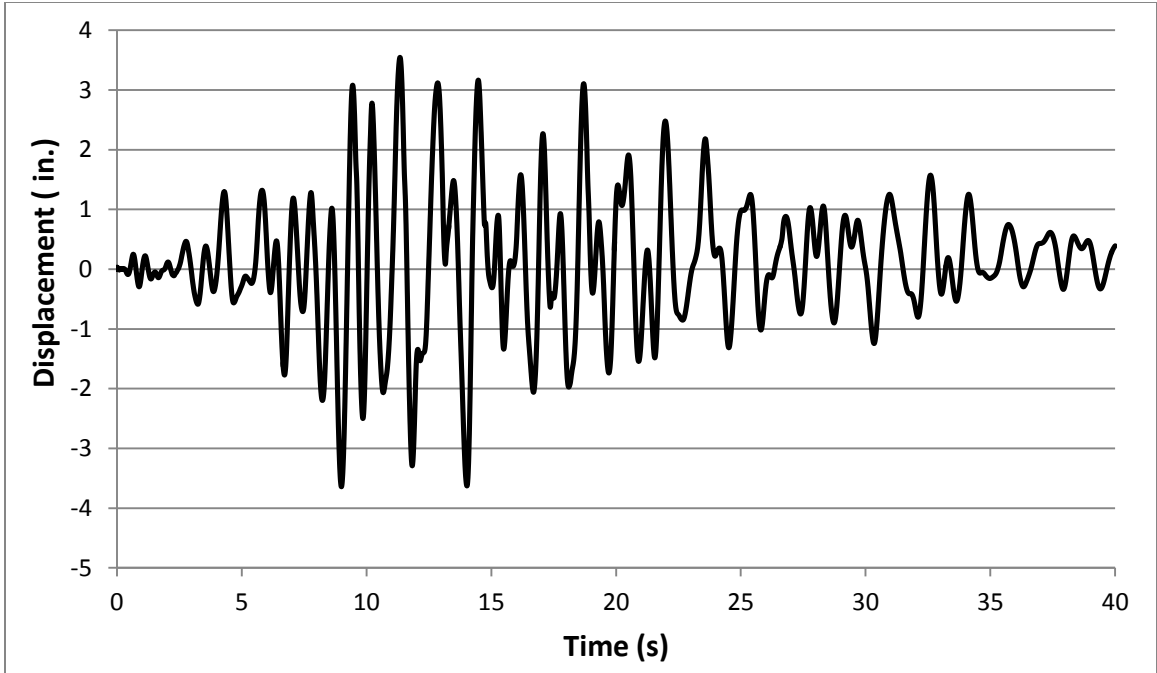


**Figure 3.11: Relative Displacement of Top and Bottom of Element 3, Pier 2**

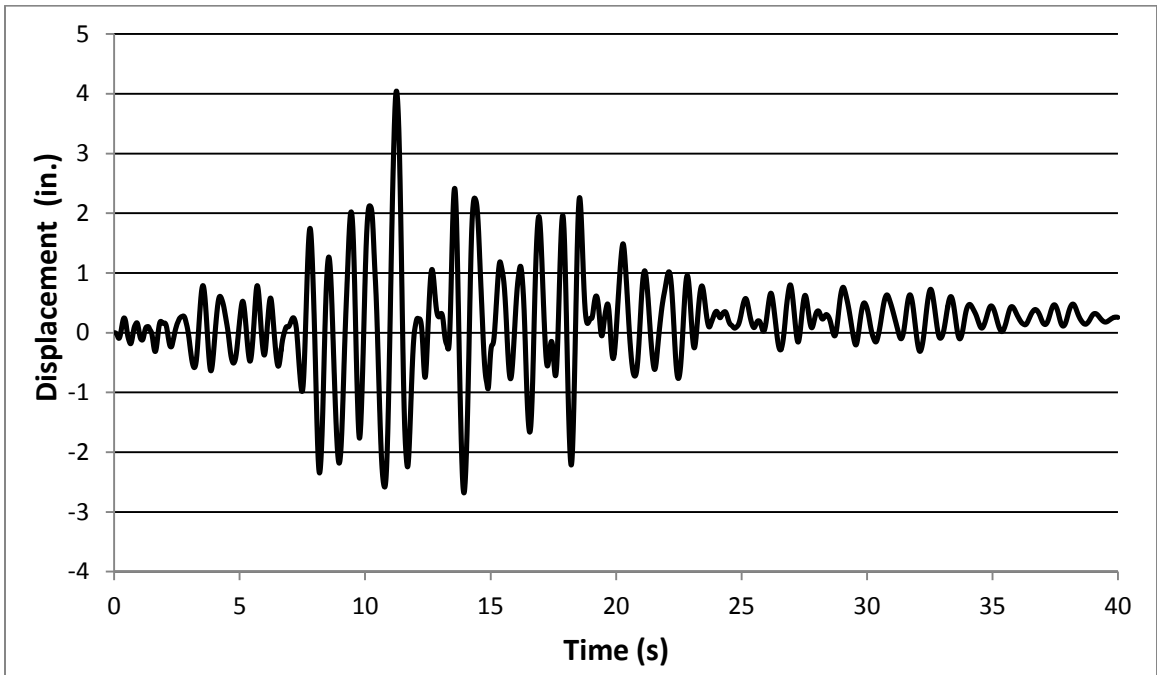


**Figure 3.12: Relative Displacement of Top and Bottom of Element 3, Pier 4**

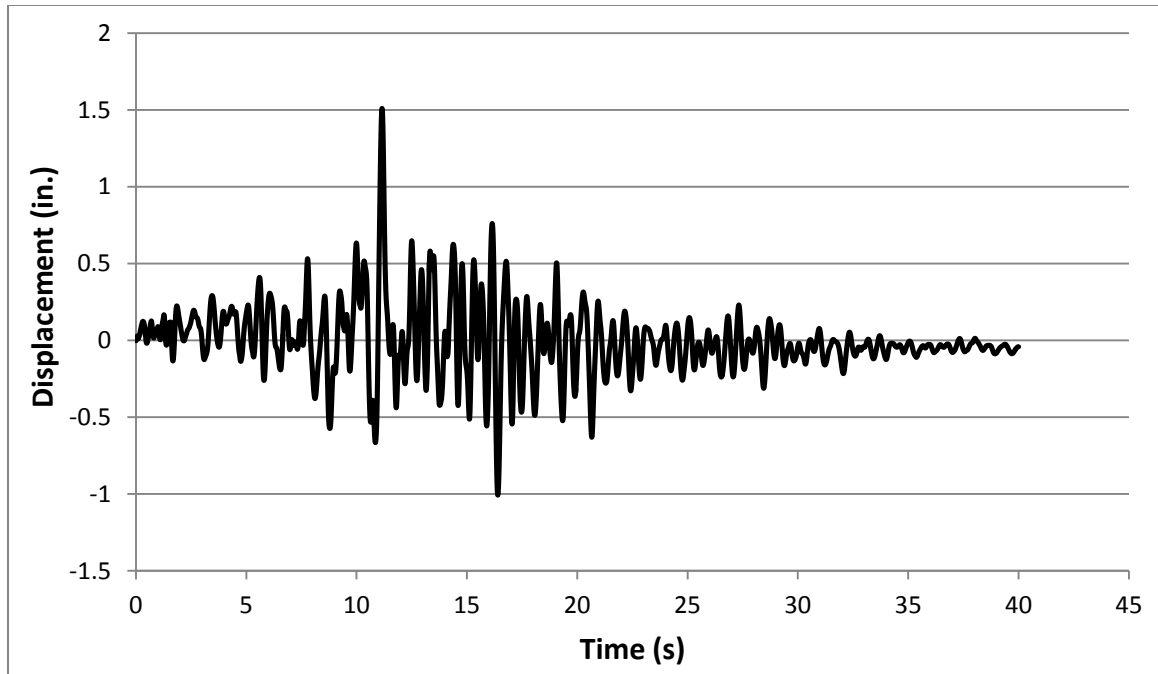


**Figure 3.13: Relative Displacement of Top and Bottom of Element 3, Pier 6**

The demand to capacity ratio of bending moment, shear force and displacement of Elements 3 of Piers 2, 4 and 6 are tabulated in Table 3.2.

**Table 3.2: Demand to Capacity Ratio of Bending Moment, Shear Force and Displacement of Element 3 of Piers**

Piers	Demand to Capacity Ratio		
	Bending Moment	Shear Force	Displacement
2	1.0	0.9	0.9
4	1.1	1.0	1.5
6	0.9	0.9	0.8

From Table 3.2 it can be seen that the displacement ductility is greater than 1 in only Pier 4. This shows that the displacement demand exceeds the capacity (yield displacement) of the element.

The aforementioned results are obtained from the improved bridge model that includes contact elements and gaps in all location of expansion joints. However one of the major objectives of this project is to compare the response obtained from the improved bridge model (with contact elements and gaps) and the bridge model (without contact elements and gaps) from the first phase of this project when subjected to the earthquake loading. Tables 3.3, 3.4 and 3.5 summarize these results.

**Table 3.3: Comparison of Bending Moment Demand (Kip-in.) to Capacity Ratio of Elements 2 and 3 of Piers 2, 4 and 6 of Bridge Model With and Without Contact Element (CE)**

Pier No.	Maximum seismic induced demand, OpenSees bridge model (Kip-in.)		Estimated capacity, OpenSees pushover (Kip-in.)	Estimated capacity, hand calculation (Kip-in.)	Demand to capacity ratio	
	without CE	with CE			without CE	with CE
2	15,700	15,700	14,200	15,500	1.0	1.0
4	19,800	19,700	18,600	18,200	1.1	1.1
6	16,600	17,500	20,400	20,300	0.8	0.9

**Table 3.4: Comparison of Shear Force (Kip) Demand to Capacity Ratio of Elements 2 and 3 of Piers 2, 4 and 6 of Bridge Model With and Without Contact Element (CE)**

Pier No.	Maximum seismic induced demand, OpenSees bridge model (Kip)		Estimated capacity, hand calculation (Kip)	Demand to capacity ratio	
	without CE	with CE		without CE	with CE
2	120	129	151	0.8	0.9
4	197	183	184	1.1	1.0
6	137	164	178	0.8	0.9

**Table 3.5: Comparison of Displacement Ductility of element 2 and 3 of Piers 2, 4, and 6 of Bridge Model With and Without Contact Element**

Pier No.	Yield displacement (in.)	Demand displacement (in.)		Displacement ductility	
		without CE	with CE	without CE	with CE
2	3.9	3.7	3.6	0.9	0.9
4	2.6	4.6	3.9	1.8	1.5
6	2.0	1.5	1.5	0.8	0.8

From the tables it can be observed that the inclusion of contact elements and gaps in the bridge model does not change the bridge response significantly. However the displacement ductility of the Element 3 of Pier 4 reduced to 1.5 from 1.8. This was the maximum change that was seen among the bending moment, shear force and displacement demand to capacity ratio in the elements of the piers.

Shear force in each guide angles and key plates were also observed to see if the elements fail. Figures 3.14 through 3.18 show the shear in the elements in all locations.

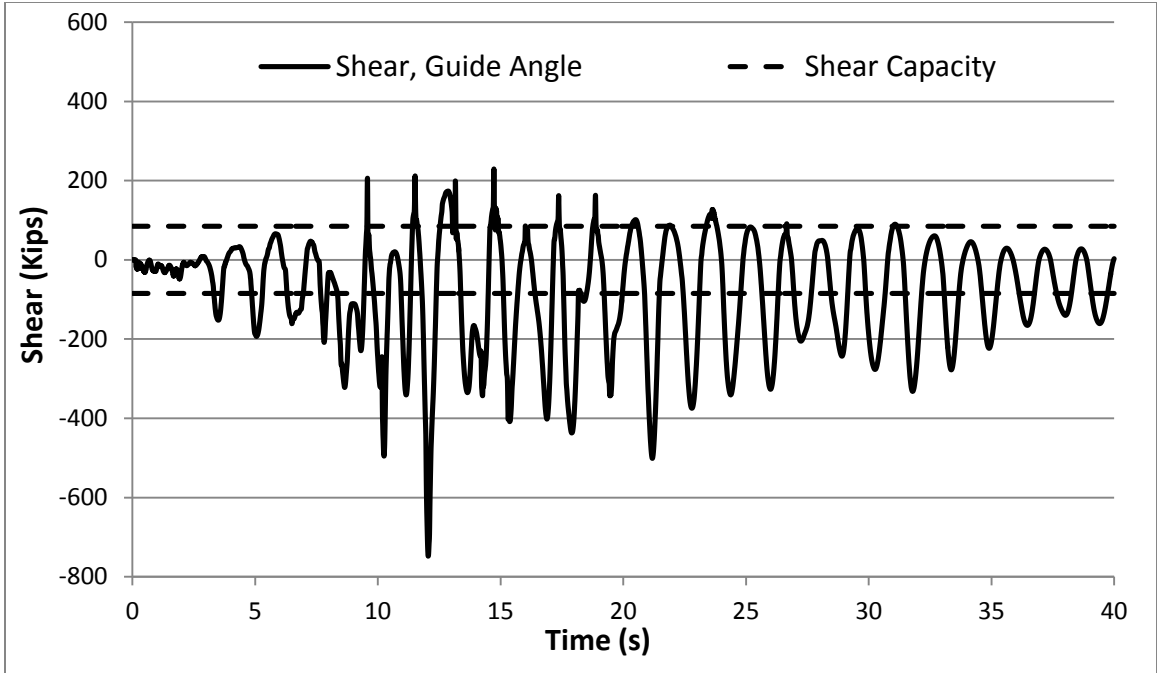


**Figure 3.14: Shear Force in Guide Angles, Pier 2**

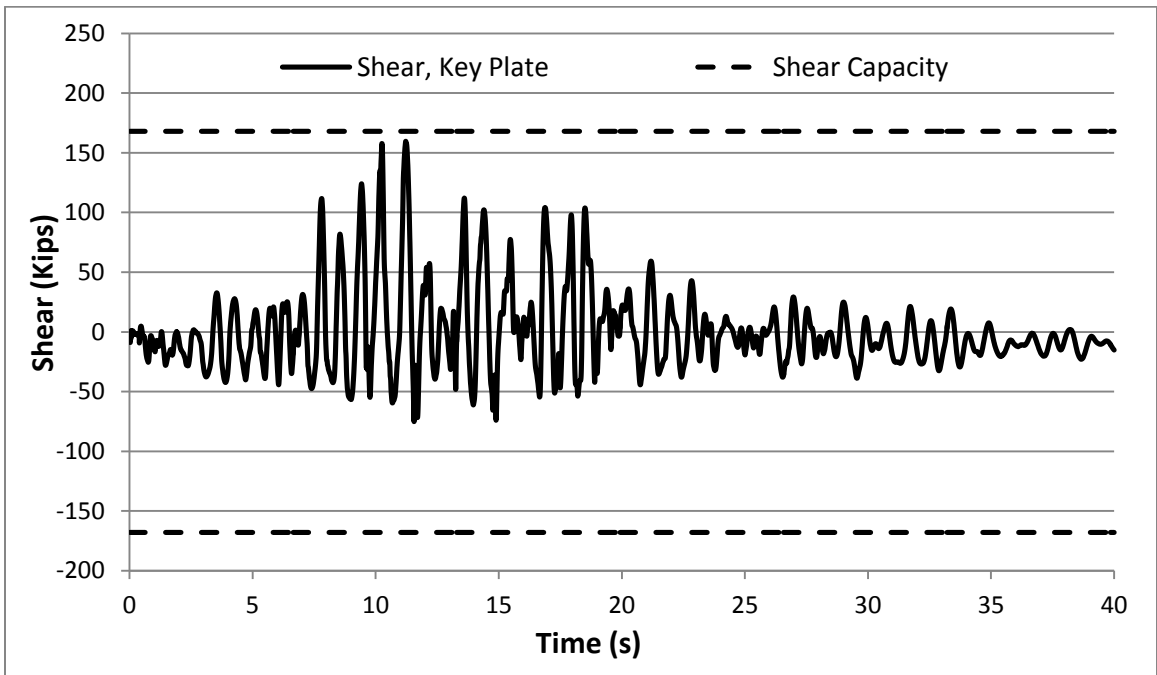


**Figure 3.15: Shear Force in Key Plates, Pier 3**

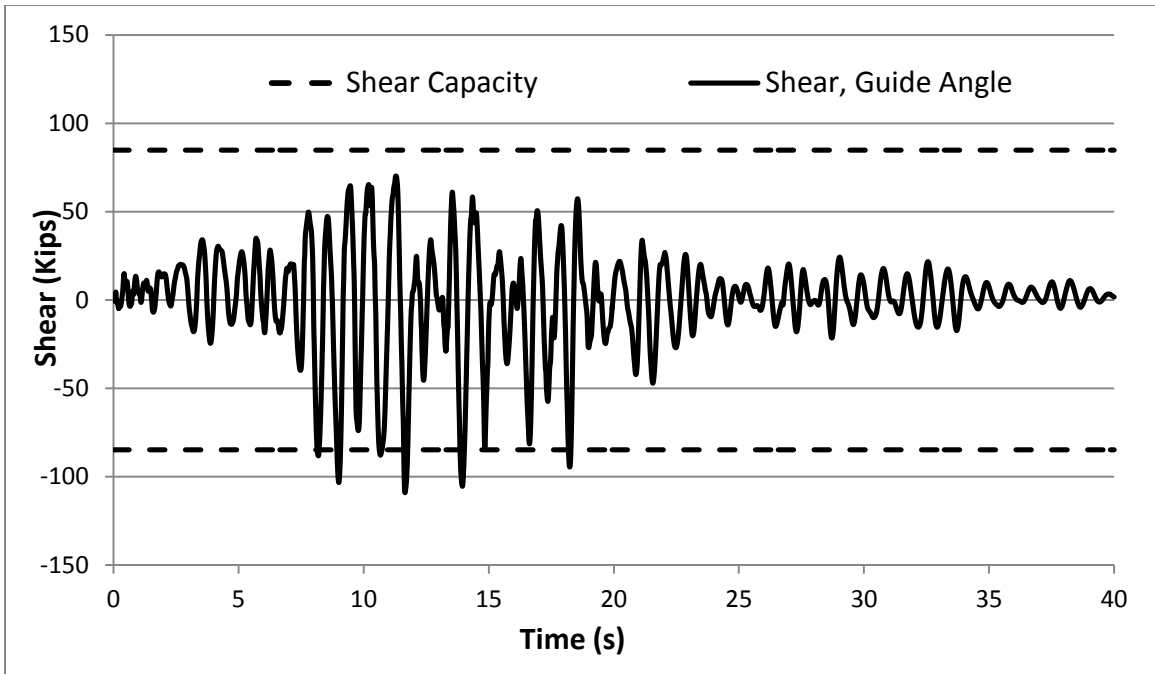


**Figure 3.16: Shear Force in Guide Angles, Pier 4**

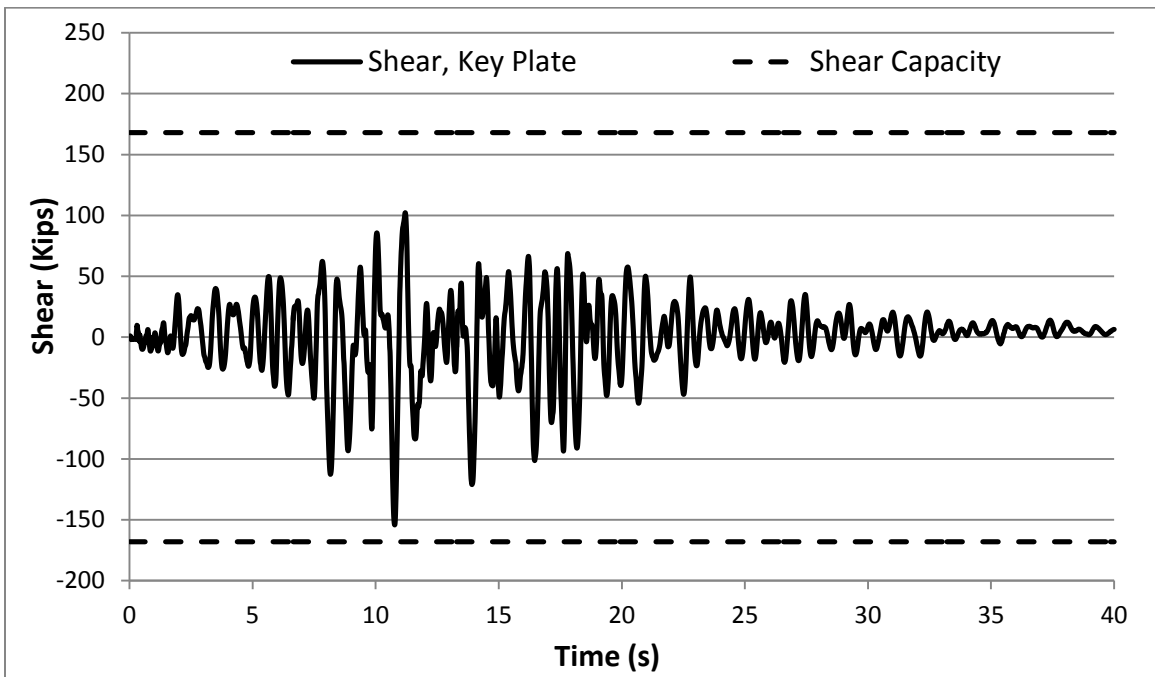


**Figure 3.17: Shear Force in Key Plates, Pier 5**

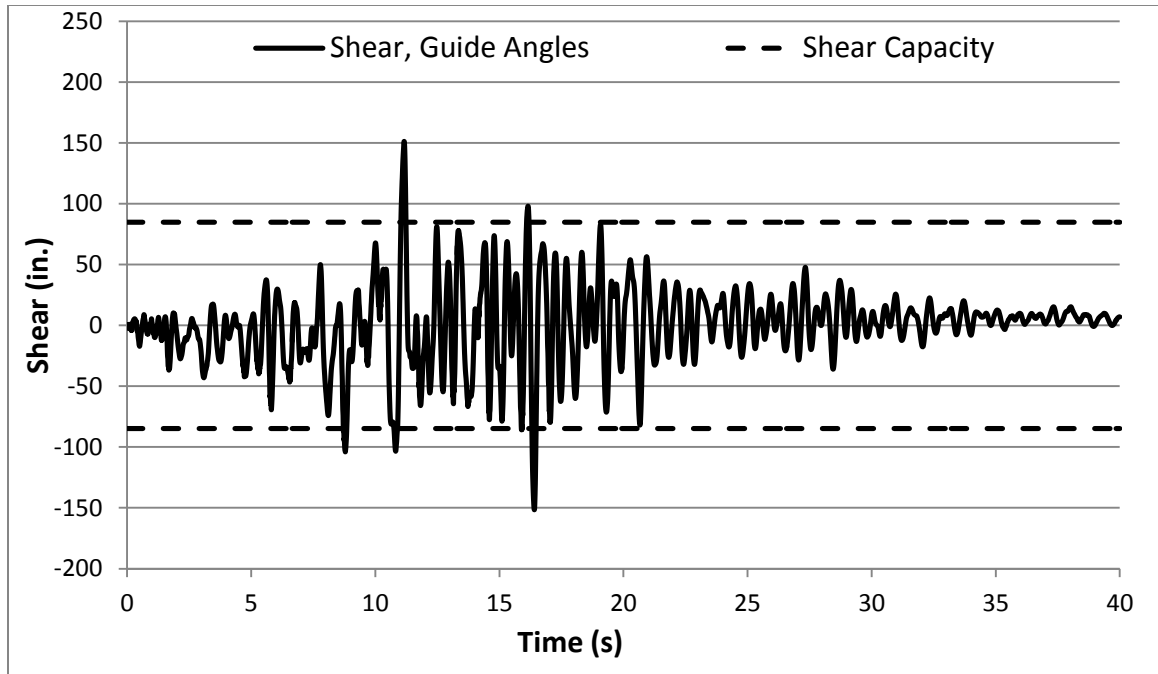


**Figure 3.18: Shear Force in Guide Angles, Pier 6**

As it can be seen from the above figures, the shear demand in guide angles in all locations exceeded their capacities whereas the shear demand in key plates does not reach their capacities. The guide angles on Pier 2 may fail because the shear demand exceeds the capacity by a large amount. Guide angles in other location may not fail, but may be deformed. Hence the superstructure may be still held in place by some of the restrainers.

To study the worst case scenario of the bridge vulnerability to the probable earthquake, another analysis was performed to see if the superstructure becomes unseated from the substructure by removing the key plates and guide angles in all locations leaving only the neoprene bearings. The total lateral displacement of the deck and the lateral relative displacement of the superstructure and top of the substructure were observed. Figures 3.19 to 3.22 show the results of the analysis.

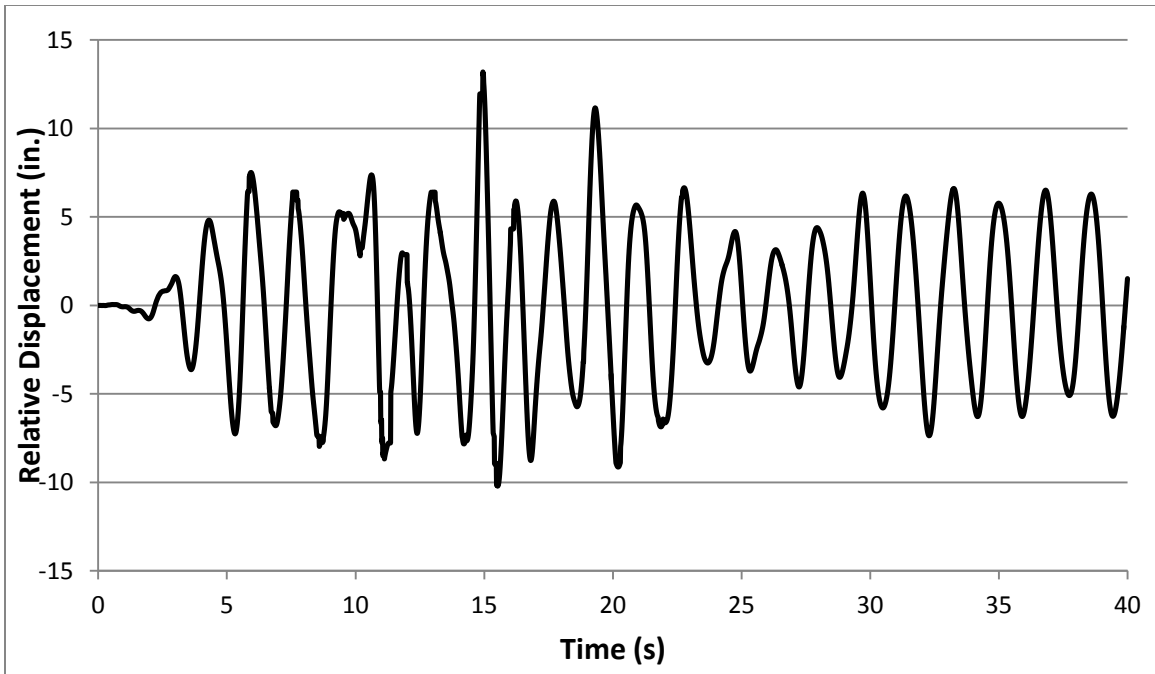


**Figure 3.19: Relative Displacement of Abutment 1 and Bridge Deck, Z-direction**

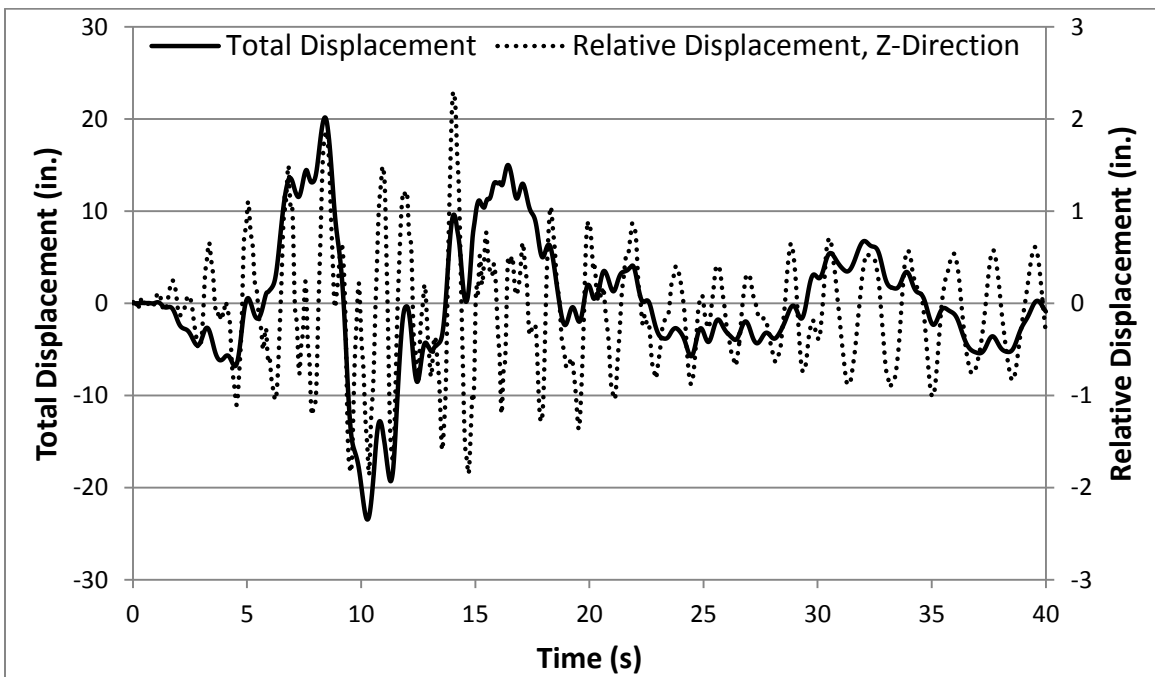


**Figure 3.20: Total Displacement of the Deck and the Relative Displacement of Deck and Top of the Pier 2, Z-Direction**

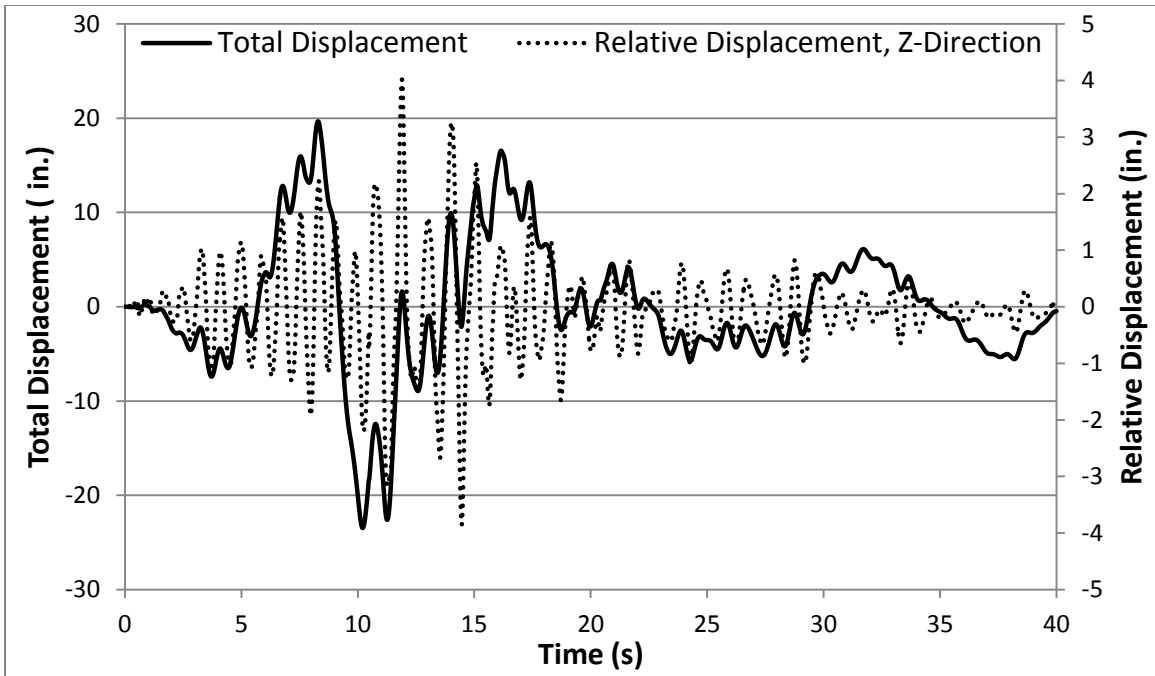


**Figure 3.21: Total Displacement of the Deck and the Relative Displacement of Deck and Top of the Pier 4, Z-Direction**

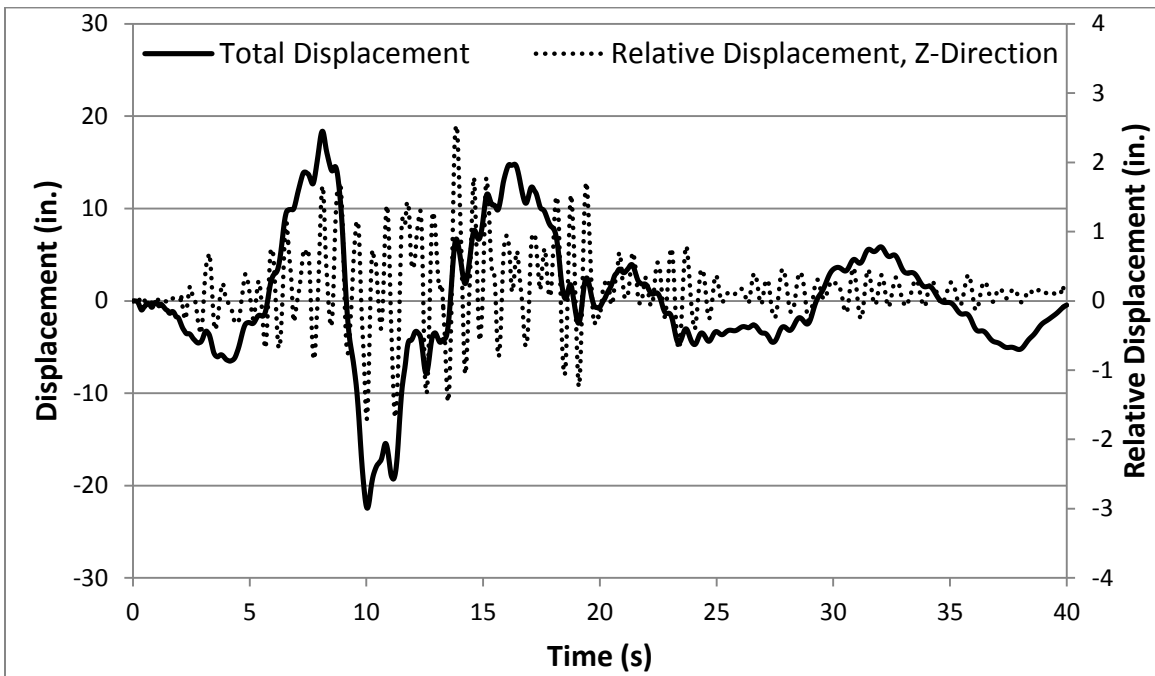


**Figure 3.22: Total Displacement of the Deck and the Relative Displacement of Deck and Top of the Pier 6, Z-Direction**

Figure 3.19 shows the maximum relative transverse displacement at Abutment 1 is approximately 13 in. It was also observed from the Figures 3.20, 3.21 and 3.22, that the maximum relative displacement of the deck to the top of the piers was about 4 in. The bridge box girders are 6 feet wide. Therefore, the bridge superstructure does not unseat from the piers in transverse direction. To see if the bridge superstructure becomes unseated in longitudinal direction, the relative displacement of the deck to the top of the Pier 4 was observed in X-direction. The longitudinal relative displacement of the deck and abutments were also observed. Followings are the results.

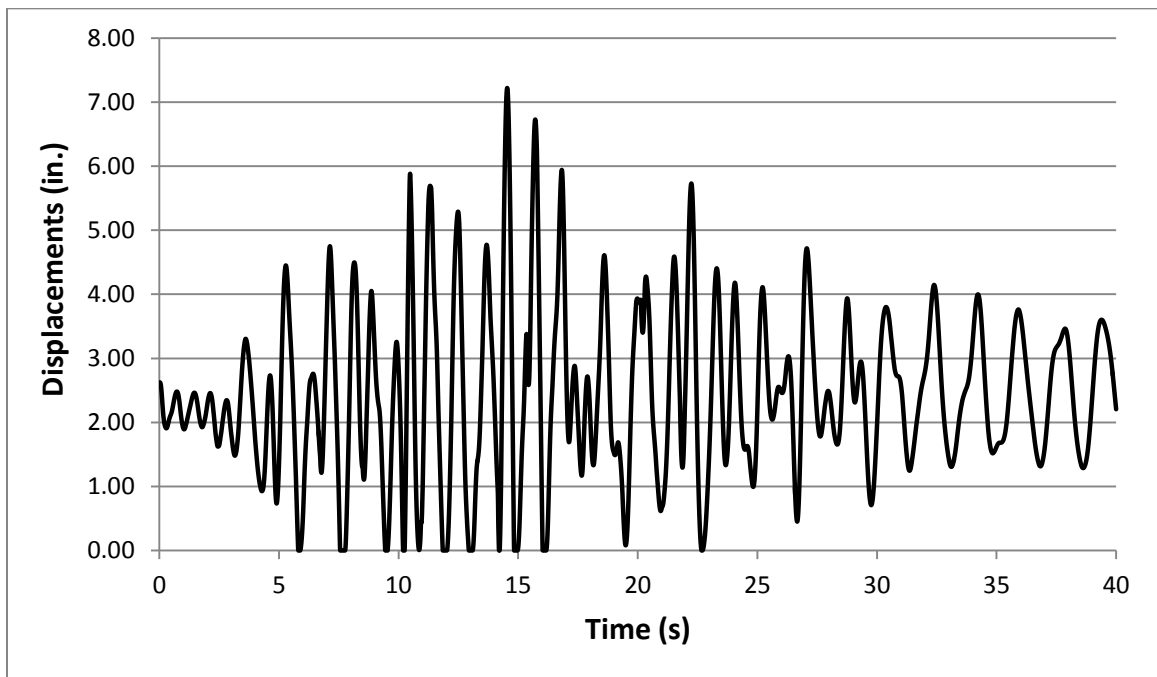


**Figure 3.23: Relative Displacement of Abutment 1 and Bridge Deck, X-Direction**

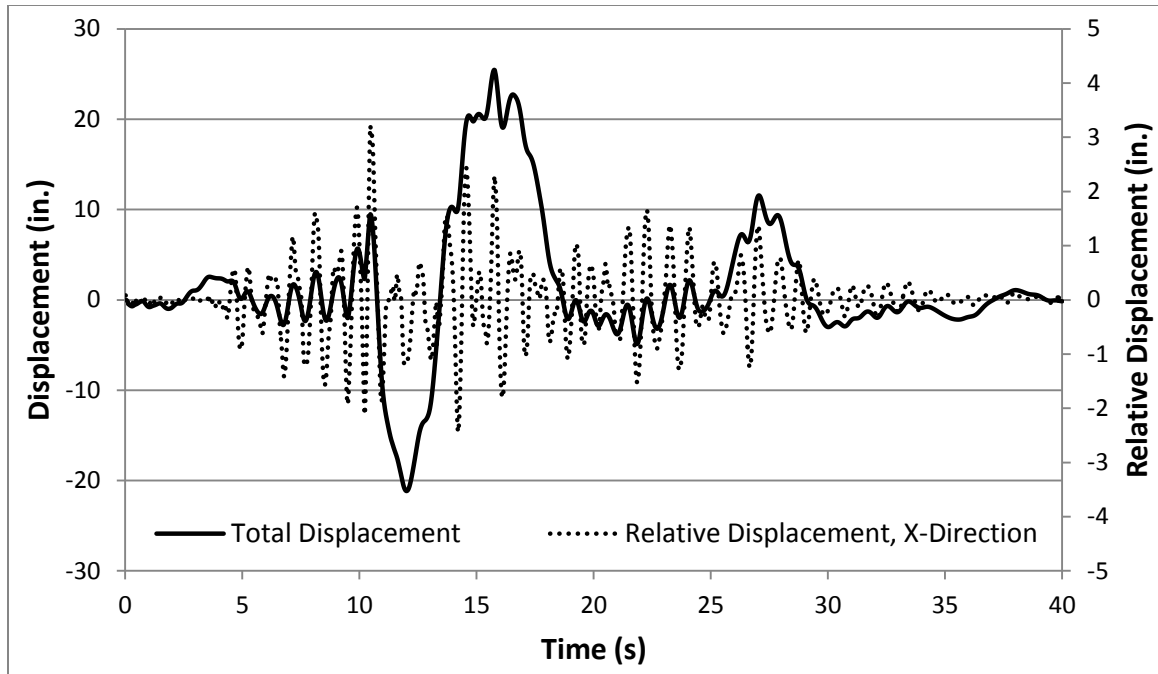


**Figure 3.24: Relative Displacement of the Deck to the Top of Pier 4, X-Direction**

The longitudinal relative displacement of the abutments and decks were observed. Figure 3.23 shows that the maximum relative displacement is 7.2 in. at Abutment 1. The maximum relative displacement of the deck to top of the Pier 4 where an expansion joint is located was observed to be less than 4 in. The relative displacement is less than the width (9.8 in.) on top of the pier available for decks to move freely. Hence, the bridge superstructure does not unseat from the substructure.

Now from the observation made, it has been shown that the bridge is unlikely to fail, but the bridge has to be in a good shape and position to be usable after an earthquake event. Hence, one more nonlinear time history analysis was performed using the same earthquake loading. This time the bridge was allowed to move freely for 40 seconds after the earthquake event. Then the relative displacement of the deck to their supports was

checked to see if there exists any residual displacement. Figure 3.25 shows the relative displacement of Abutment1 and deck for 80 seconds.

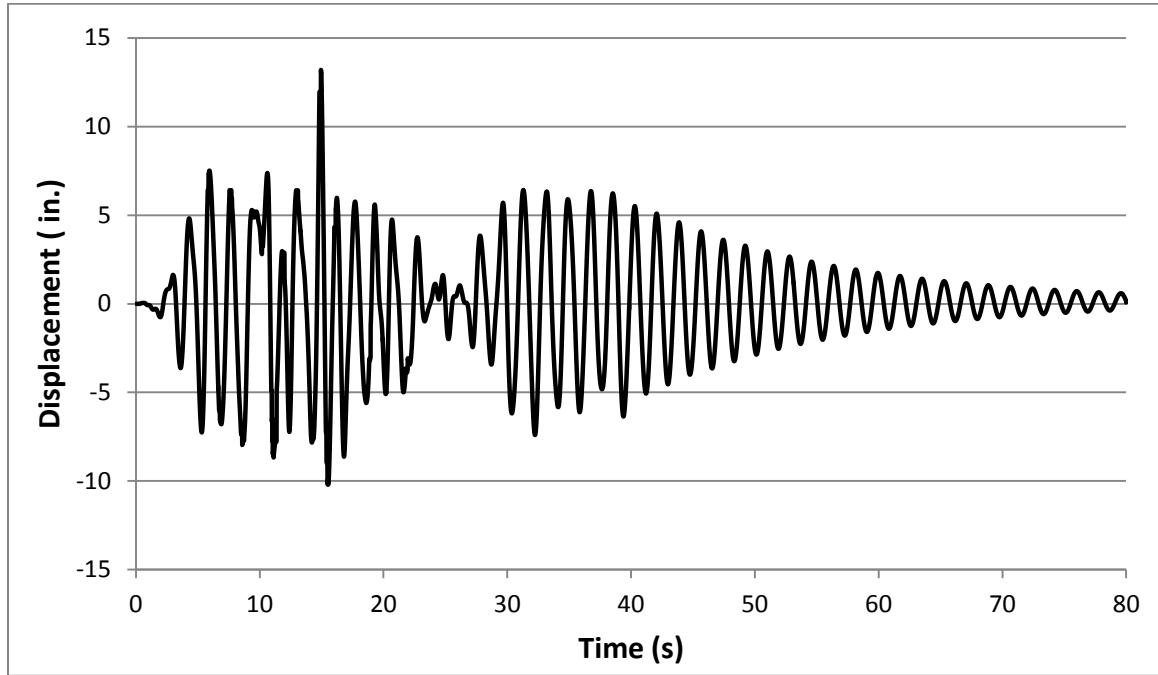


**Figure 3.25: Relative Displacement at Abutment 1, Z-direction, for a Total of 80 Seconds**

The relative displacement of the deck and Abutment 1 decreased to zero after the earthquake event. This shows that there does not exist residual displacement in transverse direction.

### **3.2 Sensitivity Analysis**

Sensitivity analysis was carried out for investigation of the bridge seismic response to certain input parameters. The input parameters considered for the study were compressive strength of concrete, damping constant of the bridge and coefficient of friction of contact elements. The bridge model with contact elements and gaps in all

expansion joints was used for the sensitivity study. Bidirectional Landers earthquake loadings were applied to each of the abutments and bottom of the piers. The results obtained from the bridge model by varying the input parameters values were considered for the sensitivity study.

Sensitivity of each parameter to the bending moment, shear force and displacement of Element 3 of Piers 2, 4 and 6 were studied. The relative displacement of the top and bottom of the Element 3 of piers was considered to evaluate the sensitivity of the input parameters to displacement of the pier element. The Root Mean Square (RMS) values of the bridge responses from 5 to 20 seconds were used for the sensitivity study. The reason for using RMS values for the 15-second interval considered was based on the fact that the bridge response is the greatest during this time period. The RMS values will not be affected by the localized peaks which for seismic analysis are very unpredictable. Results obtained from the analyses are shown in Figures 3.26 through 3.34.

Figures 3.26, 3.27, and 3.28 show the result obtained for the sensitivity analysis of bending moment, shear force and displacement of Element 3 of Piers 2, 4 and 6 respectively to compressive strength of concrete. Similarly Figures 3.29, 3.30 and 3.31 present the results obtained for the sensitivity analysis of the bridge response to coefficient of friction of contact elements. Finally, Figures 3.32, 3.33 and 3.34 present the results obtained for sensitivity analysis of the bridge response to damping constant of the bridge system.

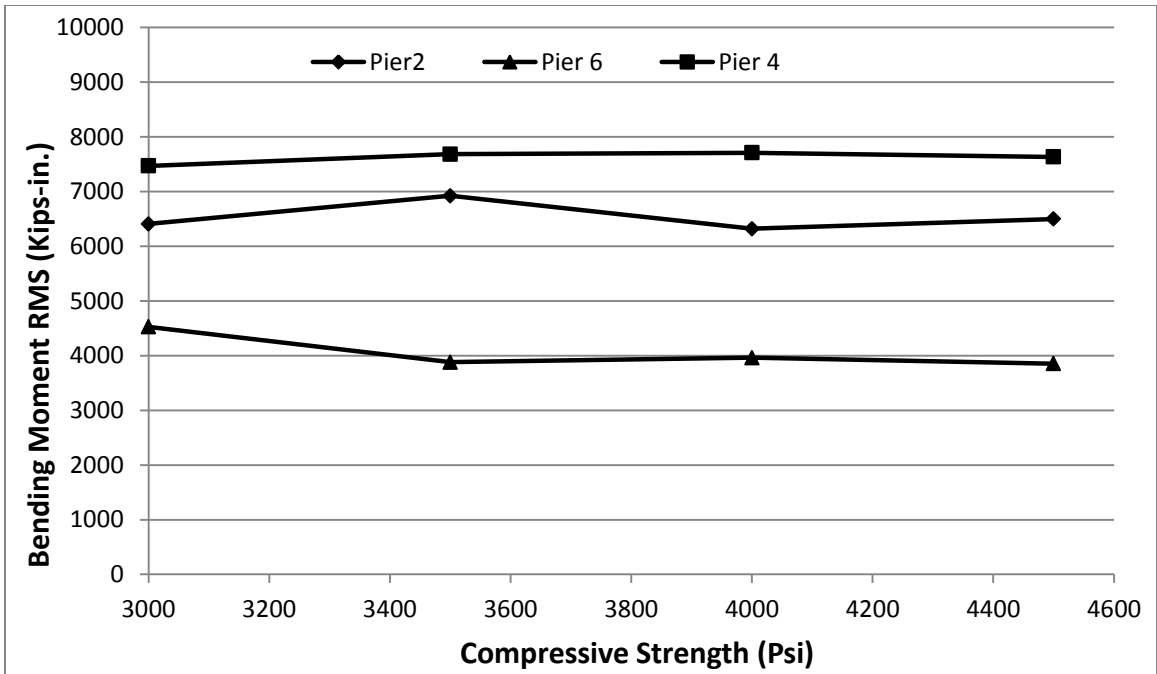


Figure 3.26: Sensitivity of Bending Moment to Compressive Strength of Concrete

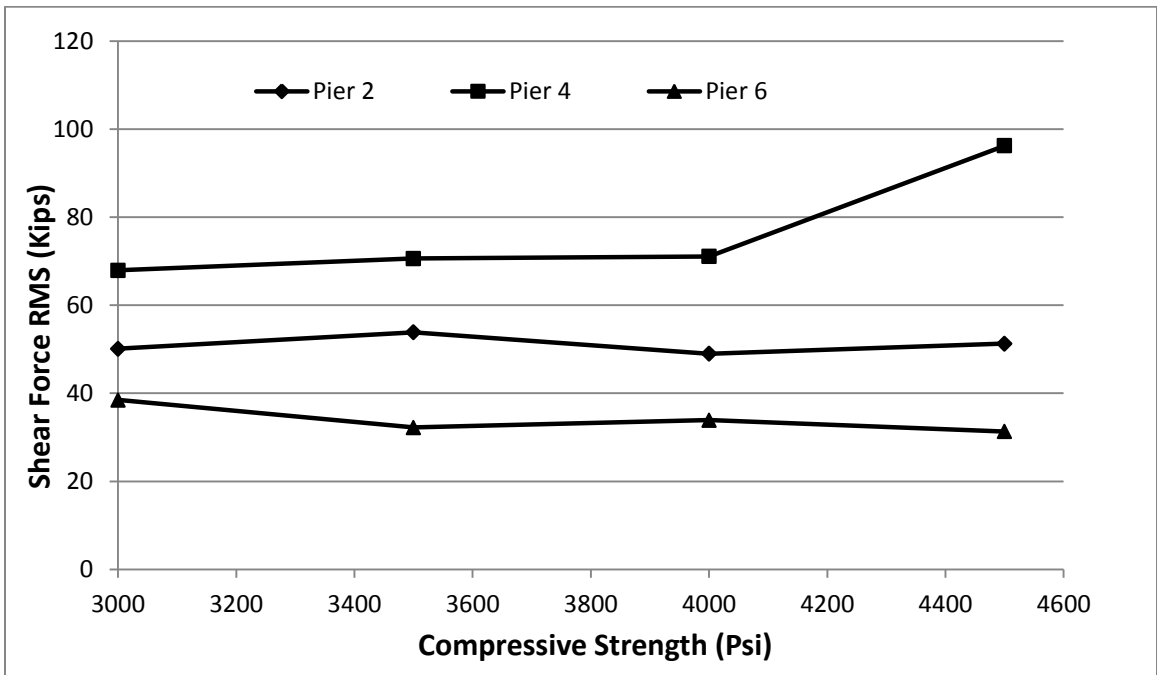
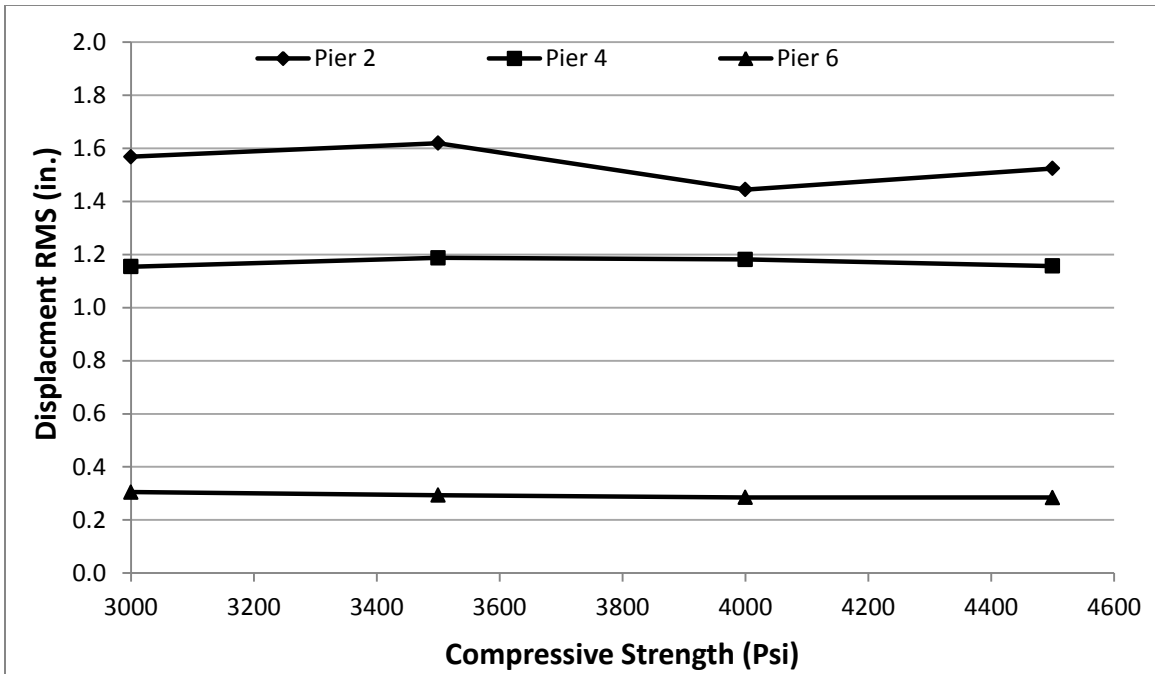
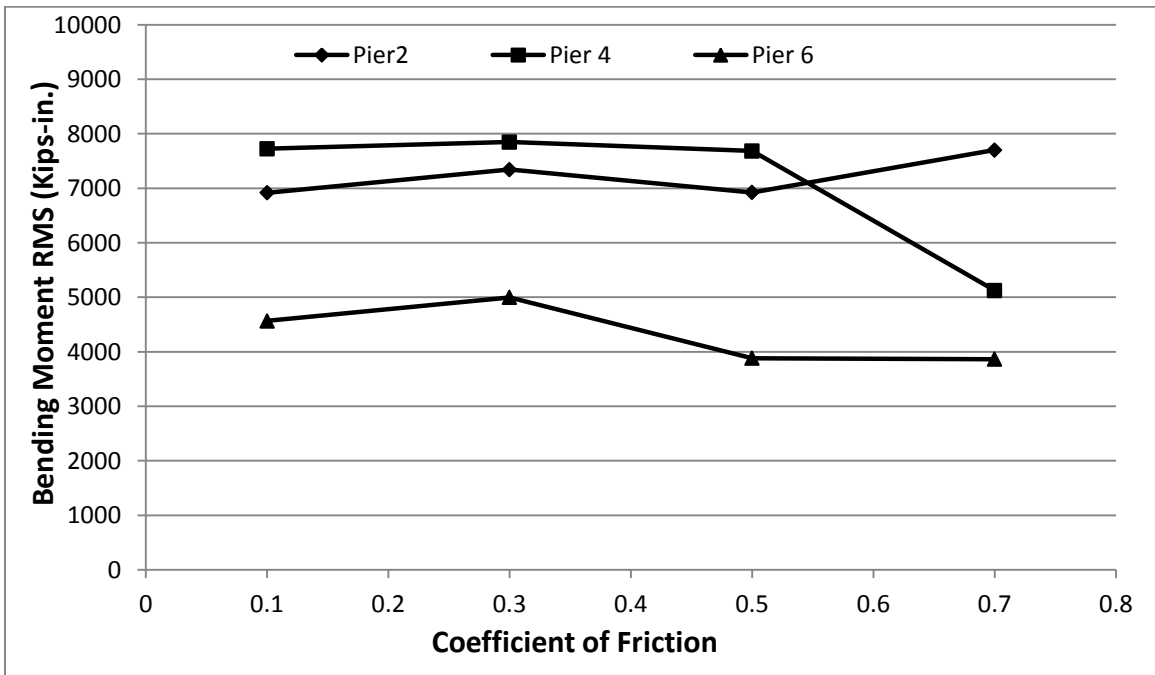


Figure 3.27: Sensitivity of Shear Force to Compressive Strength of Concrete



**Figure 3.28: Sensitivity of Displacement to Compressive Strength of Concrete**



**Figure 3.29: Sensitivity of Bending Moment to Coefficient of Friction of Contact Element**

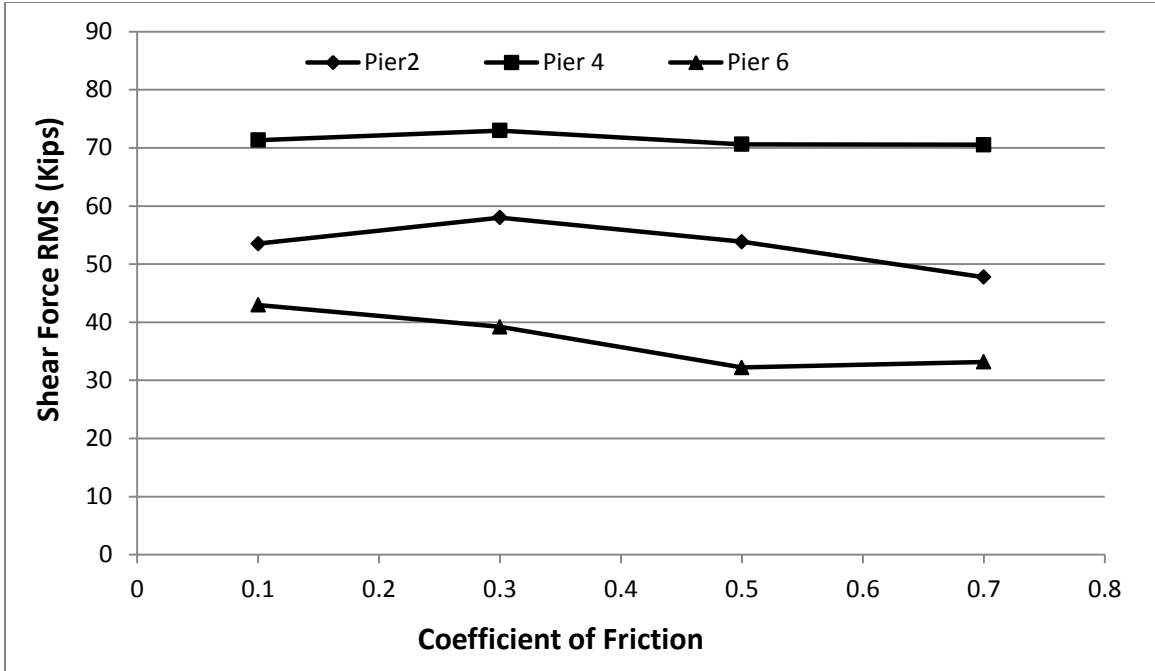


**Figure 3.30: Sensitivity of Shear Force to Coefficient of Friction of Contact Elements**

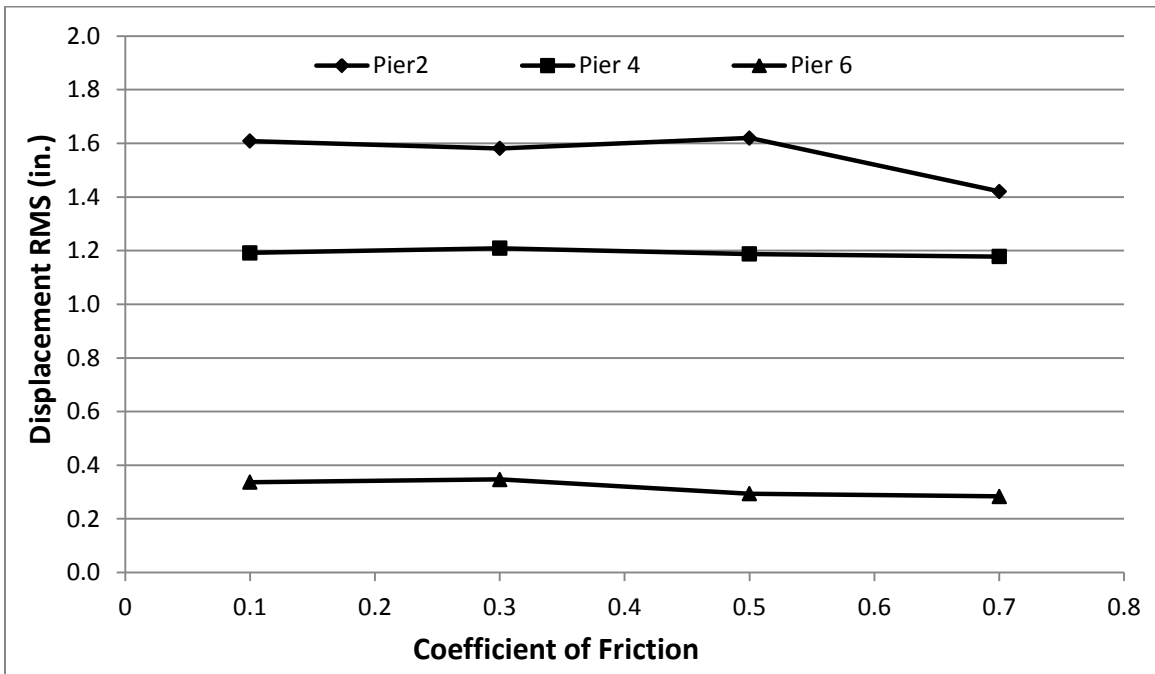


**Figure 3.31: Sensitivity of Displacement to Coefficient of Friction of Contact Elements**

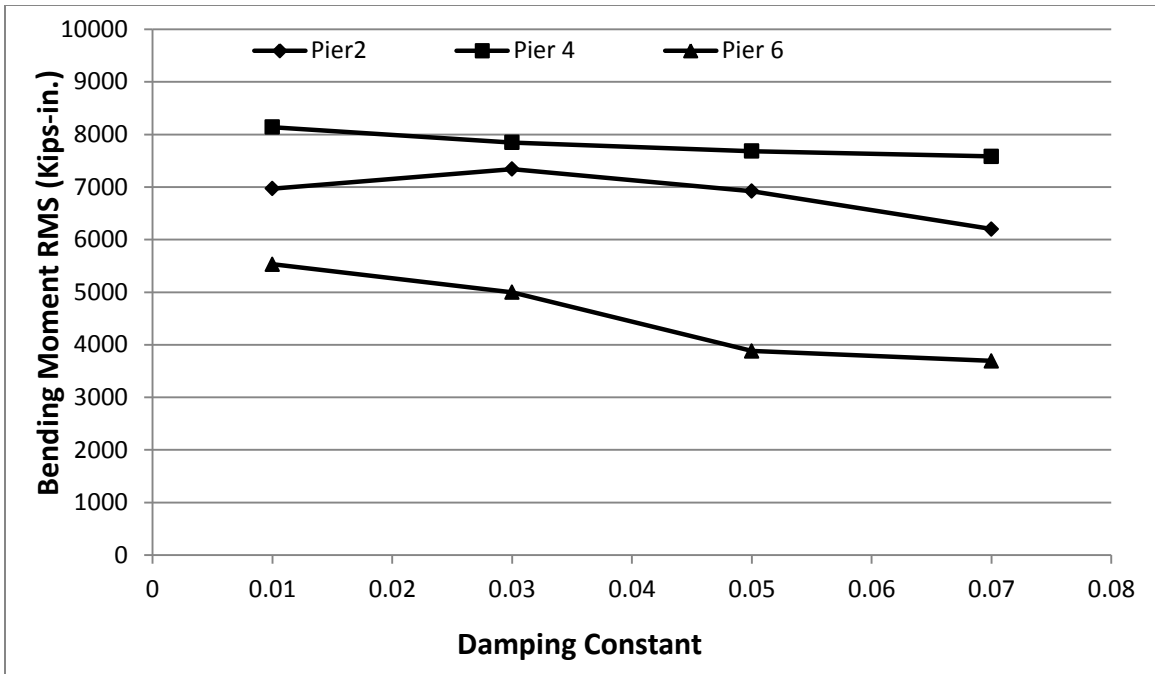


**Figure 3.32: Sensitivity of Bending Moment to Damping Constant**

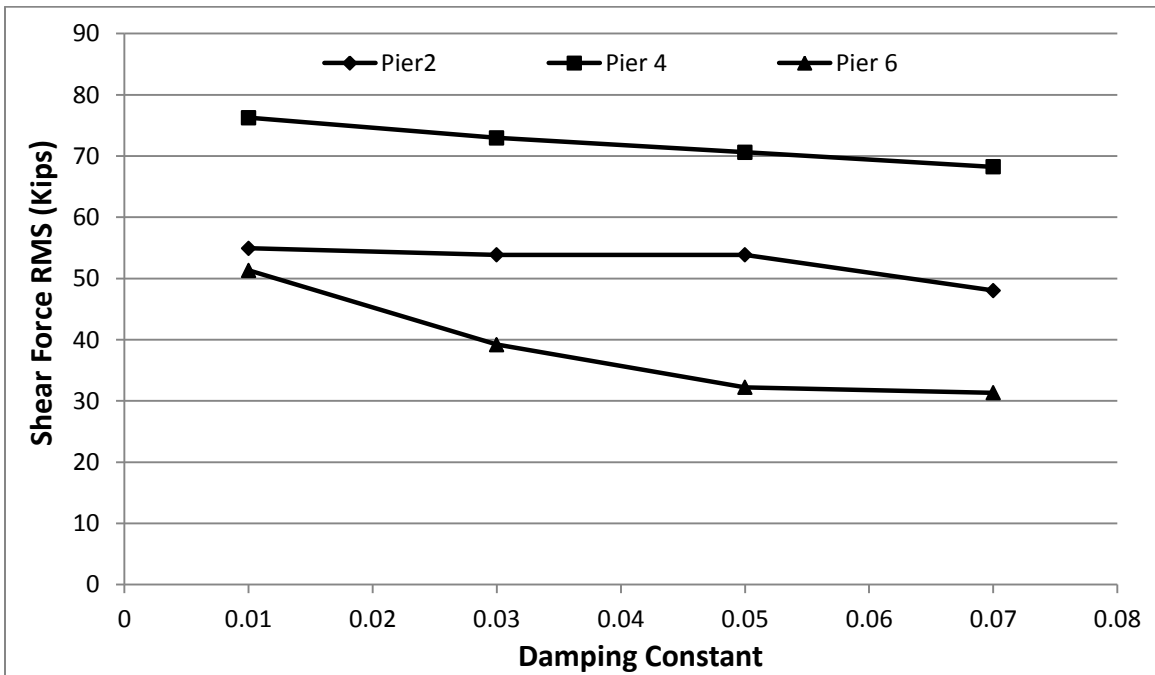


**Figure 3.33: Sensitivity of Shear Force to Damping Constant**

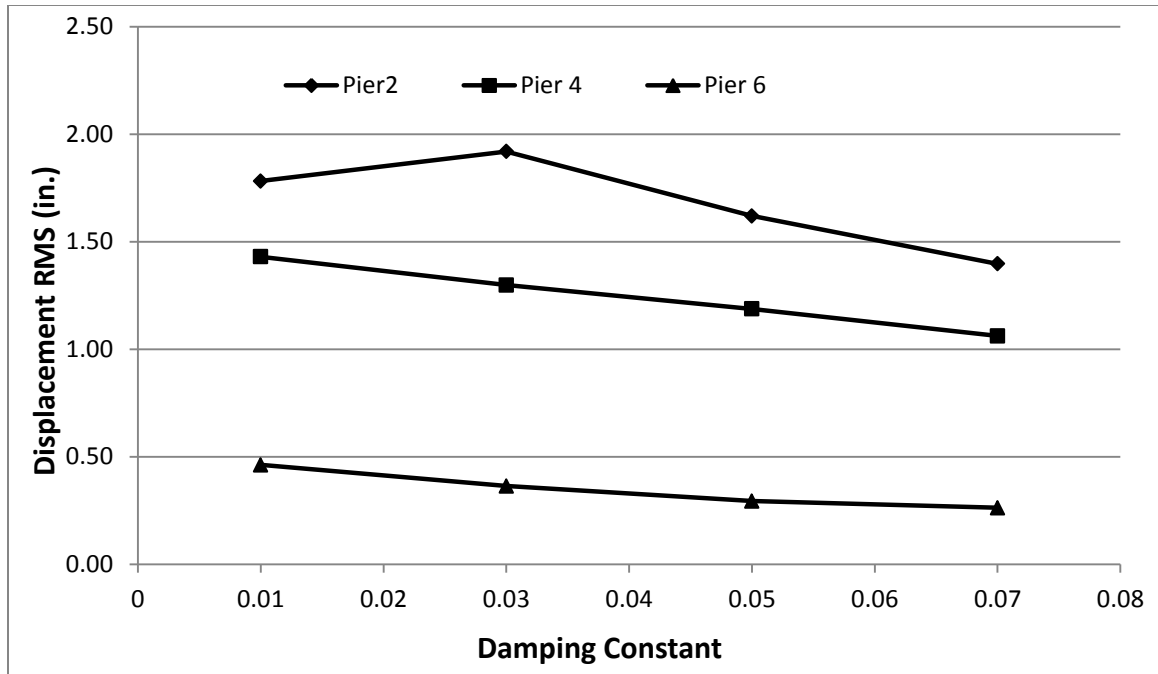


**Figure 3.34: Sensitivity of Displacement to Damping Constant**

From the above figures, it can be concluded that the damping constant affects all the bridge responses more than the other two parameters. The changes in the bending moment, shear force and displacement of the element are larger in case of the damping constant. On the average, the bridge response decreased with the increasing damping constant of the bridge. However the coefficient of friction did not have much effect on the responses as they remained approximately constant for all range of values. Compressive strength of concrete ranging from 3000 to 4500 psi did not have significant effect on the bridge responses, as well.

## CHAPTER 4

### DISCUSSION

The Washington Street Overpass was built in 1971 prior to the major changes in seismic design code. The bridge being situated in a seismically active region of Idaho, a study was conducted to investigate the performance of the bridge during a probable earthquake event using *AASHTO Guide Specifications for LRFD Seismic Bridge Design* (2009). OpenSees software was used to develop an analytical three-dimensional bridge model.

The OpenSees bridge model with all the bridge components was subjected to the bidirectional lateral Landers earthquake loading; it indicated that the internal forces induced in pier elements due to the earthquake motion were not large enough to cause the collapse of the bridge. Internal forces in Piers 2, 4 and 6 were evaluated for the analysis.

Elements of Pier 4 had the maximum bending moment, shear force and displacement ductility. The Bending moment demand to capacity ratio was 1.1 which shows that the bending moment did not exceed the capacity by a large amount. The shear force in Pier 4 reaches the capacity but does not exceed the capacity. The bending moment and shear force induced fail to form failure mechanism like a plastic hinge, but the Pier 4 elements exhibit inelastic deformation as the displacement ductility was more than 1 (1.5).

Shear force in the lateral restrainers that hold the superstructure in place was evaluated and found that the guide angles' shear demand exceeded their capacity. Guide angles on Pier 2 may fail as the shear force excessively exceeded the capacity; however

the guide angles in other locations may not fail. Shear force induced in key plates of all the locations did not exceed their capacity. Hence the superstructure is likely to stay in place by the restrainers.

To evaluate the extreme case of the earthquake damage to the bridge system, another analysis was performed. This second analysis was performed on the same bridge but removing all the restrainers (guide angles and key plates) except neoprene bearings. This enables the superstructure to move with less constraint on top of the piers and abutments. The relative displacement of the deck segments and top of the piers and abutments in both longitudinal and transverse direction was evaluated which showed that the superstructure does not become unseated from the supports.

The maximum transverse relative displacement of the deck with respect to the substructure was approximately 13 in. at Abutment 1 which is not enough to unseat the 6 feet wide girder from the abutment. The maximum longitudinal relative displacement was about 7 in. which also occurred at Abutment 1. The displacement was less than the width (9.8 in.) available at the abutment to allow the deck to move freely. The analysis shows that the superstructure is unlikely to become unseated from the substructure.

The bridge was subjected to the earthquake loading and allowed to move freely after the earthquake event for 40 seconds more. The relative displacement of the deck to their support in the transverse direction was analyzed and found that there was no residual displacement indicating the bridge comes back to the original position after the earthquake event. There may be minor damages on the bridge restrainers and piers, which has to be repaired after the earthquake event.

It was noted that the implementation of the contact element and gaps in all the expansion joints do not make significant difference in the bridge response due to the earthquake loading.

To specify the damage level that the bridge experienced after the earthquake event, the HAZUS-MH MR3 Technical Manual [10] by Federal Emergency Management Agency (FEMA) was referred. HAZUS-MH MR3 classifies the bridge damage into five states. These are none (ds1), slight/minor (ds2), moderate (ds3), extensive (ds4) and complete (ds5). More specifically, ds3 is defined by “any column experiencing moderate (shear cracks) cracking and spalling (column structurally still sound), moderate movement of the abutment (<2 in.), extensive cracking and spalling of shear keys, any connection having cracked shear keys or bent bolts, keeper bar failure without unseating, rocker bearing failure or moderate settlement of the approach.” The damage state ds4 is defined by “any column degrading without collapse – shear failure - (column structurally unsafe), significant residual movement at connections, or major settlement approach, vertical offset of the abutment, differential settlement at connections, shear key failure at abutments.” The damage state ds5 is defined by “any column collapsing and connection losing all bearing support, which may lead to imminent deck collapse, tilting of substructure due to foundation failure.” For the bridge under consideration, ds5 is likely not to apply. However, the level of damage is more likely to be either ds3 (moderate) or ds4 (extensive).

Further sensitivity analyses were performed to evaluate the sensitivity of the bridge response to selected input parameters when subjected to the earthquake loading. The selected input parameters for sensitivity analysis were the 28-day compressive

strength of concrete, the coefficient of friction of the contact elements, and the damping constant of the bridge. From the analysis it was found that the damping constant affected the bridge response the most. The other two parameters did not cause significant changes in the bridge response.

## CHAPTER 5

### CONCLUSION

This chapter provides the conclusions drawn from this research and recommendations for future research.

#### 5.1 Conclusions of the Research

##### 5.1.1 Seismic Analysis

From the seismic analysis performed for the concrete and steel Washington Street Overpass, the following conclusions have been drawn.

- A probable seismic ground motion with a 1,033-year return period is likely not cause the bridge collapse by failing the piers or by unseating the superstructure from its supports.
- Pier 4 is likely to deform permanently from the observation of displacement ductility demand, but it is likely not collapse.
- Guide angles are likely to fail leaving key plates as the only lateral movement restrainers for the superstructure.
- Residual transverse displacement of the superstructure relative to the support is unlikely. Hence, there is a good chance that the bridge will be usable immediately after the earthquake event. However, minor damages in the bridge have to be repaired.
- Based on these information and damage states described in HAZUS-MH MR3 Technical Manual by FEMA, the bridge damage is likely to be ds3 (moderate) or ds4

(extensive). There is the possibility that the bridge may not be usable by vehicles without repair.

### **5.1.2 Response of the Model With Contact Elements Versus the Bridge Model**

#### **Without Contact Elements**

For the research presented here, the improved bridge model (i.e., the model with contact element and gaps in all locations) was subjected to the Landers earthquake loading. The response obtained was compared to the response obtained from the first phase of this project (i.e., the bridge model without contact elements and gaps in expansion joints). There were no significant changes in the responses of the two bridge models.

### **5.1.3 Sensitivity Analysis**

Sensitivity analyses were performed in order to determine the parameters that have the most influence on the bridge seismic response. The input parameters selected for the study were compressive strength of concrete, coefficient of friction of contact elements and damping constant of the bridge system. The damping constant affects the bridge response, whereas the other two input parameters did not have much effect on the response.

## **5.2 Future Research Recommendations**

This research provided the degree of vulnerability of the bridge incorporating the simulation of the interaction of the adjacent parts of the structure when subjected to the ground motion which are scaled to the site response spectrum. This research also

provided an understanding of the seismic behavior of the bridge to some parameters by conducting sensitivity analysis. Future research may include the following.

- Consideration of the vertical component of the ground motion along with longitudinal and transverse components could give more accurate response of the bridge. For the research presented here, inclusion of all three components of Landers earthquake was tried, but there were numerical issues which could not be resolved.
- Use of more appropriate OpenSees elements for modeling the bridge components could provide better bridge response. In future “*Elastic-Perfectly Plastic Material*” could be used for modeling the guide angles and key plates of the bridge. This material deforms plastically when yield occurs in tension and compression.

## REFERENCES

1. AASHTO, *Guide Specifications for LRFD Bridge Design*, Washington, DC, 2009.
2. American Society of Civil Engineers (ASCE), *Minimum Design Loads for Buildings and other Structures*, ASCE/SEI 7-05, Reston, VA, 2006.
3. Arora, J. S., and Haug, E. J., "Methods of Design Sensitivity Analysis in Structural Optimization," *AIAA Journal*, Vol. 17, No. 9, 1979, pp. 970-974.
4. Caltrans, *Bridge Design Practice*, 1995, Section 8, "Seismic Analysis of Bridge Structures".
5. Cooper, J. D., Reilly, R. J., and Vumbaco, J. B. "FHWA R&D Program Produces Major Improvements in Seismic Design of Highway Bridges," U. S. Department of Transportation, 1983.
6. DesRoches, R., and Muthukumar, S., "Implications of Seismic Pounding on the Longitudinal Response of Multi-span Bridges-an Analytical Perspective," *Earthquake Engineering and Engineering Vibration*, Vol. 3, No. 1, 2004, pp. 57-65.
7. Dryden, G. M., and Fenves, G. I., "The Integration of Experimental and Simulation Data in the Study of Reinforced Concrete Bridge Systems Including Soil-Foundation-Structure Interaction." PEER Report 2009/03, College of Engineering, University of California, Berkeley, 2009.
8. Fishman, K. L., and Richards, R., "Seismic Analysis and Design of Bridge Abutments Considering Sliding and Rotation," *Report NCEER, 97-0009*, Buffalo, New York, 1997.

9. Hamby, D. M., "A Review of Techniques for Parameter Sensitivity Analyses of Environmental Models." *Environmental Monitoring and Assessment*, No. 32, 1994, pp. 135-154.
10. HAZUS-MH MR3 Technical Manual, Multi-hazard Loss Estimation Methodology, Washington, D.C., 2003.
11. Idaho Transportation Department (ITD), "720' Steel & Concrete Overpass US. 89 (Washington St.) Over U.P.R.R. and 12th St," State of Idaho Department of Highways, 20 May, 1970.
12. Itani, A. M., and Pekcan, G., "Seismic Performance of Steel Plate Girder Bridges with Integral Abutments," *Report No. FHWA-HIF-11-043*, Department of Civil And Environmental Engineering, University of Nevada, Reno, 2011.
13. Karantzikis, M. J., and Spyrakos, C. C., "Seismic Analysis of Bridges Including soil-Abutment Interaction." 12WCEE, 2000.
14. Kunnath, S., Heo, Y., and Mohle, J., "Nonlinear Uniaxial Material Model for Reingforcing Steel Bars," *Journal of Structural Engineering*, Vol. 135, No. 4, 2009, pp. 335-343.
15. Lou, L., "Effect of the Spatial Variability of Ground Motions on the Seismic Response of Reinforced Concrete Highway Bridges," Doctoral Dissertation, Drexel University, 2006.
16. Mackie, K. and Stojadinovic, B., "Bridge Abutment Model Sensitivity for Probabilistic Seismic Demand Evaluation," University of California, Berkeley, CA, 2002.

17. Mander, J. B., Priestley, M. J. N., and Park, R., "Theoretical Stress-Strain Model for Confined Concrete," *Journal of the Structural Division, American Society of Civil Engineers*, Vol. 114, No. 8, 1988, pp. 1804-26.
18. Miller, A., Ebrahimpour, A., and Shrestha, N., "Seismic Performance of a Four-Decade-Old Overpass in Southeast Idaho." *Journal of Performance of Constructed Facilities, American Society of Civil Engineers*, CF.1943-5509.0000486, June 13, 2013.
19. Miller, A. L., "Seismic Analysis of US-89 Overpass at Union Pacific Railroad in Montpelier, Idaho." M.S. thesis, Department of Civil and Environmental Engineering, Idaho State University, Pocatello, Idaho, 2012.
20. PEER Ground Motion Database, Pacific Earthquake Engineering Research Center, [http://peer.berkeley.edu/peer\\_ground\\_motion\\_database](http://peer.berkeley.edu/peer_ground_motion_database). accessed on June 2011.
21. Pietra, D., "Evaluation of Pushover Procedures for the Seismic Design of Buildings," M.S. Thesis, Earthquake Engineering, Rose School, 2008.
22. Priestley, M. J. N., Seible, F., and Calvi, M., *Seismic Design and Retrofit of Bridges*, John Wiley and Sons, Inc., New York, 1996.
23. Spears, R. E., "Unique Method for Generating Design Earthquake Time Histories," *American Society of Mechanical Engineers (ASME) Pressure Vessels and Piping Division Conference*, Chicago, 2008.
24. Symans, M.D., Shatterat, N.K., McLean, D.I., and Cofer, W.F., "Evaluation of Displacement-Based Methods and Computer Software for Seismic Analysis of Highway Bridges," *Washington State Transportation Center (TRAC)*, 2003.

25. University of California Berkeley, “OpenSees: Open System for Earthquake Engineering Simulations,” 2006, <http://opensees.berkeley.edu>.
26. “Visual Catalog of Reinforced Concrete Bridge Damage,” California Department of Transportation Structure Maintenance and Investigations, June 20, 2006.
27. Vosooghi, A., and Buckle, I. G., “Evaluation of the Performance of a Conventional Four-Span Bridge During Shake Table Tests,” *Report No. CCEER-13-02*, University of Nevada, Reno, January 2013.
28. Zadeh, M. S., and Saiidi, M. S., “Pre-test Analytical Studies of NEESR-SG 4-Span Bridge Model Using OpenSees,” *Report No. CCEER-07-3*, Department of Civil Engineering, University of Nevada, Reno, 2007.

## **APPENDIX**

## Appendix A: Confined Concrete Properties Calculations

As recommended by the AASHTO *Guide Specifications for LRFD Bridge Design* Mander's model is used for determining the confined concrete properties of piers. Following procedures and Equations C.1 through C.7 are followed to determine the appropriate confined concrete properties.

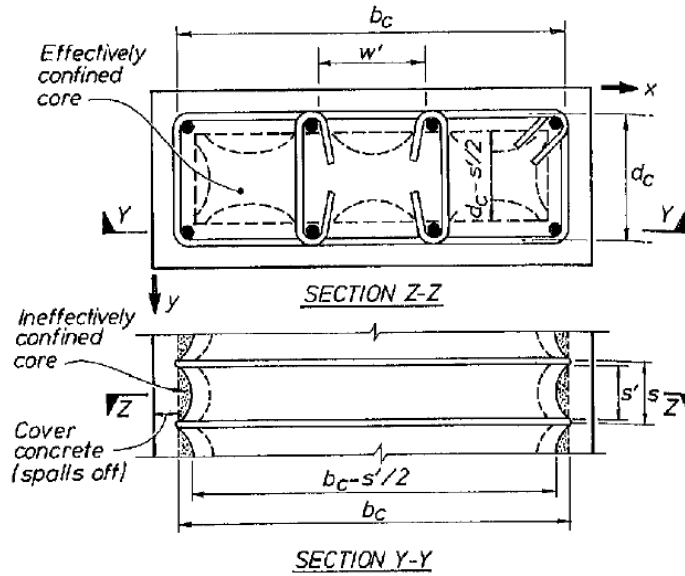


Figure A. 1: Confined Core Rectangular Hoop Reinforcement [17]

$$k_e = \frac{\left(1 - \sum_{i=1}^n \frac{(w'_i)^2}{6b_c d_c}\right) \left(1 - \frac{s'}{2b_c}\right) \left(1 - \frac{s'}{2d_c}\right)}{1 - \rho_{cc}} \quad (C.1)$$

Where,

$w'_i$  -  $i$ th clear distance between adjacent longitudinal bars

$b_c$  - Largest core dimension to centerline of perpendicular hoop

$d_c$  - Smallest core dimension to centerline of perpendicular hoop

$s'$  - Clear vertical spacing between spiral or hoop bars

$\rho_{cc}$  – Ratio of area of longitudinal reinforcement to area of core of section

$$f_l = \frac{f_{yh}}{s} \left( \frac{A_{sx}}{d_c} + \frac{A_{sy}}{b_c} \right) \quad (C.2)$$

Where,

$f_{yh}$  - Yield strength of transverse reinforcement

$s$  – Center to center spacing or pitch of hoop

$A_{sx}$  – Total area of transverse bars running in x – direction

$A_{sy}$  – Total area of transverse bars running in y – direction

$$f'_l = f_l * k_e \quad (C.3)$$

$$k_1 = -1.254 + 2.254 \sqrt{1 + \frac{7.94 f'_l}{f'_{co}}} - \frac{2 f'_l}{f'_{co}} \quad (C.4)$$

Where,

$f'_{co}$  – Maximum strength of cover concrete

$$f'_{cc} = f'_{co} * k_1 \quad (C.5)$$

Where,

$f'_{cc}$  – Maximum strength of confined concrete

$$k_2 = 1 + 5 \left( \frac{f'_{cc}}{f'_{co}} - 1 \right) \quad (C.6)$$

$$\varepsilon_{cc} = \varepsilon_{co} * k_2 \quad (C.7)$$

Where,

$\epsilon_{cc}$  - Strain at maximum strength of confined concrete

$\epsilon_{co}$  - Strain at maximum strength of cover concrete

**Table A. 1: Element Concrete Properties for 3500 psi 28- day Compressive Strength**

<b>Pier</b>	<b>Element</b>	<b>Max. compressive Strength, fpc (psi)</b>	<b>Strain at Max. Strength, epsc0</b>
2	1	4686	0.002298
	2,3	4819	0.002591
	4a,b,d,e	5064	0.00313
	4c	4768	0.002479
3	1	4680	0.002285
	2,3	4815	0.002582
	4a,b,d,e	5064	0.00313
	4c	4768	0.002479
4	1	4667	0.002257
	2,3	4792	0.002531
	4a,b,d,e	5037	0.003069
	4c	4761	0.002464
5	1	4674	0.002273
	2,3	4792	0.002532
	4a,b,d,e	5064	0.00313
	4c	4768	0.002479
6	2,3	4792	0.002532
	4a,b,d,e	5064	0.00313
	4c	4768	0.002557
<b>Crushing Strength, fpcu</b>		0.7*fpc	
<b>Strain at Crushing Strength, epsu</b>		0.01	

**Table A. 2: Element Concrete Properties for 4000 psi 28-day Compressive Strength**

<b>Pier</b>	<b>Element</b>	<b>Max. compressive Strength, fpc (psi)</b>	<b>Strain at Max. Strength, epsc0</b>
2	1	5336	0.002261
	2,3	5469	0.002518
	4a,b,d,e	5717	0.002994
	4c	5418	0.00242
3	1	5350	0.002249
	2,3	5466	0.002511
	4a,b,d,e	5717	0.002994
	4c	5418	0.00242
4	1	5317	0.002225
	2,3	5442	0.002466
	4a,b,d,e	5689	0.00294
	4c	5411	0.002406
5	1	5324	0.002239
	2,3	5443	0.002467
	4a,b,d,e	5717	0.002994
	4c	5418	0.00242
6	2,3	5443	0.002467
	4a,b,d,e	5717	0.002994
	4c	5418	0.00242
<b>Crushing Strength, fpcu</b>		0.7*fpc	
<b>Strain at Crushing Strength, epsu</b>		0.01	

**Table A. 3: Element Concrete Properties for 4500 psi 28-day Compressive Strength**

<b>Pier</b>	<b>Element</b>	<b>Max. compressive Strength, fpc (psi)</b>	<b>Strain at Max. Strength, epsc0</b>
2	1	5986	0.002232
	2,3	6120	0.002462
	4a,b,d,e	6369	0.002887
	4c	6069	0.002374
3	1	5980	0.002222
	2,3	6116	0.002455
	4a,b,d,e	6369	0.002887
	4c	6069	0.002374
4	1	5967	0.0022
	2,3	6093	0.002415
	4a,b,d,e	6341	0.002839
	4c	6062	0.002362
5	1	5975	0.002213
	2,3	6093	0.002416
	4a,b,d,e	6369	0.002887
	4c	6069	0.002374
6	2,3	6093	0.002416
	4a,b,d,e	6369	0.002887
	4c	6069	0.002374
<b>Crushing Strength, fpcu</b>		0.7*fpc	
<b>Strain at Crushing Strength, epsu</b>		0.01	

## Appendix B: OpenSees Commands

### Node Commands to Define Contact Elements in All Location

The nodes created in order to form all the required rigid links and contact elements are given by the following nodes.

#nodes of contact element at abutment1

node 33	82.49	380.86	210.3834
node 44	82.49	380.86	210.3834
node 55	-82.49	380.86	-210.3834
node 66	-82.49	380.86	-210.3834

#nodes of contact element at abutment2

node 77	6666.27	126.04	184.3182
node 88	6666.27	126.04	184.3182
node 99	6521.73	126.04	-184.3182
node 100	6521.73	126.04	-184.3182

#nodes of contact element at expansion joint on pier 4

node 122	3347.458	351.1	184.3182
node 133	3347.458	351.1	184.3182
node 144	3191.731	351.1	-184.3182
node 155	3191.731	351.1	-184.3182

model BasicBuilder -ndm 3 -ndf 6;

# Nodes of rigid links for abutment and expansion joint

#abutment#1

node 11	0	380.86	0
node 3	82.49	380.86	210.3834
node 4	82.49	380.86	210.3834
node 5	-82.49	380.86	-210.3834
node 6	-82.49	380.86	-210.3834

#abutment#2

node 22	6594	126.04	0
node 7	6666.27	126.04	184.3182
node 8	6666.27	126.04	184.3182
node 9	6521.73	126.04	-184.3182
node 10	6521.73	126.04	-184.3182

#Pier#4 expansion joint

node 481	3325.083	351.1	184.3182
node 482	3180.543	351.1	-184.3182

node	483	3347.458	351.1	184.3182
node	484	3202.918	351.1	-184.3182
node	12	3347.458	351.1	184.3182
node	13	3347.458	351.1	184.3182
node	14	3191.731	351.1	-184.3182
node	15	3191.731	351.1	-184.3182

### Command For Modeling the Confined Concrete (4000 psi)

Concrete for reinforced concrete piers has been modeled by the “*concrete01*” model. The following describes the material model used for Element 2 of Pier 4.

```
# Pier No.....4
# Element No.....2

# Units: Kip, inch, second
# Define Material

set fcc42 -5.442384;           # 4000 psi Concrete
set Ecc42 [expr 57*sqrt(-$fcc42*1000)]; # Elastic Modulus
set epscc42 -0.002466;       # Strain at Maximum Strength
set fccu42 [expr 0.7*$fcc42]; # Crushing Strength
set epsccu42 -0.01;         # Strain at Crushing Strength

uniaxialMaterial Concrete01 $matTagConfConcrete42 $fcc42 $epscc42 $fccu42
$epsccu42;

puts "Confined Concrete Material42"
```

### Commands for Contact Element

The “*zeroLengthContact3D*” elements are used to simulate the interaction of the adjacent structure in each expansion joints. Total of six elements have been used in the bridge model and two of them on each expansion joint. The following describes the assigned values of the input parameters used for the contact element.

## #Contact Element

```
element zeroLengthContact3D 20 44 33 1e8 1e8 0.1 0 1;  
element zeroLengthContact3D 30 66 55 1e8 1e8 0.1 0 1;  
element zeroLengthContact3D 40 77 88 1e8 1e8 0.1 0 1;  
element zeroLengthContact3D 50 99 100 1e8 1e8 0.1 0 1;  
element zeroLengthContact3D 60 133 122 1e8 1e8 0.1 0 1;  
element zeroLengthContact3D 70 155 144 1e8 1e8 0.1 0 1;
```

```
puts "contact element"
```

```
equalDOF 3 33 1 2 3;  
equalDOF 4 44 1 2 3;  
equalDOF 5 55 1 2 3;  
equalDOF 6 66 1 2 3;
```

```
equalDOF 8 88 1 2 3;  
equalDOF 7 77 1 2 3;  
equalDOF 10 100 1 2 3;  
equalDOF 9 99 1 2 3;
```

```
equalDOF 12 122 1 2 3  
equalDOF 13 133 1 2 3  
equalDOF 14 144 1 2 3  
equalDOF 15 155 1 2 3
```

## #Rigidlinks for abutment and expansion joint

```
rigidLink beam 11 3;  
rigidLink beam 11 5;  
rigidLink beam 2000 4;  
rigidLink beam 2000 6;
```

```
rigidLink beam 22 8;  
rigidLink beam 22 10;  
rigidLink beam 7020 7;  
rigidLink beam 7020 9;
```

```
rigidLink beam 471 481  
rigidLink beam 471 482  
rigidLink beam 472 483  
rigidLink beam 472 484
```

```
rigidLink beam 481 12  
rigidLink beam 482 14  
rigidLink beam 483 13  
rigidLink beam 484 15
```

## Appendix C: Verification

### Appendix C.1: Concrete01 Material Behavior Verification

A patch of “Concrete01” sample of dimension 1” x 1” x 1” was developed in OpenSees. Material properties for the concrete such as elastic modulus, strain at maximum strength, crushing strength, and strain at crushing strength were calculated according to the example provided in the OpenSees command manual. The developed sample concrete cube was applied to a compressive load, P as shown in Figure C.11

The stress applied to the sample and its corresponding resulting strain obtained was plotted which was nonlinear. Figure C.12 shows the stress strain relationship obtained. Figure C.12 shows that the maximum concrete compressive strength, strain at the compressive strength, ultimate compressive strength and strain at the ultimate compressive strength are same as the input values. This proves that the “Concrete01” material is behaving as desired.

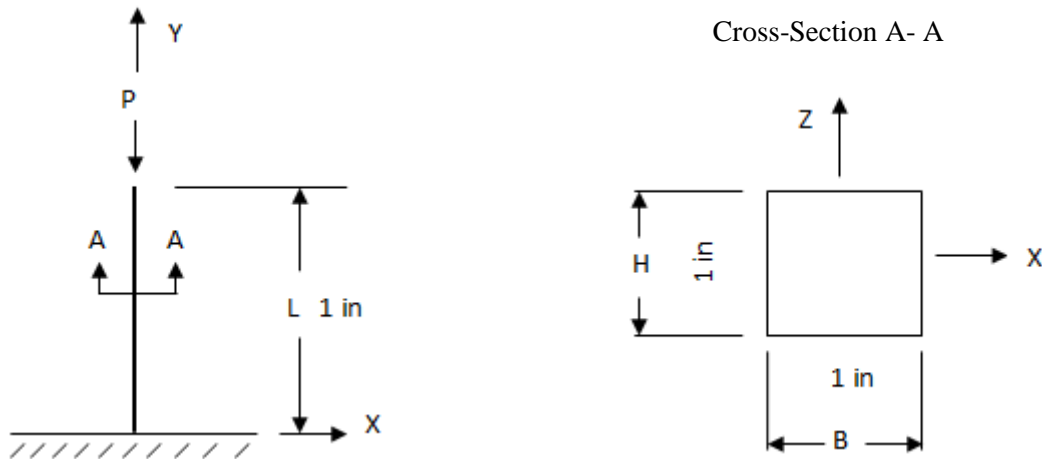


**Figure C.11: Concrete Patch and Cross-Section**

Concrete Properties:

Concrete Compressive Strength,  $f_c = -4168$  psi

Elastic Modulus,  $E_c = 57 \cdot \sqrt{-f_c} = 3680$  psi

Strain at Maximum Strength,  $\epsilon_{sc} = -0.0027$  psi

Crushing Strength,  $f_{cu} = 0.7 \cdot f_c = -2917$  psi

Strain at Crushing Strength,  $\epsilon_{scu} = -0.01$

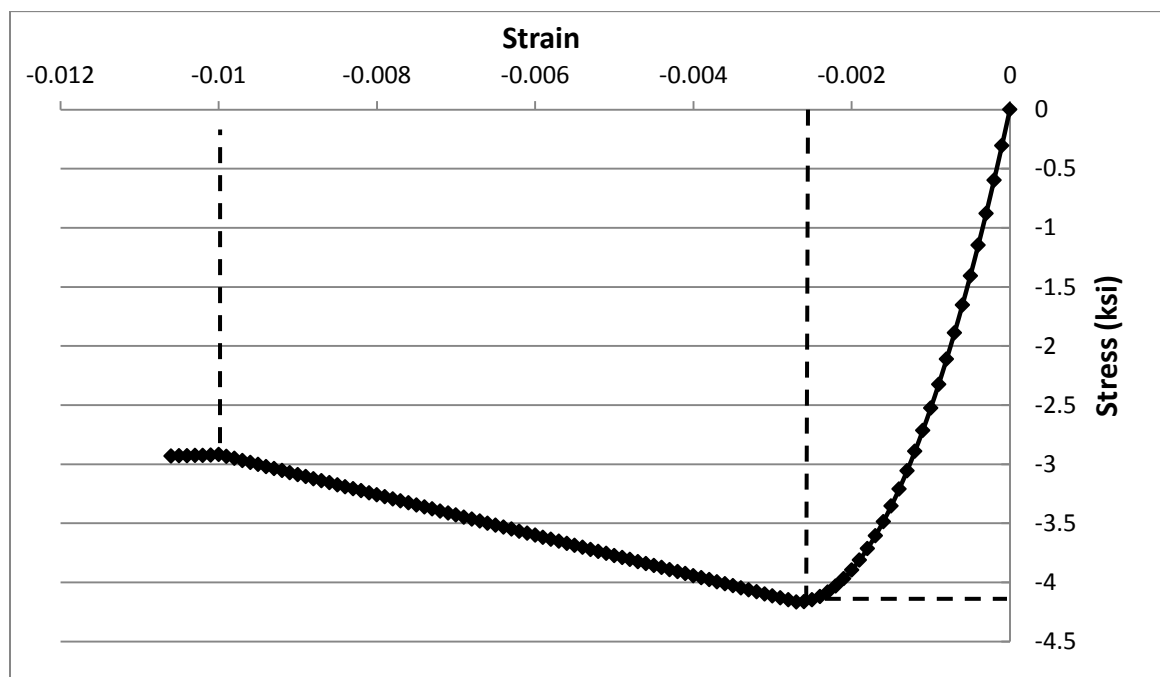


**Figure C.12: Concrete01 Stress-Strain Relationship**

### Opensees Source Code for Concrete01 Material Behavior Verification

```
# Concrete01 Material Behavior Verification
```

```
# Units: Kip, inch, second
```

```
model BasicBuilder -ndm 2 -ndf 3; # Define the model builder, ndm=#dimension, ndf=#dofs
```

```
wipe;
```

```

file mkdir Data;

#Define GEOMETRY -----
set LCol 1.0;          # column length

#Define section geometry
set HCol 1.0;         # Column Depth
set BCol 1.0;         # Column Width

#Nodal coordinates:
node 1 0.0 0.0 ;
node 2 0.0 $LCol ;

#Fix all degrees of freedom except axial at node 2
fix 1 1 1 1 ;
fix 2 1 0 1 ;

#Define Material
set fc -4.167772;      # Concrete Compressive strength
set Ec [expr 57*sqrt(-$fc*1000)];    # Elastic Modulus
set epsc -0.002687;   # Strain at Maximum Strength
set fcu [expr 0.7*$fc];    # Crushing Strength
set epscu -0.01;        # Strain at Crushing Strength
uniaxialMaterial Concrete01 1 $fc $epsc $fcu $epscu;
puts "Concrete Material"

#Define cross-section for nonlinear columns
set y1 [expr $HCol/2.0];
set z1 [expr $BCol/2.0];
section Fiber 1 {
    patch rect 1 10 10 [expr -$y1] [expr -$z1] [expr $y1] [expr $z1];
};

#Define geometric transformation: performs a linear geometric transformation of beam stiffness
and resisting force from the basic system to the global-coordinate system

```

```

set ColTransfTag 1;                # associate a tag to column transformation
set ColTransfType Linear ;        # options, Linear PDelta Corotational
geomTransf $ColTransfType $ColTransfTag ;
#Element connectivity:
set colsectag 1;

element nonlinearBeamColumn 1 1 2 5 $colsectag $ColTransfTag;          # self-
explanatory when using variables

#Define RECORDERS -----
recorder Node -file Data/DFree.out -time -node 2 -dof 2 disp;          #
displacements of free nodes

recorder Element -file Data/FCol.out -time -ele 1 globalForce;        # element
forces -- column

recorder Element -file Data/DCol.out -time -ele 1 deformation;        # element
deformations -- column

pattern Plain 1 Linear {;
    load 2 0.0 1.0 0.0;          # node#, FX FY MZ
};

integrator DisplacementControl 2 2 -0.0001;

#Define Analysis Parameters:
system SparseGeneral -piv;      # Overkill, but may need the pivoting!
test NormUnbalance 1.0e-9 10;  # determine if convergence has been achieved at the end of
an iteration step
numberer Plain;                # renumber dof's to minimize band-width (optimization), if
you want to
constraints Plain;             # how it handles boundary conditions
algorithm Newton;              # use Newton's solution algorithm: updates tangent
stiffness at every iteration

analysis Static;               # define type of analysis static or transient
analyze 1000;                  # apply 1000 steps

```

## Appendix C.2: Contact Element Verification

Verification was performed for “*ZeroLengthContact3D*” element that is used to represent the abutment-deck interaction and the interaction between the adjacent decks in expansion joint of the Washington Street Overpass. A simple structural frame was developed in OpenSees. Figure C.21 shows the model developed in OpenSees program.

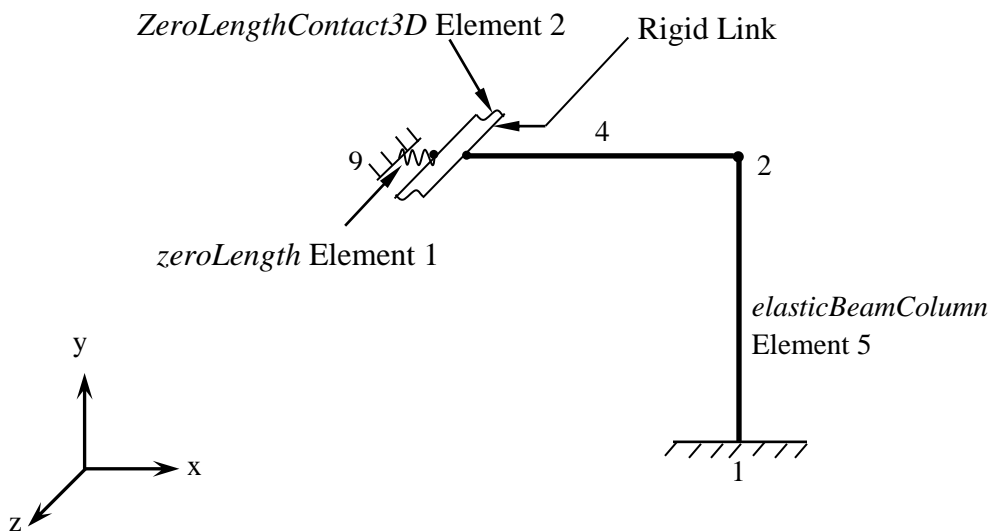


**Figure C.21: A Frame with Contact Elements**

The frame is comprised of four types of elements. They are “*zeroLengthSection*” element at the end of Element 4, two “*ZeroLengthContact3D*” elements, four rigid links and two “*elasticBeamColumn*” elements. 0.1 coefficient of friction of contact element was used for this verification.

The bases of Elements 1 and 5 are fixed. Ground motion with constant displacement of 1 in. was applied to the Nodes 9 and 1 in X and Z-direction respectively. The forces induced in element 4 were observed. It was seen that the transverse forces of the element was 10% of the normal forces. The results are tabulated as shown in Table C.1. The model was run for few more times varying the coefficient of friction of contact

elements ranging from 0.1 to 0.9. In all the cases, transverse forces were reduced to the assigned corresponding coefficient of friction of contact elements.

**Table C.21: Forces Induced in Element 4 for Coefficient of Friction of 0.1**

Time (s)	Force	
	Normal Direction	Transverse Direction
0.01	91.17	-9.04
0.02	91.17	-9.04
0.03	91.17	-9.04
0.04	91.17	-9.04
0.05	91.17	-9.04
0.06	91.17	-9.04
0.07	91.17	-9.04
0.08	91.17	-9.04
0.09	91.17	-9.04
0.1	91.17	-9.04

### OpenSees Source Code for Contact Element Verification

```
# Verification for contact element
#Constant displacement at node 9 in X-direction and at node 1 in Z- direction
```

```
wipe;
file mkdir ContactEleData;
```

```
model BasicBuilder -ndm 3 -ndf 3;
node 88 0 20 0.1;
node 44 0 20 0.1;
node 66 0 20 -0.1;
node 55 0 20 -0.1;
```

```
model BasicBuilder -ndm 3 -ndf 6;
node 9 0 20 0;
node 7 0 20 0;
node 8 0 20 0.1;
node 4 0 20 0.1;
node 6 0 20 -0.1;
node 5 0 20 -0.1;
node 3 0 20 0;
node 2 20 20 0;
node 1 20 0 0;
```

```

#constraints
fix 1 1 1 1 1 1 1;
fix 9 1 1 1 1 1 1;

fix 6 0 1 1 1 1 1;
fix 7 0 1 1 1 1 1;
fix 8 0 1 1 1 1 1;

geomTransf Linear 1 0 1 0;
geomTransf Linear 2 0 0 -1;

#elastic element

uniaxialMaterial Elastic 50 100;
section Uniaxial 60 50 P;
element zeroLengthSection 1 9 7 60;

#Contact Element

element zeroLengthContact3D 2 55 66 1e12 1e12 0.1 0 1;
element zeroLengthContact3D 3 44 88 1e12 1e12 0.1 0 1;

# connectivity:
#           $eleTag $iNode $jNode $A $E  $G  $J  $Iy $Iz $transfTag

element elasticBeamColumn 4 3 2 10 29e3 10e3 200 100 100 1;
element elasticBeamColumn 5 1 2 10 29e3 10e3 200 100 100 2;

equalDOF 8 88 1 2 3;
equalDOF 44 4 1 2 3;
equalDOF 6 66 1 2 3;
equalDOF 55 5 1 2 3;

rigidLink beam 7 6;
rigidLink beam 7 8;
rigidLink beam 3 4;
rigidLink beam 3 5;

#RECORDER

recorder Node -file ContactEleData/Node2.out -time -node 2 -dof 1 2 3 disp
recorder Element -file ContactEleData/Element1.out -time -ele 1 force
recorder Element -file ContactEleData/Element2.out -time -ele 2 force
recorder Element -file ContactEleData/Element3.out -time -ele 3 force
recorder Element -file ContactEleData/Element4.out -time -ele 4 force
recorder Element -file ContactEleData/Element5.out -time -ele 5 force

```

```

# Define earthquake (Displacements)
set dt 0.01
set const "Path -filePath const.txt -dt $dt -factor 2"

puts "earthquake loaded"

# Create Load Pattern
pattern MultipleSupport 1 {
  groundMotion 1 Plain -disp $const
  imposedMotion 9 1 1
  imposedMotion 1 3 1
}

test NormUnbalance 1.0e-6 25

algorithm Newton

#system ProfileSPD
system UmfPack
#system BandGeneral
#system SparseGeneral

#constraints Transformation
constraints Penalty 1e14 1e14

#          gamma beta
integrator Newmark 0.5 0.25

numberer RCM

analysis Transient

set ok 0
set maxNumIter 20;
set tol 1e-8;
set testtype NormDispIncr

set DtAnalysis 0.01;

set tFinal 2
set tCurrent 0.0

while {$tCurrent < $tFinal && $ok == 0} {

```

```

# original algorithm and time step
test $stesttype $tol $maxNumIter 0;
set ok [analyze 1 $DtAnalysis]

# analysis did not converge – reduce time step

if {$ok != 0} {

    puts "$ok != 0"
    set ok [analyze 1 [expr $DtAnalysis/20.0]];

}
# analysis did not converge – reduce time step

if {$ok != 0} {

    puts "$ok != 0"
    set ok [analyze 1 [expr $DtAnalysis/100.0]];

}
# analysis did not converge – reduce time step

if {$ok != 0} {

    puts "$ok != 0"
    set ok [analyze 1 [expr $DtAnalysis/500.0]];

}
# analysis did not converge – reduce time step

if {$ok != 0} {

    puts "$ok != 0"
    set ok [analyze 1 [expr $DtAnalysis/2500.0]];

}
# analysis did not converge – reduce time step

if {$ok != 0} {

    puts "$ok != 0"
    set ok [analyze 1 [expr $DtAnalysis/10000.0]];

}
# analysis did not converge – reduce time step

```

```

if {$ok != 0} {
    puts "$ok != 0"
    set ok [analyze 1 [expr $DtAnalysis/50000.0]];
}
# analysis did not converge – reduce time step

if {$ok != 0} {
    puts "$ok != 0"
    set ok [analyze 1 [expr $DtAnalysis/250000.0]];
}
# analysis did not converge – reduce time step

if {$ok != 0} {
    puts "$ok != 0"
    set ok [analyze 1 [expr $DtAnalysis/1000000.0]];
}
# analysis did not converge – reduce time step

if {$ok != 0} {
    puts "$ok != 0"
    set ok [analyze 1 [expr $DtAnalysis/5000000.0]];
}
# analysis did not converge – reduce time step

if {$ok != 0} {
    puts "$ok != 0"
    set ok [analyze 1 [expr $DtAnalysis/25000000.0]];
}
# analysis did not converge – reduce time step and try Newton w/ initial tangent

if {$ok != 0} {
    puts "$ok != 0"
    test $stesttype $tol 1000 2;
    algorithm Newton -initial
    set ok [analyze 1 [expr $DtAnalysis/100000.0]]
    test $stesttype $tol $maxNumIter 2;
}
# analysis did not converge – reduce time step and try Broyden

```

```

    if {$ok != 0} {
        puts "Trying Broyden .."
        algorithm Broyden 8
        set ok [analyze 1 [expr $DtAnalysis/100000.0]]
    }

# analysis did not converge – reduce time step and try Newton w/ with line search

    if {$ok != 0} {
        puts "Trying NewtonWithLineSearch .."
        algorithm NewtonLineSearch .8
        set ok [analyze 1 [expr $DtAnalysis/100000.0]]
        algorithm Newton
    }
    set tCurrent [getTime]
    puts $tCurrent
}

```

### **Appendix C.3: Validation of the OpenSees Bridge Model Using the Concept of Forces**

In order to validate that the entire bridge model developed in OpenSees works appropriately; the concept of equilibrium of forces is used. Figure 2.24 shows the entire bridge model. The bridge system comprises of all the components including the contact elements and gaps in all expansion joints. A gravitational load of Pier 4 (102 Kips) was applied only on the top (Nodes 422 and 423) of the Pier 4. The rest of the loads (including the nodal self-weights) were removed from all the locations. A displacement time history with the values of zero was applied to the bases of the piers and abutments of the bridge in longitudinal and transverse directions. The bridge model with 3500 psi 28-day compressive strength concrete, damping constant of 5% and 0.5 coefficient of friction of contact elements was used for this validation performance.

The vertical reactions of each of the piers and abutments were recorded. The sum of the forces was found to be 101.92 kips. The error percentage calculated for the applied load and reaction forces obtained is 0.08%, which is very minimal. Therefore, it is verified that the bridge model works appropriately as a system which includes superstructure with reinforced concrete bridge deck segments and two steel box girders, five reinforced concrete piers, deep pile foundation, abutments, three expansion joints with contact elements and gaps, steel guide angles, steel key plates and neoprene bearings.